

AD600515

SSC-161

**MICROMECHANISMS OF CLEAVAGE FRACTURE
IN POLYCRYSTALLINE IRON**

BY

CHARLES J. McMAHON, JR.

SHIP STRUCTURE COMMITTEE

SHIP STRUCTURE COMMITTEE

MEMBER AGENCIES:

BUREAU OF SHIPS, DEPT. OF NAVY
MILITARY SEA TRANSPORTATION SERVICE, DEPT. OF NAVY
UNITED STATES COAST GUARD, TREASURY DEPT.
MARITIME ADMINISTRATION, DEPT. OF COMMERCE
AMERICAN BUREAU OF SHIPPING

ADDRESS CORRESPONDENCE TO:

SECRETARY
SHIP STRUCTURE COMMITTEE
U. S. COAST GUARD HEADQUARTERS
WASHINGTON 25, D. C.

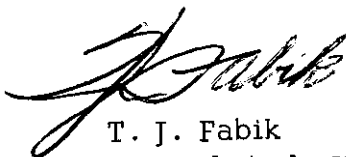
Dear Sir:

The Ship Structure Committee is sponsoring a study at the Massachusetts Institute of Technology of the influence of metallurgical structure on the fracture behavior of ship steel. Herewith is the Sixth Progress Report, SSC-161, of this project entitled Micromechanisms of Cleavage Fracture in Polycrystalline Iron by Charles J. McMahon, Jr.

This project is being conducted under the advisory guidance of the Ship Hull Research Committee of the National Academy of Sciences—National Research Council.

This report is being distributed to individuals and groups associated with or interested in the work of the Ship Structure Committee. Comments concerning this report are solicited.

Sincerely yours,



T. J. Fabik
Rear Admiral, U. S. Coast Guard
Chairman, Ship Structure
Committee

SSC-161

Sixth Progress Report
of
Project SR-136
"Metallurgical Structure"

to the
Ship Structure Committee

MICROMECHANISMS OF CLEAVAGE FRACTURE
IN POLYCRYSTALLINE IRON

by

Charles J. McMahon, Jr.
Massachusetts Institute of Technology

under

Department of the Navy
Bureau of Ships Contract NObs-88279

Washington, D. C.
National Academy of Sciences-National Research Council
May 1964

ABSTRACT

The initiation and propagation of cleavage microcracks in coarse-grained vacuum-melted ferrite, containing 0.035 and 0.007 per cent carbon, were studied by means of tensile tests carried out between room temperature and -196°C , and by special metallographic procedures. The latter involved surface replication of prepolished tensile specimens at various stages along the stress-strain curve, and also the progressive sectioning of such specimens to reveal the internal details. In this way, the effects of carbides and mechanical twinning were related to the low temperature yielding behavior, initiation and propagation of cleavage, and the ductile-brittle transition.

Cleavage microcracks develop in ferrite during the strain-hardening portion of the stress-strain curve at low temperatures, and are initiated mainly by cracks which form in the carbides. Twinning does not play an important role in crack initiation over the entire temperature range studied. Carbide cracks during plastic deformation at all temperatures investigated, but they lead to microcracks in the ferrite only when the applied stress is high enough to permit the carbide cracks to act as Griffith cracks. The ductile-brittle transition temperature closely follows the temperature at which microcrack formation starts. The lower carbon ferrite has a transition temperature 70°C below that of the higher carbon ferrite because its carbide particles are fewer in number and smaller in size.

Carbide cracks also lead to the formation of large voids during the necking of specimens tested in the ductile and transition temperature regions; these voids tend to lower the fracture stress and decrease the reduction in area at fracture.

Pre-existing twins provide strong barriers to microcrack propagation, and can act as a refinement of grain size to raise both the fracture stress and fracture strain in the brittle region. Twinning also causes the disappearance of the discontinuous-yield phenomenon at low temperatures.

A model for microcrack initiation by carbide cracking is proposed, and the conditions leading to brittle fracture are discussed. The applicability of these findings to the low-temperature brittle behavior of mild steel is also considered.

CONTENTS

	<u>Page</u>
INTRODUCTION	1
REVIEW OF THE LITERATURE	1
The Griffith Theory	1
Theories of Brittle Fracture Initiation	2
Theory of Crack Propagation	8
Intergranular Fracture	9
Microcracks in Polycrystals	9
OBJECTIVES AND PLAN OF THE WORK	10
EXPERIMENTAL PROCEDURE	10
Materials	10
Heat Treatments	11
Electropolishing	12
Grain Size Measurements	13
Tensile Testing	13
Metallographic Studies	15
RESULTS	17
Tensile Properties of Ferrite	17
Microcrack Studies on Fractured Specimens	22
Unloading Effects in Interrupted Tensile Tests	24
Surface Replication Studies	25
Sub-Surface Observations on Ground Specimens	30
Role of Carbides in Ductile-Fracture Region	42
DISCUSSION OF RESULTS	42
Crack Initiation	42
Conditions for Brittle Fracture	45
Role of Twins in Crack Propagation	47
Applicability of Results to other Materials	49
SUMMARY AND CONCLUSIONS	49
ACKNOWLEDGMENTS	51
REFERENCES	52

NATIONAL ACADEMY OF SCIENCES-NATIONAL RESEARCH COUNCIL

Division of Engineering & Industrial Research

SR-136 Project Advisory Committee
"Metallurgical Structure"

for the

Ship Hull Research Committee

Chairman:

C. S. Barrett
University of Chicago

Members:

J. H. Bechtold
Westinghouse Electric Corp.

L. S. Darken
U. S. Steel Corp.

Maxwell Gensamer
Columbia University

J. R. Low, Jr.
General Electric Co.

INTRODUCTION

The phenomenon of cleavage fracture, which tends to occur on the brittle side of the ductile-brittle transition in body-centered cubic and hexagonal close-packed metals, has long presented a special challenge to those interested in the fracture of materials. The challenge exists partly from the need to understand and control the tendency for sudden catastrophic failure, with low energy absorption, in such important engineering materials as mild steel, but it also stems from the interest in cleavage fracture as a purely scientific phenomenon. Cleavage is, by virtue of its crystallographic nature, the simplest mode of fracture which occurs in metals, and it should be the most easily understood. Nevertheless, although the efforts expended in the study of cleavage have been many and great, the problem is far from completely solved.

Because of their great technological importance, ferrous materials have received a large portion of the attention directed toward the brittle-fracture problem, and since their technology is generally more advanced than that of other b.c.c. metals, this situation is likely to continue into the near future. Most approaches to this problem have involved analyses of strength and ductility properties measured in various mechanical tests, or theoretical treatments of models proposed to explain the nature of the high stress concentrations necessary for the initiation of cleavage. One approach which has not been fully explored, however, is the study of the incipient stages of cleavage fracture, or the formation of microcracks. These microcracks can exist in deformed, though unfractured, specimens and are, in essence, cleavage fractures which have propagated over very small areas, relative to the cross-section of the specimen, before coming to rest. They offer an opportunity for a study of cleavage fracture on a fine scale, from which it may be possible to deduce some of the mechanisms of crack initiation, propagation, and arrest. The present work was undertaken with this end in mind.

By means of tensile testing at sub-ambient temperatures and careful metallographic analysis of deformed or fractured specimens of high-purity iron-carbon alloys, it is hoped to arrive at a clearer understanding of the micro-mechanisms of cleavage fracture of iron and steel, with the possibility of relating this to

other b.c.c. transition metals.

REVIEW OF THE LITERATURE

Ever since the early attempts of Ludwik¹ to explain the ductile-brittle transition by the existence of a fracture stress curve, which was supposed to intersect a yield stress curve at some low temperature, an explanation of brittle fracture in terms of microscopic and atomic mechanisms has been sought. Most theories of low-temperature brittle fracture in metals have emphasized the initiation stage; however, more recently the propagation stage has received an increasing share of attention.

In this chapter, the various hypotheses of the mechanics of brittle fracture are reviewed, along with the experimental observations which support or fail to support these hypotheses. In an effort to present a unified treatment of the subject, the discussion of theory and experiment is combined. This review is mainly concerned with cleavage fracture; the intergranular mode of low-temperature brittleness will be mentioned only briefly.

The Griffith Theory

The fundamental concept which forms the basis for modern treatments of brittle fracture was established by Griffith² in 1920. Griffith postulated that the generally observed tendency of brittle materials to fracture at stresses which are a few orders of magnitude below their estimated cohesive strengths is due to the existence of minute crack-like flaws which propagate under an applied "traction" if the strain energy released in the volume of material through which the crack passes is greater than the energy consumed in the formation of new crack surfaces. He assumed that the energy consumed by other dissipative processes is negligible (and herein lies the essence of "ideal" brittleness).

If the component of applied tensile stress normal to the major axis of an elliptical crack in a plate is σ and the length of the crack is $2c$, then the crack will propagate if

$$\sigma = \text{const.} \times \sqrt{\frac{E\gamma}{c}}$$

where E is the elastic modulus and γ is the surface energy of the material (assumed to be isotropic). The value of the constant depends

Theories of Initiation of Brittle Fracture in Metals

The Zener Hypothesis

The idea of pre-existing Griffith cracks cannot be used to explain the low cleavage strengths of metal crystals. The observed cleavage strength of zinc crystals would require cracks of several millimeters in length, and these should be easily observed. Furthermore, it is now almost universally accepted that cleavage fracture of metals is always preceded by some amount of plastic deformation. The first theoretical models which linked cracked initiation with plastic deformation involved the concept of the dislocation pileup.

In 1948 Zener⁹, considering the inhomogeneous nature of plastic flow in crystals, suggested that a slip band behaves like a temporarily viscous region in an elastic continuum and that the high stress concentration at the head of such a configuration, due to the relaxation of the shear stress across it, could lead to formation of a crack if the band were blocked by some obstacle such as a grain boundary or precipitate (Figure 1a). Alternatively, stated in terms of dislocation theory, this crack initiation could be viewed as the coalescence of edge dislocations whose movement on the slip plane has been similarly blocked (Figure 1b).

Eshelby, Frank and Nabarro¹⁰ have calculated the spacings of the dislocations in such an array, as well as the shear stress at its head, and Koehler¹¹ has extended this to a calculation of the tensile stress at the head of the pileup. Stroh¹²⁻¹³⁻¹⁴ and Petch⁸ have examined this model of crack initiation in detail.

The Grain Size Effect

It has been widely observed that in b.c.c. metals the yield stress and fracture stress behave similarly with respect to the grain size, in that they both increase linearly with the inverse square root of the average grain diameter. This $d^{-1/2}$ - yield stress behavior was first reported by Hall¹⁵ for mild steel and later by Petch¹⁶ for mild steel and iron (Figure 2a). It was Petch¹⁶ who first pointed out that the cleavage stress obeyed a similar $d^{-1/2}$ relation (Figure 2b), although his plotted values were

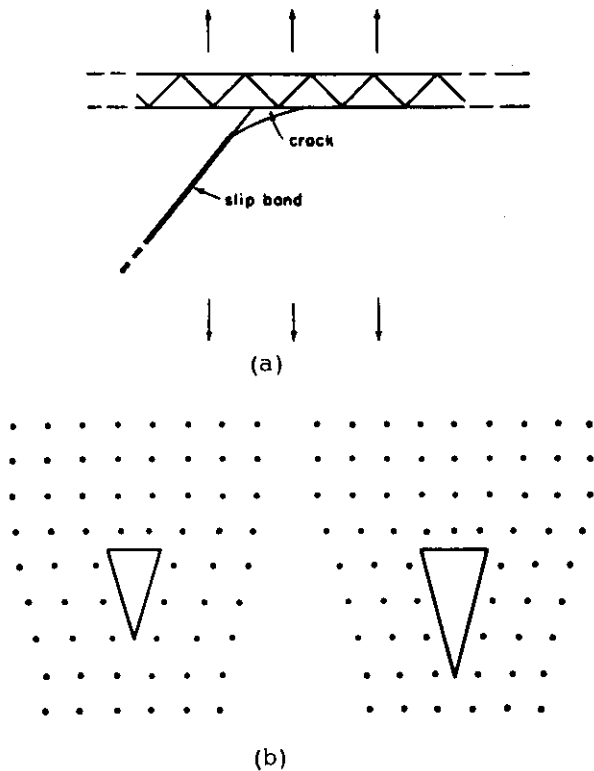


FIG. 1. CRACK INITIATION MODELS OF ZENER (a) BLOCKAGE OF A SLIP BAND BY A PRECIPITATE PLATE, (b) COALESCENCE OF EDGE DISLOCATIONS⁹.

on whether a plane stress or plane strain condition is being described and is of order unity in either case.

Griffith was able to support his theory by measurements of the fracture stress of glass tubes and bulbs as a function of the depth of artificially introduced surface scratches and by the near-theoretical strengths which he found in freshly-drawn glass fibers. Later, Andrade and Tsien³ made direct observations of surface flaws in glass. Although there have been objections to this use of macroscopic elastic theory on the atomic scale⁴, and although there is some reason to suspect that brittle crack propagation may occur in more than one stage⁵, the Griffith theory still stands pre-eminent in the fracture of brittle elastic materials⁶. Griffith, himself, noted⁷ that this theory could not be applied to plastic crystals in which rupture is preceded by plastic flow, but he suggested that it could be used in the case of brittle crystals if the anisotropy of the surface energy were taken into account.

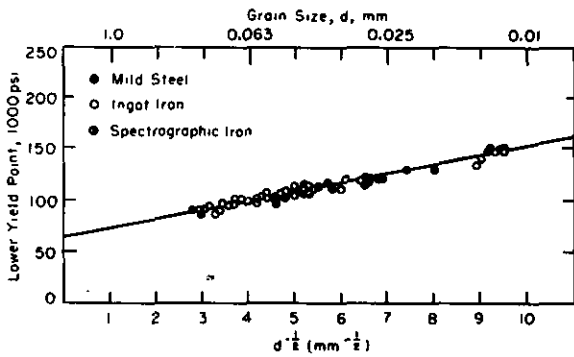


FIG. 2a. LOWER YIELD STRESS OF FERRITE AT -196 C AS A FUNCTION OF GRAIN SIZE¹⁶.

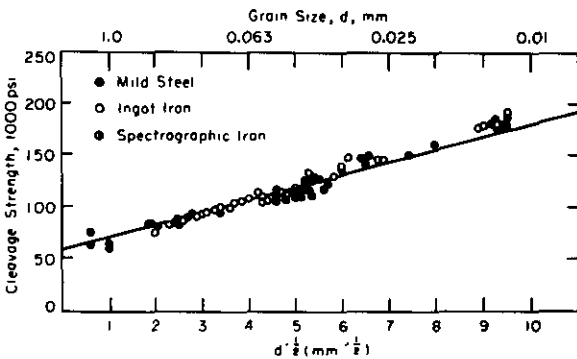


FIG. 2b. CLEAVAGE STRENGTH OF FERRITE AT -196 C AS A FUNCTION OF GRAIN SIZE¹⁶.

normalized to zero percent plastic strain to "correct" for the enhancing effect of plastic strain on the fracture stress. Others, however, have shown that uncorrected values of cleavage stress of various b.c.c.¹⁷⁻¹⁸ and h.c.p.¹⁹⁻²⁰ metals also follow this relation.

The $d^{-1/2}$ dependence of the yield stress can be attributed to the piling-up of dislocations, not necessarily in a linear array, at the head of a slip band which is blocked by a grain boundary. Since the effect was originally observed in iron and steel, it was at first confused with the yield-point effect found in those metals and explained in terms of the Cottrell theory of discontinuous yielding²¹. It has been shown, however, that not only does the flow stress at various strain levels obey a similar relation in iron²² and chromium²³, but that the yield and flow stresses of f.c.c. polycrystals also follow a $d^{-1/2}$ line²⁴⁻²⁵⁻²⁶. Thus, it is now apparent that the $d^{-1/2}$ relationship has more to do with strain hardening in polycrystals than with yielding²⁷.

Petch⁸⁻¹⁶ derived the first explanation which

connected the $d^{-1/2}$ behavior of cleavage stress with the Zener idea of crack initiation by a dislocation pileup.

The Theory of Petch

Petch considered that cleavage ensues when the stress σ at the head of a pileup reaches the theoretical cleavage strength σ_{TCS} . Making use of the approximation¹¹

$$\sigma = \alpha n \tau \quad (1)$$

where n is the number of dislocations piled-up by the applied shear stress τ and α a constant of order unity, and the Eshelby, Frank and Nabarro¹⁰ estimate of the length of the pileup array in terms of n and τ , which he set equal to $d/2$, he obtained the expression

$$\sigma = \frac{\alpha}{2D} (\tau - \tau_0)^2 d, \quad D = \frac{Gb}{2\pi(1-\nu)} \quad (2)$$

τ_0 is the "friction" stress opposing dislocation motion, which must be subtracted from τ to get the net shear stress acting on the pileup. G is the shear modulus, b the Burger's vector of the dislocations and ν is Poisson's ratio. By letting the applied tensile stress be twice τ and setting

$$\sigma = \sigma_{TCS} = \text{constant}$$

Petch obtained the following cleavage stress--grain size relation

$$\sigma_c = \sigma_0 + kd^{-1/2} \quad (3)$$

where k is a constant and σ_0 is twice τ_0 .

The Theory of Stroh

Stroh¹⁴ has developed a theory of fracture which, again, uses the concept of cracks initiated by the stress concentration of a dislocation pileup. He calculated that for a brittle metal, in which crack growth is not damped-out by plastic flow, the condition for initiating a crack is given by the following expression

$$\tau = \sqrt{\frac{3\pi G\gamma}{8(1-\nu)L}} \quad (4)$$

where τ is the resolved shear stress acting of the pileup, γ is the surface energy of the cleavage plane, and L is the length of the dis-

location pileup.

To get this relation Stroh first calculated the maximum normal stress in the grain adjacent to the pileup as a function of the resolved applied shear stress and the distance from the head of the pileup. He then supposed that a crack formed in the plane normal to this maximum stress and substituted this stress into the Griffith equation for crack propagation. He used the Eshelby, Frank and Nabarro estimate of the length of a pileup of n dislocations to get

$$\tau = \frac{3\pi^2 \gamma}{nb} \quad (5)$$

as the condition for crack initiation expressed in terms of n . Stroh estimated from reasonable values of τ that a pileup of about 100 dislocations would produce a crack, and further concluded that this crack would propagate catastrophically under the applied stress. By equating L to $d/4$ he was able to rationalize the $d^{-1/2}$ behavior of cleavage stress.

Stroh assumed that the dislocation sources in the grain adjacent to the pileup are locked by Cottrell atmospheres and thus prevented from relieving the stress concentration by slip. He thereby implies that this mechanism will operate only during yielding, when the density of operative sources is low and the few sources which do operate can be expected to form a large pileup in a short time. He states that the probability of brittle fracture is the same as the probability that the dislocations near a piled-up group will not be released by yielding in the next grain.

Biggs and Pratt³⁹ suggested that mechanical twins may take the place of grain boundaries in single crystals and that this may not only extend Stroh's theory to single crystals, but also explain the role of twinning in cleavage fracture. (They found that by prestraining iron single crystals at room temperature, both twinning and brittle fracture could be suppressed at -196 C.)

Stroh's prediction that cracks formed during low-temperature yielding will propagate to failure is not entirely supported by the results of Low¹⁷. Low found that, in mild steel at -196 C, cleavage fracture took place at the yield stress for large-grained specimens, but that for specimens of less than a particular

grain size, cleavage fracture occurred only after yielding and subsequent work hardening (Figure 3). Furthermore, he observed cleavage microcracks in specimens which had yielded

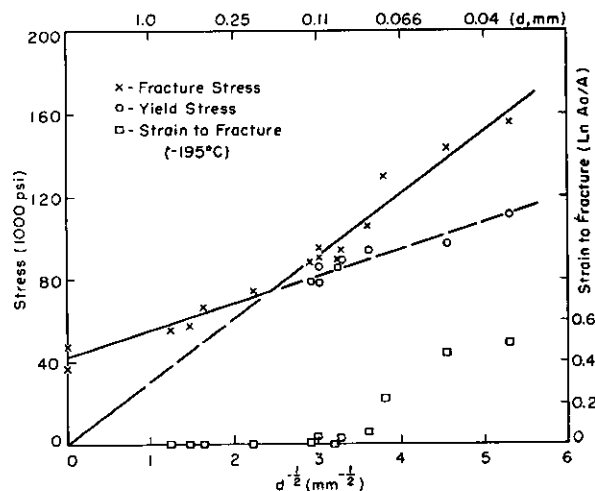


FIG. 3. YIELD AND FRACTURE STRESSES AT -195 C AS A FUNCTION OF GRAIN SIZE FOR A LOW CARBON STEEL. TRANSCRYSTALLINE CLEAVAGE FRACTURES¹⁷.

but not fractured.

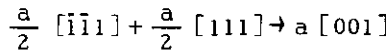
Low³⁸ believes that the existence of a barrier strong enough to form a pileup is unlikely, since a concentrated shear stress approaching the theoretical shear strength of the material would have to be reached in order to produce a pileup large enough to exceed the theoretical cleavage strength. In addition, he points out that large pileups have never been observed in the many etch-pit and electron transmission studies carried out in search of them. Finally, the models of both Petch and Stroh pre-suppose that Frank-Read sources operate during yielding to produce pileups, each lying on a single glide plane. There is reason to believe that a variant of the double cross slip mechanism of Koehler⁴³ is more likely in some of the materials which undergo cleavage fracture⁴⁴⁻⁴⁵, and cross slipping mechanisms of dislocation multiplication should not produce large pileups.

On the other hand, Hornbogen⁴⁶ has recently found that cross slip is rare in iron - 3 atomic percent phosphorus (an alloy which exhibits extreme brittleness) and that yielding is initiated by the operation of sources in the grain boundaries and subboundaries. He has also shown that very large pileups can be formed by the dislocations issuing from the

tips of mechanical twins.

The Theory of Cottrell

Cottrell³⁰ has proposed a model for crack initiation which does not involve grain boundaries, but rather the coalescence of $\frac{a}{2} \langle 111 \rangle$ dislocations moving on intersecting $\{110\}$ slip planes, by the reaction



Continued intersection and coalescence of the slip dislocations is supposed to form a pure edge $[001]$ dislocation of increasing Burger's vector, which is pictured as a cleavage knife being wedged into the (001) plane (Figure 4).

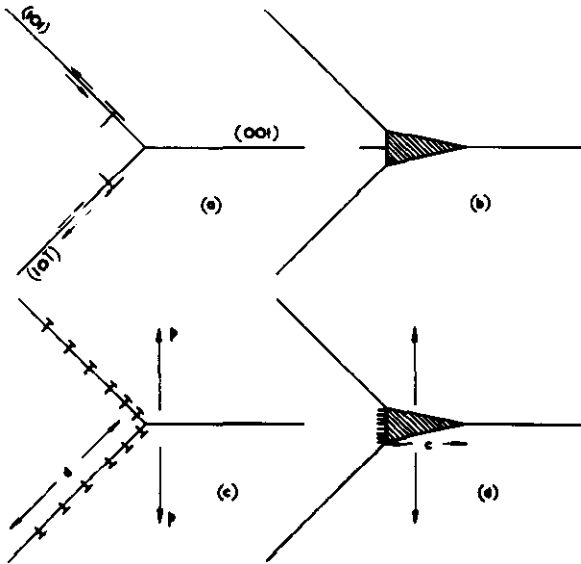


FIG. 4. (a) COALESCENCE OF TWO SLIP DISLOCATIONS TO FORM A CRACKED DISLOCATION ON A CLEAVAGE PLANE (b). (c) COALESCENCE OF TWO SLIP BANDS TO FORM A CLEAVAGE CRACK (d).³⁰

Cottrell derives a criterion for brittle fracture based on this model, which should apply as well to any crack initiation mechanism which employs intersecting slip or twin bands. This derivation requires that cracks be formed during yielding (either at the upper yield stress

or during Lüder's band propagation) and gives the expression

$$\sigma_y k_y d^{1/2} = \beta G \gamma \tag{6}$$

as the criterion for the ductile-brittle transition, where σ_y is the lower yield stress, $2d$ is the grain diameter, k_y is the slope of the σ_y versus $d^{-1/2}$ curve and β is a numerical factor (≈ 1 in the unnotched tension test).

The transition is so defined, that when the left-hand side exceeds the right-hand side, the yield stress is sufficient to propagate the crack formed in this model. This will tend to occur at large values of k_y , d or σ_0 (the friction stress) and will give rise to cleavage fracture at the yield stress. When the left-hand side is too small, cracks are supposed to form during yielding but they will be unable to propagate beyond a certain length. Plastic deformation can then take place before the occurrence of cleavage fracture at higher stress levels. Thus, a ductile-brittle transition can be obtained with a decreasing temperature, for a given grain size, or with increasing grain size at a given temperature, both of which are commonly observed.

The "certain length" at which a crack is supposed to stop in a specimen tested just above the transition temperature is arrived at from purely mathematical considerations and has no connection with any microstructural parameter, such as grain size. Although Cottrell seems to imply that this length will be the grain diameter, there is no reason to expect this from the derivation, since the grain size enters only through the yield stress relation. Hence, the importance of the grain boundary, per se, in polycrystals is found only in the surface-energy term, γ , which becomes a general expression of all the ways in which energy can be expended in crack propagation. These include slip or twinning caused by the high stress concentration at the tip of the moving crack (which increases with crack velocity³¹⁻³³), formation of cleavage steps or so-called "river markings"³³, and breaking through barriers such as twins and grain boundaries.

Stroh³⁴ has given a calculation which seems to show that the dislocations of Cottrell's model should dissociate rather than coalesce

after meeting at the slip plane intersection. However, calculations by Chou, Garofalo and Whitmore³⁵ indicate that such a double pileup would produce a much higher stress concentration than a single pileup, and that if the dissociation envisaged by Stroh were somehow prevented, such a dislocation array could indeed initiate a cleavage crack.

Cottrell³⁶ stated that a yield drop, which involves a sudden avalanche of slip dislocations, is needed for such a mechanism to operate. That is, pileups from unlocked or fresh dislocation sources must form the crack before further unlocking of other sources or generation of new dislocations can relieve the stress concentration. Thus, he visualizes that the influence of low temperature and high strain rate comes mainly from their effect of raising k_v (which contains the stress necessary to unpin a locked dislocation, according to the Cottrell theory of yielding). The fact that k_v has been found to be temperature insensitive over a wide range of temperatures by many investigators³⁷⁻³⁹⁻³⁸ in different materials does not offer much support for either the discontinuous yielding theory or the explanation of why brittleness accompanies a decrease in temperature.

It should be noted that the initiation of cleavage cracks by slip-band intersection in ionic crystals has been observed³⁹⁻⁴⁰, but to explain this we need only require that, under certain conditions, one slip band offers an impenetrable barrier to another which intersects it, and that continued slip on the secondary system produces a stress concentration large enough to exceed the theoretical cleavage strength. Here the primary slip band takes the place of the grain boundary in the Zener-Stroh model, and it is not necessary to call upon a special type of dislocation interaction to account for the crack.

The Later Theory of Petch

Petch⁴¹ has approached the brittle fracture problem from the standpoint of the transition in mode of fracture from ductile (or fibrous) to cleavage. He considers that crack formation by either a Stroh or Cottrell dislocation mechanism is the first stage of both ductile and cleavage fracture, and that cleavage will result if the applied tensile stress is sufficient to propagate the crack as a Griffith crack. Ductile fracture is thought to be due

to the linking-up of non-propagating dislocation cracks by ductile tearing of the bridges between them. In the transition temperature region the ductile "crack" or void, which forms first in the interior of the neck in a round tensile specimen, is supposed to gain speed and propagate as a Griffith crack at critical values of velocity and triaxial stress state.

By using Stroh's calculation of the shear stress and pileup size necessary to start a crack, and his own observation⁴² that the ductile fracture stress (corrected to constant fracture strain) follows the $d^{-1/2}$ relation

$$\sigma_f = \sigma_0 + k_f d^{-1/2} \quad (7)$$

he derives the following expression

$$\sigma_f = \frac{4G\gamma'}{k_f d^{1/2}} \quad (8)$$

as the criterion for the change from ductile to cleavage fracture. Here, again, the various energies expended in crack propagation are all contained in γ' , the effective surface energy. The effect of temperature resides mainly in the large increase in σ_0 at low temperatures, which raises the stress to produce the pileup, and partly in the supposed increase in k_v with decreasing temperature, which indicates stronger pinning and a lower γ' . (Stronger pinning means that dislocation sources are less likely to operate, thus less energy is absorbed by slip.) Both an increasing σ_0 and a decreasing γ' would favor cleavage.

The theories of Stroh, Cottrell and Petch are all based on the initiation of cracks by dislocation pileups, and they all yield roughly similar expressions for the stress to produce cleavage fracture. The only direct experimental evidence of slip-induced cleavage which has been reported so far is found in the work of Honda⁵⁰. He showed that cleavage cracks can form parallel to the tensile axis in [110] iron-silicon crystals, apparently at the intersection of slip lines.

Crack Initiation Mechanisms Involving Twins

Hull⁴⁷⁻⁴⁸⁻⁴⁹ and Honda⁵⁰ have recently given clear evidence of the initiation of cleavage by the intersection of mechanical twins in single crystals of iron-silicon. Honda used iron - 2.9 percent silicon crystals in the form

of sheets with a $\{110\}$ surface in tensile tests at -196°C . His crystals always failed by cleavage which started at the intersection of pairs of $\langle 111 \rangle \{112\}$ twins whose line of intersection was parallel to the (100) plane, when the tensile axis lay in the $[100]$ direction. The mechanism by which twin A forms an impenetrable barrier to twin B (Figure 5a), thereby causing a highly concentrated tensile stress on the cleavage plane, is explained in terms of the rotation of the $(11\bar{2})$ plane in the twinned region of A to an orientation which is unfavorable for the operation of system B (Figure 5b). The estimated stress concentra-

tion is comparable with the theoretical cleavage strength. Honda also found that crystals pulled in $\langle 110 \rangle$ and $\langle 111 \rangle$ directions cleaved without twinning and that the results can best be explained by a slip band intersection mechanism.

Hull⁴⁸ obtained results similar to those of Honda's $\langle 100 \rangle$ specimens with iron - 3 percent silicon sheet crystals having a (100) face pulled in the $[100]$ direction at -196°C . He also found that similar crystals⁴⁹ fractured by cleavage at 20 K, likewise initiated by twin intersections, when pulled in directions ranging from $[010]$ to $[110]$.

Honda⁵¹ has recently tested iron single crystals over a range of temperatures down to -196°C and has verified that the twin intersection mechanism of crack initiation applies to iron as well. In this case, it appears that the intersection of a twin with the boundary of an included grain can be an equally important source of cleavage.

Edmondson⁵² has reported further substantiation of the twinning mechanism for iron single crystals, and Cahn⁵³ and Bell and Cahn⁵⁴ have shown that it operates in molybdenum and zinc as well. So far, the evidence for this mechanism has been obtained in single crystals, and it is not at all certain that it is of equal importance in polycrystals.

Hornbogen⁵⁵⁻⁵⁶ has observed twin-initiated cleavage in iron-phosphorus crystals and his results indicate that some of these cracks were formed by the elastic waves emitted by a moving twin (which may be considered to be a linear plastic wave) being reflected from the boundary of another twin lying across its path. This dynamic model should be considered separately from the quasi-static one of Honda and Hull. Honda (private communication) has observed that a twin intersection, which existed prior to fracture, was the cause of cleavage when the stress was later raised to a higher level; thus, cracking was not the immediate result of the twin intersection. No evidence of this shock-induced cracking has been reported for other materials, and the phenomenon may be peculiar to iron-phosphorus alloys.

Sleeswyk⁵⁷ has proposed a model for crack initiation based on a modification of the Cottrell mechanism³⁰ and his own concept of dislocations emitted from the tip of a moving twin,

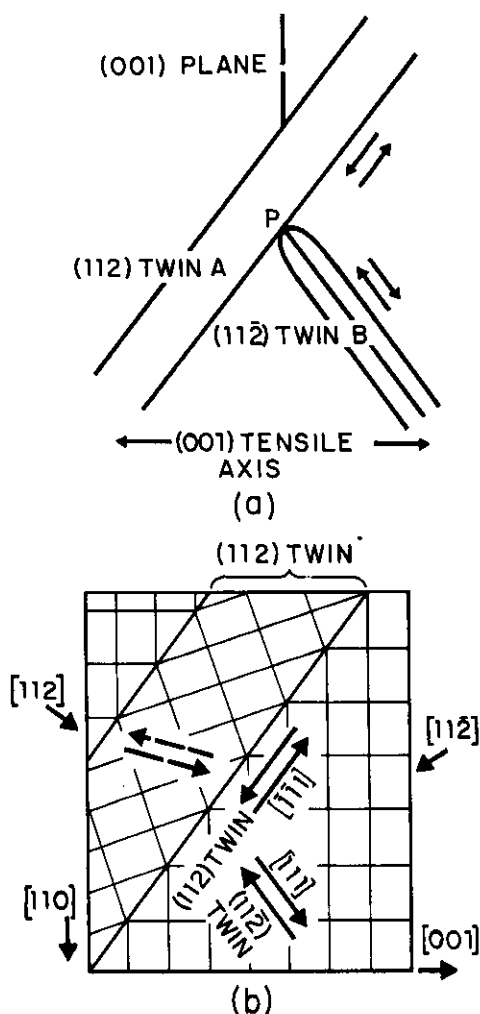


FIG. 5(a) and (b). (a) TYPE OF TWIN INTERSECTION WHICH CAN PRODUCE CLEAVAGE ON (001) PLANE (b) REORIENTATION OF LATTICE IN TWIN A WHICH PREVENTS PENETRATION OF TWIN B⁵⁰.

which he has termed "emissary dislocations"⁵⁸. His idea is that the dislocations emitted by two twins, which are travelling so as to arrive at their line of intersection at nearly the same time, will intersect on a {100} plane to give <100> dislocations, i.e., a Cottrell type of crack nucleus.

He concludes that the microcracks which Hahn⁶⁶ found in his mild steel tensile specimens were formed by this mechanism, and he predicts that in both poly- and single crystals, the cleavage stress should be about 1.1 times the twinning stress at all temperatures in the brittle region. Sleeswyk's conclusions can be evaluated in the light of the results of the current study and they will be discussed in a later section.

Crack-Initiation Hypothesis of Allen

In order to account for the observations that single crystals of iron may fracture by cleavage apparently without prior deformation⁵⁹, that polycrystalline specimens of iron-phosphorus⁶⁰ and notched mild steel⁶¹ may fracture by cleavage at stresses well below the expected yield stress, and that anomalous effects may be obtained by prestraining mild steel in compression, Allen⁶² has suggested that cleavage may be initiated in certain closely spaced dislocation arrays which may exist in annealed metals. The idea still lacks any direct experimental support, and cannot be evaluated at this point.

Cracking of Iron Carbide in Iron and Steel

It has long been known that the brittle iron carbide phase in steel can crack during deformation⁶³. These cracks can generally be ignored at normal temperatures and strain rates, where the ductility of the ferrite matrix is sufficient to accommodate such stress-raising discontinuities. However, in the case of low-temperature (or high strain-rate) deformation, the carbide phase must be considered as a possible source of ferrite cleavage. Indeed, Bruckner⁶⁴ and Allen et al⁶⁵ have published photographs of microcracks in mild steel and in iron, respectively, which apparently originated at cracked carbide films in the grain boundaries. Hahn⁶⁶ has observed similar cracks in mild steel and high purity iron-carbon alloys. The work of Josefsson⁶⁷, Allen et al⁶⁵, Danko and Stout⁶⁸ and Brick⁶⁹ has demonstrated that the impact transition temperature of low-carbon ferrite can be radically lowered by

changes in the carbide morphology brought about by subcritical heat treatments. Figure 6 taken from the work of Danko and Stout shows that when carbide formation is suppressed in a low carbon iron by quenching from the alpha region, the impact transition temperature is about 200 F lower than that of the same material in which grain boundary carbide has been allowed to form in a slow cooling process. The importance of iron carbide has been largely overlooked in most theories of brittle fracture, however, and part of the present work will be devoted to a study of its effect.

Theory of Crack Propagation

The theory of crack propagation in metals, being much more complicated and less amenable to experimental study, has progressed less than the theory of initiation mechanics. Orowan⁷¹ has modified Griffith's equation for the fracture stress by substituting a plastic work term p for the surface energy γ to give:

$$\sigma = \text{const.} \times \sqrt{\frac{Ep}{C}}$$

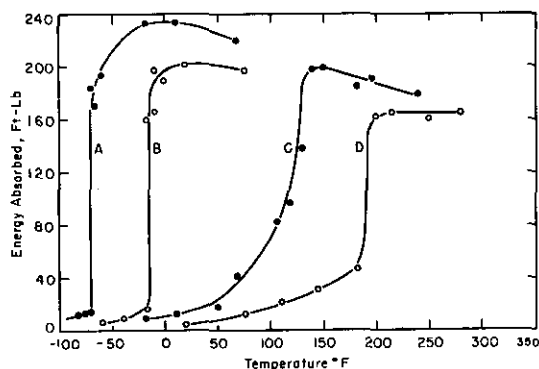


FIG. 6. THE EFFECT OF CARBIDES ON THE NOTCH TOUGHNESS OF INGOT IRON. NO GRAIN BOUNDARY CARBIDE NETWORKS IN A AND B.

Legend

- A Furnace cooled from 900 C; reheated to 705 C, water quenched; aged 200 C, 24 hours; grain size: ASTM 5.4
- B Furnace cooled from 1205 C; reheated to 705 C, water quenched; aged 200 C, 24 hours; grain size: ASTM 2.5
- C Furnace cooled from 900 C; grain size: ASTM 5.5
- D Furnace cooled from 1205 C; grain size: ASTM 2.4

and he has shown by X-ray measurements on fracture surfaces of mild steel plate⁷² that ρ is several orders of magnitude larger than the commonly accepted value of γ for iron (which is about 10^3 ergs/cm²). This "effective" surface energy should increase with increasing temperature and decreasing crack velocity and should vary with microstructural parameters which influence plastic deformation.

This approach is useful for a qualitative description of crack propagation, and ρ has been measured for various materials under different test conditions²⁸, but, so far, it has shed little light on the mechanisms of energy absorption in crack propagation.

Tetelman⁷³⁻⁷⁴ has analyzed the plastic deformation by slip which accompanies the propagation of cracks in iron - 3 percent silicon single crystals. He has concluded that, at fairly low temperatures and high crack velocities, the energy expended in crack propagation by activation of dislocation sources in the volume of material swept out by the moving stress field of the crack tip is of about the same order of magnitude as the surface energy γ .

Intergranular Fracture

In some instances of brittle behavior of metals, the mode of fracture is intergranular instead of cleavage. In these cases the fracture takes place simply by separation along grain boundaries, either because of the segregation of a brittle second phase at the boundaries, or because of segregation of some impurity element²⁸.

Iron can become embrittled and fracture in an intercrystalline manner if it contains oxygen, but this effect can be eliminated by additions of small amounts of carbon⁷⁰. Low²⁸ reports that the mode of fracture at -196 C of a decarburized rimmed steel, containing 0.02 percent oxygen and less than 0.001 percent carbon, can be changed from intercrystalline to transcrystalline by simply recarburizing back to 0.005 percent carbon.

Intercrystalline fractures can be distinguished from the cleavage facets of transcrystalline fracture by their characteristic smooth appearance and lack of cleavage steps. It is important to recognize the existence of intergranular fracture when it becomes opera-

tive in low-temperature testing, since the mechanisms discussed above pertaining to cleavage fracture would then lose their relevance.

Microcracks in Polycrystals

Cleavage microcracks in polycrystals were first observed by Bruckner⁶⁴ in mild steel tensile-impact specimens and later by many others in iron and steel and, recently, in chromium²³. Microcracks are generated in specimens deformed at low temperatures during plastic deformation prior to fracture. They are actually cleavage fractures which initiate at applied stresses too low for long-range propagation, and which are halted for one or more of the following reasons:

- (i) the crack hits a barrier, such as a grain boundary, twin, or precipitate;
- (ii) the stress concentration at the crack tip is relieved by slip or twinning ahead of the crack, causing it to slow down and, finally, stop; or
- (iii) the crack runs out of the localized high stress field in which it formed into a region of comparatively low stress.

Microcracks in iron and steel have been studied by Low¹⁷, Owen et al⁷⁵, Hahn⁶⁶ and Sullivan⁷⁶, and it has been generally found that the number of grains containing microcracks increases with the level of plastic strain at low temperatures (Figure 7). When the number of microcracks in fractured tensile

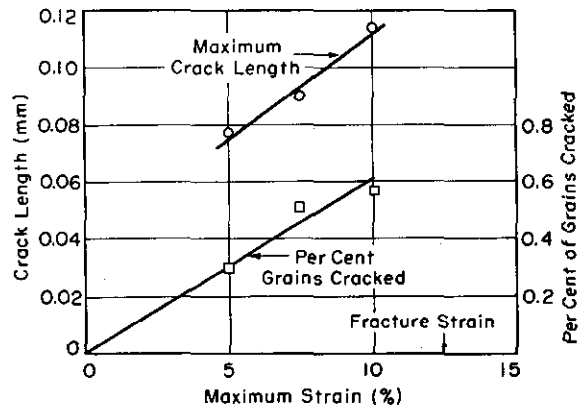


FIG. 7. NUMBER AND SIZE OF LARGEST CRACKS IN A LOW CARBON STEEL DEFORMED AT -195 C AS A FUNCTION OF STRAIN. COMPLETE FRACTURE OF AGGREGATE OCCURRED AT APPROXIMATELY 12% STRAIN¹⁷.

specimens is plotted against test temperature, a maximum is found at, or just below, the ductility transition temperature T_0 , which is the temperature of the steep decline of the percent reduction in area values of fractured tensile specimens (Figure 8). Aside from these ob-

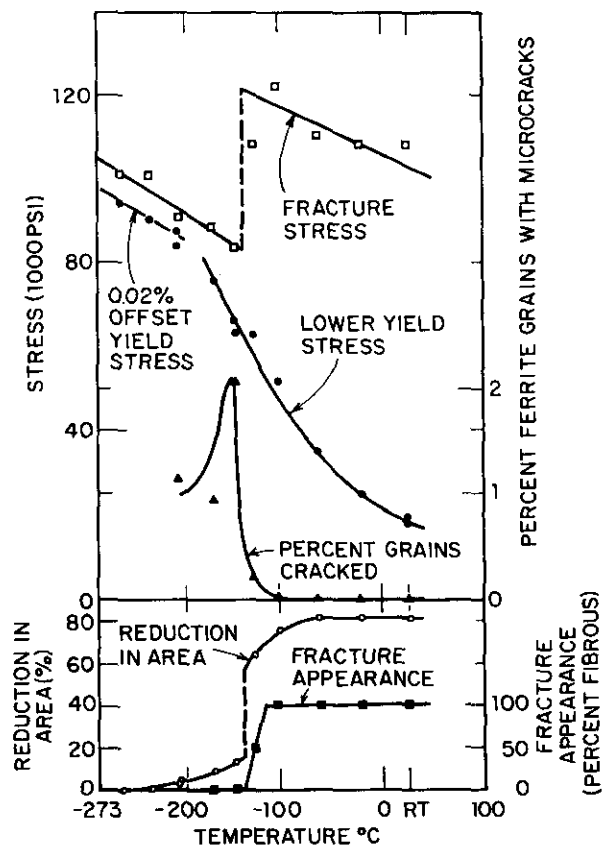


FIG. 8. TENSILE PROPERTIES OF POLYCRYSTALLINE IRON 0.04 % CARBON SPECIMENS SHOWING NUMBERS OF MICROCRACKS OBSERVED⁶⁶.

servations of the frequency of formation of cracks, there have been no detailed studies made of the mechanisms of formation of these microcracks, their behavior under increasing levels of stress, or their relevance to the overall cleavage-fracture problem.

OBJECTIVES AND PLAN OF THE RESEARCH

This research program was carried out during the period of June 1961 to May 1963 and was concerned with the following objectives:

- (1) to study the formation of cleavage microcracks in polycrystalline iron in order to determine where, in the strain history of the tensile specimens, the cracks form,

and how they behave as the stress level is raised after their formation;

- (2) to determine the mechanisms of crack formation and, in particular, to test by direct observation the various crack initiation models which have been proposed;
- (3) to determine the means by which crack propagation is arrested in the formation of "stable" microcracks, and thus to gain more insight into the process or crack propagation in polycrystalline aggregates;
- (4) to examine the role of the iron carbide phase in the ductile-brittle transition of iron and steel.

Continuous and interrupted tensile tests were carried out on coarse grained specimens of two low-carbon ferrites which had been slow cooled from the austenite region. The interrupted tests were used in conjunction with a replication technique whereby the surfaces of the tensile specimens were replicated after each strain increment. The history of deformation and crack formation could then be traced back from the fractured specimens through the series of replicas.

Selected fractured specimens were ground and polished parallel to the original surface to uncover crack sources lying beneath the surface.

EXPERIMENTAL PROCEDURE

Materials

Two 100-pound heats of high-purity vacuum-melted iron (Ferrovac E) were obtained in the form of one inch and 3/4 inch annealed rod, respectively. The former, with 0.035 percent carbon, was designated F4, and the latter, with 0.007 percent carbon, was designated F5. Their chemical compositions are given in Table I.

The rods were cold-swaged to 0.670 inch diameter and, after a one hour anneal at 800 to 850 C, were cold-rolled to 0.130 inch strip. The strips were cut into 11-inch lengths and straightened in a tensile machine within 2 hours after rolling (to prevent Lüders band formation while straightening). The strips were then cut in half and machined into tensile specimens, as shown in Figure 9.

TABLE I. CHEMICAL COMPOSITIONS OF MATERIALS STUDIED

Weight Percent	Ferrite F4	Ferrite F5
C	0.035	0.007
N	0.00045	0.0002
O	0.0017	0.0020
Mn	0.001	0.001
P	<0.001	0.003
S	0.002	0.006
Si	0.008	0.006
Ni	0.006	0.03
Cr	0.003	0.002
V	<0.001	0.004
W	<0.001	0.02
Mo	0.001	0.005
Co	0.003	0.003
Cu	0.001	0.001
Al	0.001	0.001
Pb	<0.01	
Sn	<0.006	

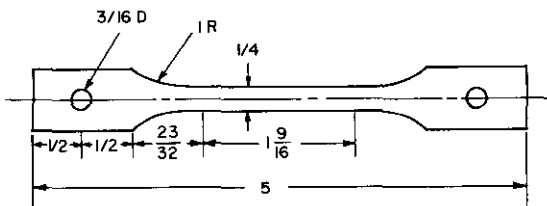


FIG. 9. TENSILE SPECIMEN.

Heat Treatments

The machined specimens were surface ground and then heat treated in an atmosphere of welding-grade argon in resistance-wound tube furnaces with a constant temperature zone of 4 to 6 inches, depending on the temperature. A summary of the treatments is given in Table II. The heat treatments are described in detail in the following paragraphs.

F4 Ferrite - The F4 ferrite was treated to produce two different coarse grain sizes by heating in the austenite region for 4 hours and furnace cooling, giving a cooling rate of approximately 3 C per minute. Most of the subsequent testing was done with the very coarse-grained material, which was austenitized at 1250 C; the material treated at 1000 C was used mainly to check the effect of a small change in grain size on the ductile-brittle transition temperature. Furnace cooling from the austenite region produced rather thick discontinuous films of Fe₃C in the ferrite grain boundaries, as well as similarly thick, but irregularly shaped, patches of Fe₃C within some of the grains. Occasional patches of pearlite surrounded by a thick carbide envelope were also present. Typical examples of these structures are shown in Figure 10. The very coarse grain size (0.29 to 0.40 mm) was used for two reasons: first, to obtain very brittle behavior (reduction in area ≤ one percent) at a temperature above that of liquid nitrogen (-196 C) so that the low-temperature tensile testing would not be unnecessarily complicated by the use of other coolants; and

TABLE II. SUMMARY OF HEAT TREATMENTS AND GRAIN SIZES

Material	Condition	Heat Treatment	Average Grain Diam. (mm)	ASTM Grain Size Number
Ferrite F4	Very Coarse	1250 C-4hrs.-FC	0.29 to 0.40	0.9 to 0
	Moderately Coarse	1000 C-4hrs.-FC	0.13 to 0.17	3.5 to 2.7
Ferrite F5	Coarse	925 C-4hrs.-FC	0.22 to 0.28	1.8 to 1.1

FC: Furnace Cooled

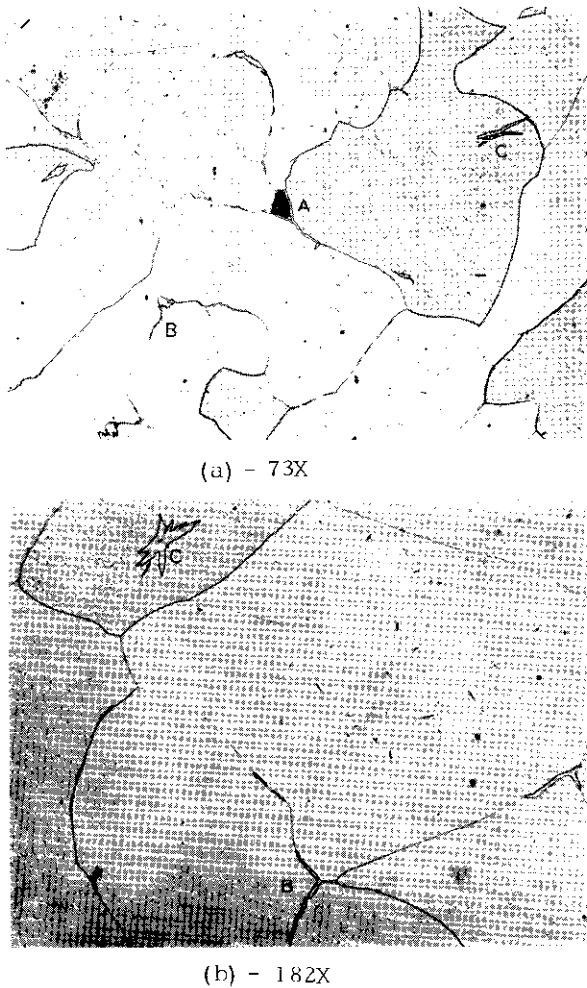


FIG. 10 (a) and (b). MICROSTRUCTURE OF VERY COARSE GRAINED F4 FERRITE SHOWING (A) PEARLITE, (B) INTERGRANULAR CEMENTITE, (C) INTRAGRANULAR CEMENTITE.

secondly, to facilitate the metallographic examinations by making the events appear on as large a scale as possible.

F5 Ferrite - This material was studied in order to gain a comparison with F4 with respect to the effect of carbides on the tensile behavior in the cleavage-fracture region. Attempts were made to match the very coarse grain size of the F4 by using various austenitizing temperatures and times while still maintaining the slow cooling rate, but it was found that the 0.22 to 0.28 mm grain size was the largest which could be obtained without encountering extremely non-uniform sizes and irregular shapes. In general, with both the F4 and F5 ferrites, as the ferritic grain size was increased, it became more difficult to obtain equiaxed and uniformly-sized grain

structures, and the number of specimens which had to be rejected because of nonuniform grain size increased.

The F5 ferrite, when furnace cooled from the austenitizing temperature of 925 C, contained very small amounts of Fe_3C as a grain-boundary precipitate. For the most part, these appeared as more or less discrete elongated particles, rather than as continuous films, and virtually no Fe_3C particles were found within the grains. Examples of the furnace-cooled F5 structures are found in Figure 11.

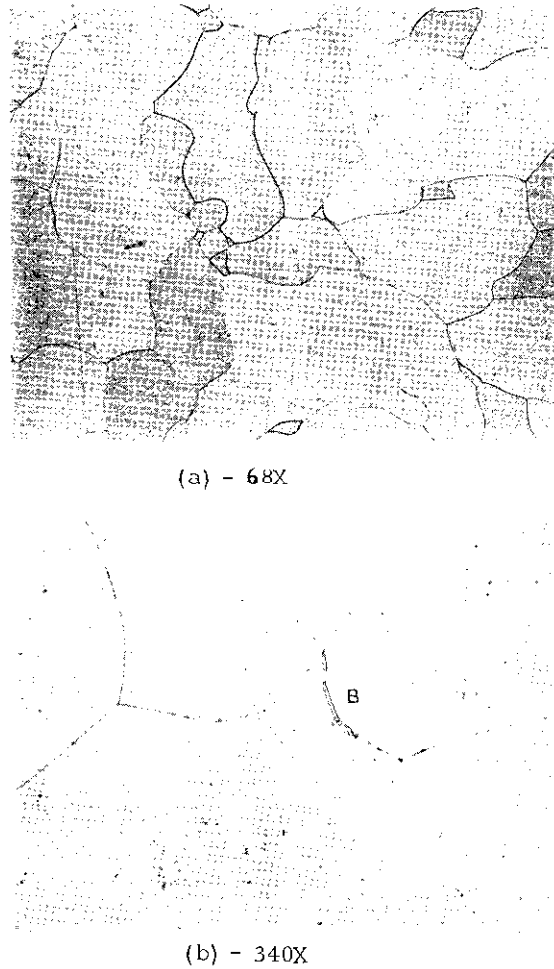


FIG. 11 (a) and (b). MICROSTRUCTURE OF COARSE GRAINED F5 FERRITE SHOWING (B) INTERGRANULAR CARBIDES.

Electropolishing

After heat treatment the specimens were electropolished in a solution of 1 part perchloric acid (sp. gr. 1.60) and 20 parts glacial acetic acid⁷⁷, for 20 minutes at a temperature

of 16 to 20 °C. The voltage and current density used were 30 to 32 volts and 2.2 to 2.7 amps per square inch. The electropolishing apparatus is illustrated in Figure 12. This treatment removed about 2 mils from the surface of the

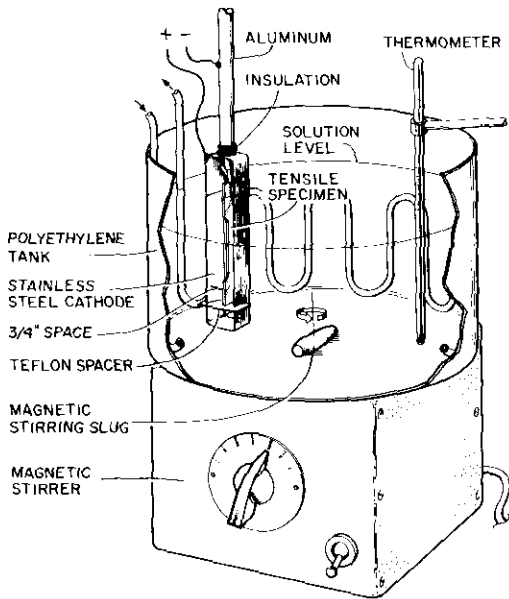


FIG. 12. APPARATUS FOR ELECTROPOLISHING TENSILE SPECIMENS.

specimens. After being polished, the specimens were etched for 5 to 10 seconds in 1 percent nital.

Grain-Size Measurements

The grain size of every specimen was measured by making a 1-inch traverse along the gauge section on each of the broad sides of the specimen, using a special micrometer stage attached to a microscope. The mean distance between grain boundaries along this traverse was multiplied by a factor of 1.65 to give a value of the average grain diameter $d^{8.0}$. This approximation involves the assumption that the grains have the shape of Kelvin's tetrakaidecahedra (cuboctahedra) with a volume equal to $\frac{\pi}{6} d^3$, and the use of the relationship of Smith and Guttman²¹

$$S_v = 2 \frac{N}{L}$$

where S_v is the grain-boundary interfacial area per unit volume of material, N is the number of grain-boundary intercepts along a linear traverse, and L is the length of the

traverse.

Tensile Testing

Tensile tests were carried out on a Tinius Olsen Electromatic 12000-pound testing machine, a "hard" screw-driven machine on which load is measured by a system of torsion bars. The strain rate used in all tests was 0.031 in./in./min. Strain was measured by crosshead movement as recorded on the chart of an autographic recorder driven by a synchronous motor. The nominal gauge length of the specimens was taken to be 1 9/16 inches, although this is an under-estimate due to the large radius of the shoulders.

The arrangement for gripping the specimens is shown in Figure 13. The grips were fitted with spherical bearings to insure proper alignment; these bearings remained free at all testing temperatures used.

The tests at subatmospheric temperatures were carried out by using the method of Wessel and Ollerman^{7,8}. Temperatures from -40 to -190 °C were obtained by spraying nitrogen as a vapor, mist or liquid on the specimen through the cooling chamber shown in Figures 14 and 15. The nitrogen was transferred from a 25 liter dewar (Figure 16) through an insulated tube under a pressure of 6 to 9 PSIG (maintained with an auxiliary tank of nitrogen gas). The flow was controlled by a solenoid valve in an on-off manner. The solenoid was actuated by hand during testing and by a Wheelco 0 to 50 mv. controller during the preliminary cooling. The input to the controller was supplied by a group of seven copper-constantan thermocouples connected in series (approximately 37.5 mv. at -196 °C) placed next to the gauge section of the specimen inside the cooling chamber.

The specimen temperature was measured with two copper-constantan thermocouples, one attached to each shoulder by means of a copper clip. During testing, these thermocouples, whose output was measured with a Leeds and Northrup Rubicon potentiometer, served both for measurement and control. The temperature fluctuation during a test was less than 1 °C; the temperature difference between the shoulders was always less than 2 °C, and usually less than 1 °C. Although the sensitivity of a copper-constantan thermocouple decreases with decreasing temperature and

becomes rather low in the vicinity of -196 C , it was at these low temperatures that the temperature uniformity characteristics of the cooling chamber were best, so that the maximum error in reported temperatures is estimated to be less than 2 C . Large temperature fluctuations caused by direct impingement of coolant on the specimen were avoided by wrapping the gauge section with a few layers of Saran plastic.

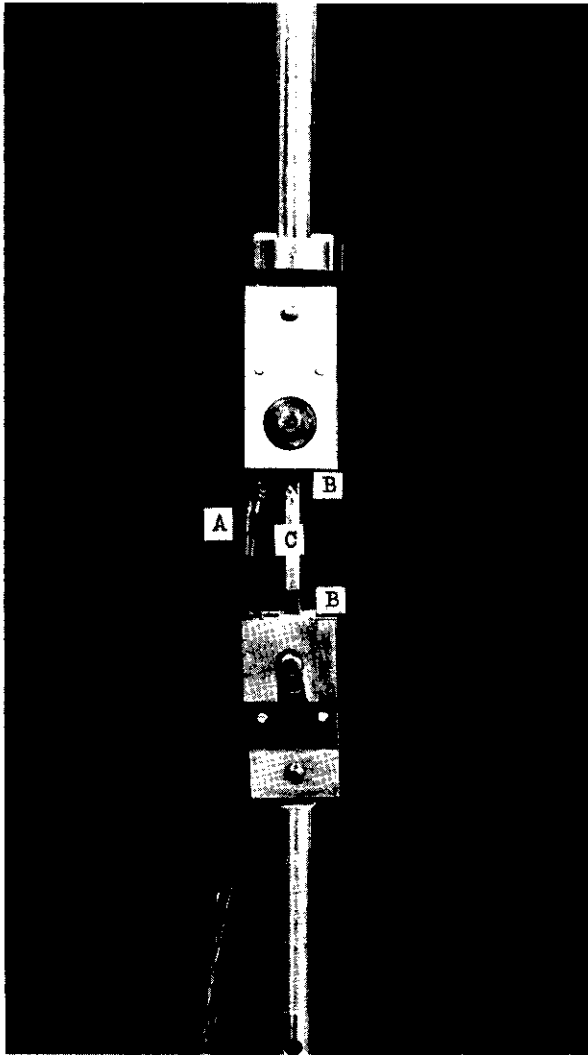


FIG. 13. GRIPS AND PULL-RODS FOR LOW-TEMPERATURE TENSILE TESTS, SHOWING (A) CONTROL THERMOCOUPLE, (B) MEASURING THERMOCOUPLES, AND (C) PROTECTIVE WRAPPING OF SARAN PLASTIC.

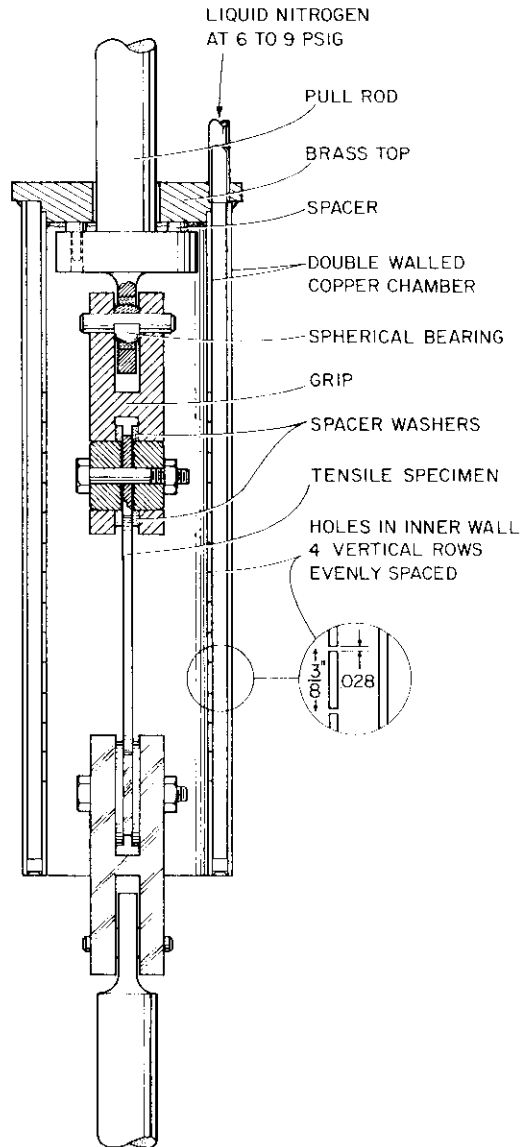


FIG. 14. LOW TEMPERATURE TENSILE TEST APPARATUS.

The test temperature of -196 C was attained by simply letting the solenoid valve remain open during the test and allowing liquid nitrogen to spray the specimen continuously.

Prior to each test at -190 C or above, the temperature was lowered to the desired level and held for about 20 minutes, during which time it was controlled automatically. The specimen was then either strained continuously to fracture or strained and unloaded repeatedly

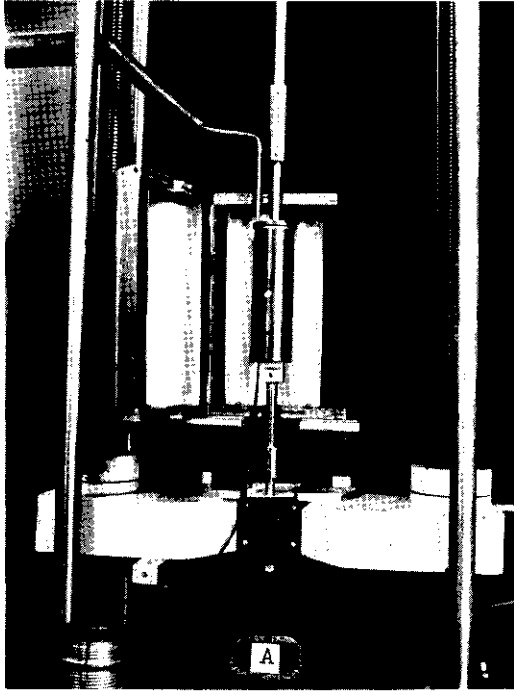


FIG. 15. COOLING CHAMBER FOR LOW TEMPERATURE TESTS. (A) IS A FOUR-POUND WEIGHT USED TO MAINTAIN ALIGNMENT DURING COOLING.

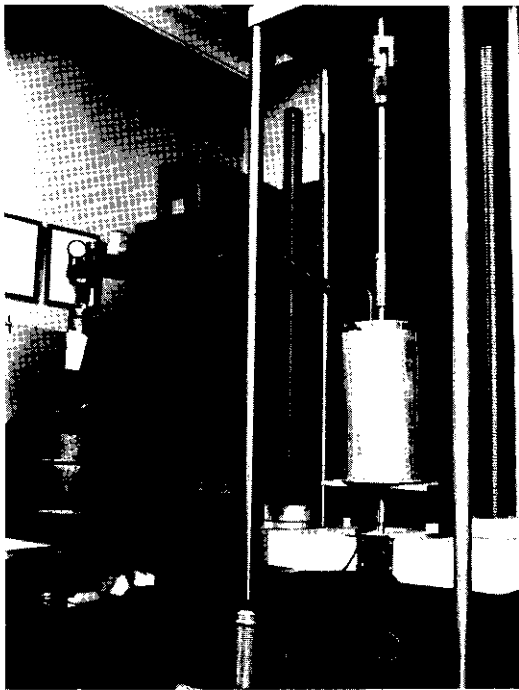


FIG. 16. LIQUID-NITROGEN TRANSFER APPARATUS.

to fracture. The later procedure was used for the surface-replication experiments which are described in the next section.

The values for upper and lower yield stress and 0.2 percent offset stress were calculated using the original cross-section area as measured with a micrometer which could be read to 0.0001 inch. The values of fracture stress were calculated using the actual cross-section area at the fracture. For the specimens which failed by cleavage with little or no necking, this area was measured with the micrometer under a stereoscopic microscope. For the specimens which necked and failed in a fibrous manner, this method was not accurate, so the fracture surfaces were photographed for area measurements with a planimeter. This method was accurate to within a few percent. The relative amounts of fibrous and cleavage fracture on the fracture surfaces were estimated under a stereoscopic microscope at magnifications up to 54X. In the temperature regions of nearly complete fibrous fracture, this determination was accurate to within a few percent, due to the ease of observing a cleavage facet in a fibrous background. In the transition region, the accuracy was probably ± 10 percent. In the region of nearly 100 percent cleavage fracture, the presence of a small amount of intergranular fracture may go undetected at the low magnifications used with the stereoscopic microscope; accordingly, spot checks were made with a standard microscope at magnifications up to 500X.

Metallographic Studies

Surface Replication

In order to record the microscopic details of deformation at low temperatures, interrupted tensile tests were carried out in which the specimens were loaded to a specified strain and unloaded. After unloading the specimens were warmed to room temperature and both sides of the gauge section were replicated on a plastic film; the specimen was then re-cooled to the test temperature and strained further. This process was repeated until the specimen fractured. The history of microcracks, twins, slip bands and other evidence of deformation observed on the fractured specimen could then be traced back through the series of replicas. In this way the origin of many microcracks could be observed directly.

The replication technique is diagrammed in Figure 17 and is a modification of a process developed by Young and Marsh^{13,2}. A 3 mil strip of cellulose acetate (2 3/4 by 5/8 inch) is attached at one end to the specimen by means of masking tape; a drop of acetone is applied at the juncture of the strip and specimen, and is immediately squeezed out along the strip-specimen interface by running a finger down the strip, as shown. A light pressure is applied for 1 to 2 minutes, after which the replica is peeled off and mounted on a glass microscope slide with double-coated cellulose tape (Scotch brand pressure sensitive tape no. 666). The sides and ends of the replica are then fastened to the tape and slide with extra pieces of standard cellulose tape to prevent curling. Following this, about 10 mg. of aluminum is evaporated onto the slide at normal incidence from a distance of about 10 cm. in a standard evaporator in a vacuum of 0.5 microns of mercury or less. The aluminum is "flashed" on in 5 to 10 second bursts to avoid burning the replica. The purpose of the aluminum is to provide reflectivity and contrast.

The tensile specimen gripping and pulling apparatus and the cooling chamber were specifically designed to facilitate the rapid removal and replacement of the specimen during the interrupted tests. After any particular

strain increment, the specimen, with grips and pull-rods attached, was hung in a room temperature water bath for 3 minutes. After it became warm enough to handle, the specimen was removed from the grips, dried with alcohol and a cool air blast and replicated. The time interval during which the specimen was at room temperature for the replication process was usually 20 to 22 minutes and never more than 30 minutes. Preliminary tensile tests were carried out to determine the effects of this room temperature aging treatment on the subsequent behavior of the specimens, and they will be described later.

The replicas were examined under the light microscope at magnifications up to 1000X and photomicrographs were made with a 35 mm camera attached to the microscope. The glass slides were set into a thin plexiglass sheet to which was attached a strip of rectangular coordinate graph paper, to aid in the location of any desired area under the microscope. In the F4 ferrite, a pearlite patch could usually be found on each side to serve as a reference mark; in F5 a Vickers hardness indentation (applied with a 100 gm. load) was made at each end of the gauge section on both sides for this purpose.

Surface-replication studies were made on F4 samples tested at -190, -180, -140, and -90 C, and on an F5 sample tested at -180 C.

Counting of Microcracks and Twins

The number of microcracks which appeared on the broad face of a tensile specimen was determined by means of a standard bench microscope with a movable stage. The specimen was traversed at a magnification of 200X in overlapping steps, so that the entire gauge section was examined. Magnifications of 500X and 1000X were available to resolve any uncertainties. Almost all specimens were counted twice, so the values reported are felt to be quite reliable. The microcrack count was expressed as the number of microcracks per 10,000 grains. If we make the approximation that the grain sections are circular with an average diameter equal to the mean distance between grain boundaries, then there are about 10,000 grains on one side of a very coarse grained F4 specimen and about 20,000 on one side of a coarse grained F5 specimen.

The amount of twinning which occurred in a

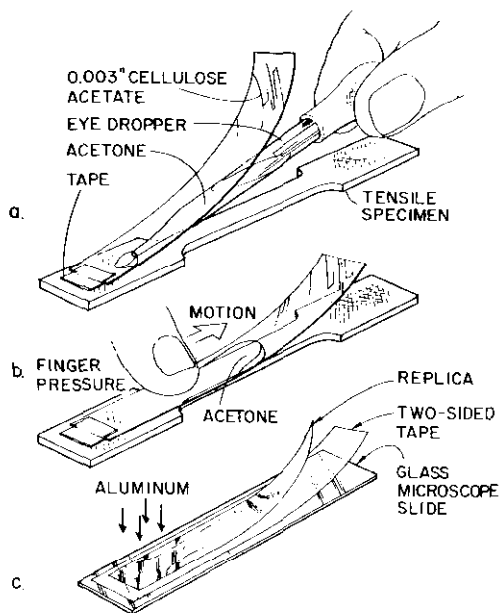


FIG. 17. REPLICATION TECHNIQUE.

specimen was measured by counting the number of grains with and without twins along a straight traverse of about 1 inch. The amount of twinning was expressed as the percentage of grains containing twins. The twin counting was done after the specimen surface had been smoothed by grinding and had been re-electropolished and etched. This was necessary since, on the original as-deformed surface, it was often impossible to distinguish twins from slip lines.

Specimen Sectioning

Two specimens of F4 ferrite and one of F5, which were tested in the temperature range -140 to -180 C, were mounted in a self-setting plastic (Quickmount) and ground parallel to the broad surface in increments of 1 mil to examine the microcracks three-dimensionally. The grinding was done with 600A grit silicon carbide paper, and after each increment of material removal, the specimens were polished on diamond-paste impregnated cloth wheels, etched lightly with 1 percent nital, and examined metallographically. In this way the origins of many cracks were determined in cases where observations made on the original surface gave insufficient information. The grinding and polishing steps were repeated until all cracks origins had been determined or until the cracks had disappeared; this ordinarily required that about 10 layers be removed.

RESULTS

Tensile Properties of F4 and F5 Ferrite

The results of tensile tests carried out on F4 ferrite in the very coarse-grained (0.29 to 0.40 mm) and moderately coarse-grained (0.13 to 0.17 mm) condition and on F5 ferrite in a coarse-grained (0.23 to 0.28 mm) condition are summarized in Figures 18 through 27.

Figures 18 and 19 show the effect of decreasing test temperature on the load-elongation curves of very coarse-grained (VCG) F4 and coarse-grained (CC) F5, respectively. These curves were traced from the chart of the autographic recorder and are not corrected for the elastic extension of the tensile machine. This correction was ignored to preserve the details of the yielding stage.

With lowering of the test temperature, the percent elongation decreases and necking

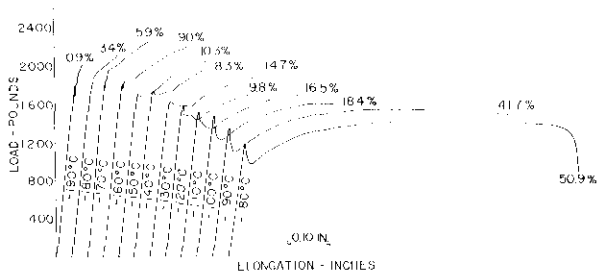


FIG. 18. LOAD-ELONGATION CURVES FOR F4 SPECIMENS 0.29 TO 0.40 MM GRAIN SIZE AS-TRACED FROM AUTO GRAPHIC RECORD. PER CENT TOTAL ELONGATION SPECIFIED.

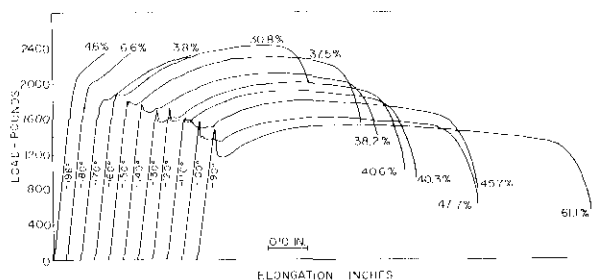


FIG. 19. LOAD-ELONGATION CURVES FOR F5 SPECIMENS 0.23 TO 0.28MM GRAIN SIZE AS-TRACED FROM AUTO GRAPHIC RECORD. PER CENT TOTAL ELONGATION SPECIFIED.

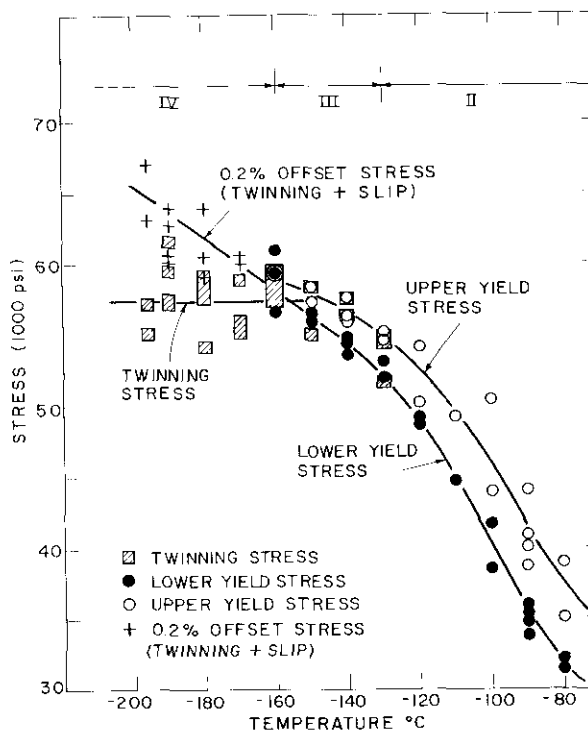


FIG. 20. LOW-TEMPERATURE YIELDING BEHAVIOR OF F4 FERRITE WITH VERY COARSE GRAIN SIZE (0.29 TO 0.40MM).

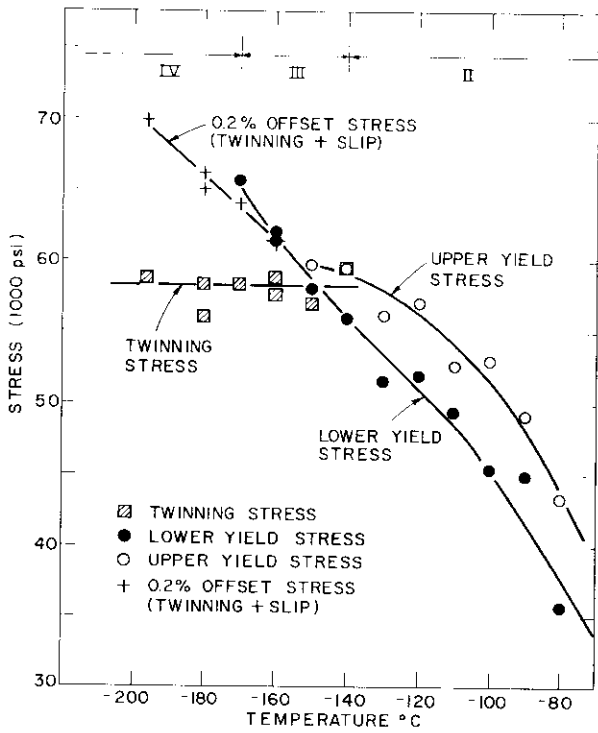


FIG. 21. LOW-TEMPERATURE YIELDING BEHAVIOR OF F5 FERRITE WITH 0.23 TO 0.28MM GRAIN SIZE.

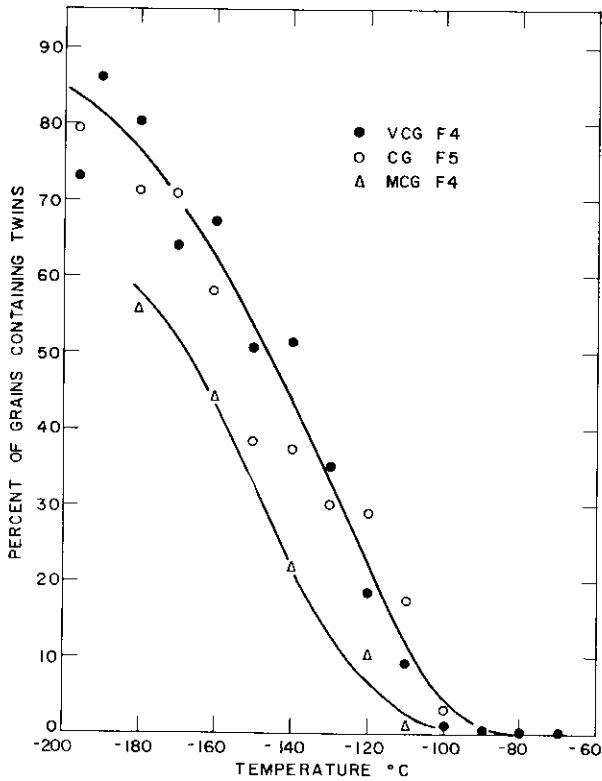


FIG. 22. INFLUENCE OF TEST TEMPERATURE AND GRAIN SIZE ON THE AMOUNT OF TWINNING IN FRACTURED FERRITE SPECIMENS.

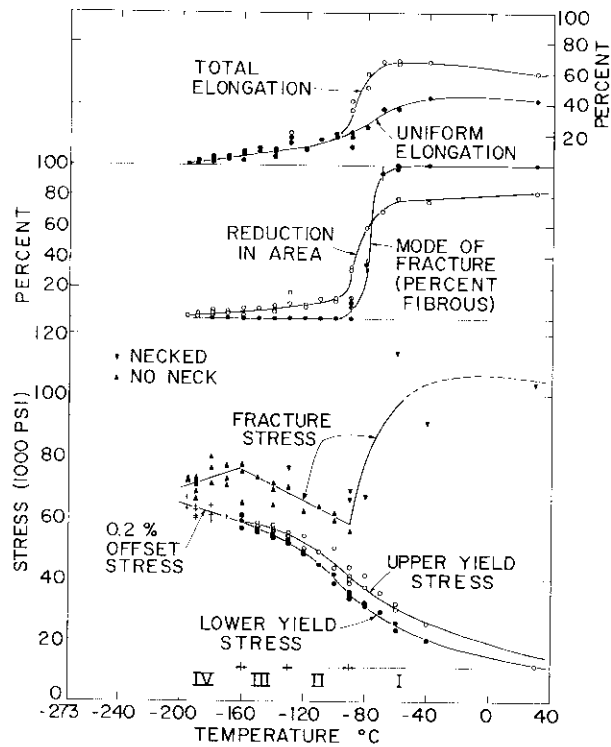


FIG. 23. TENSILE PROPERTIES OF F4 FERRITE-0.29 TO 0.40 MM GRAIN SIZE.

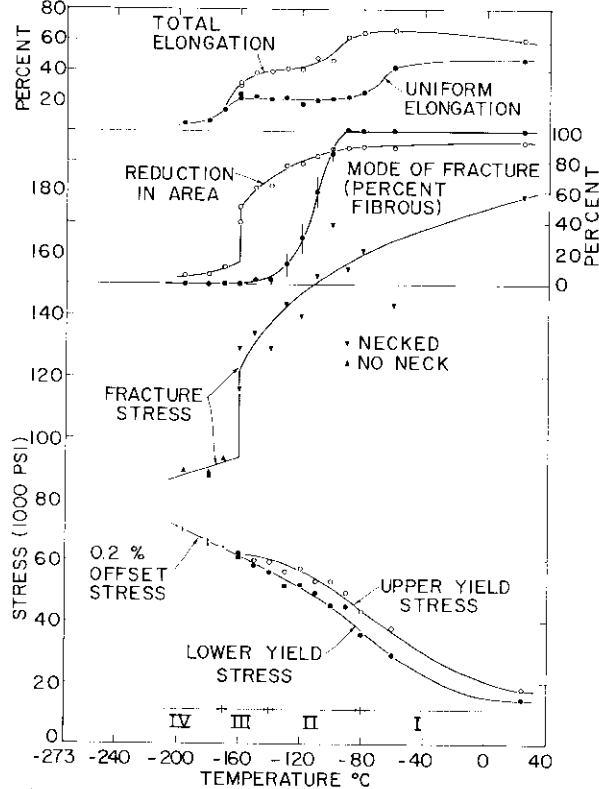


FIG. 24. TENSILE PROPERTIES OF F5 FERRITE-0.23 TO 0.28 MM GRAIN SIZE.

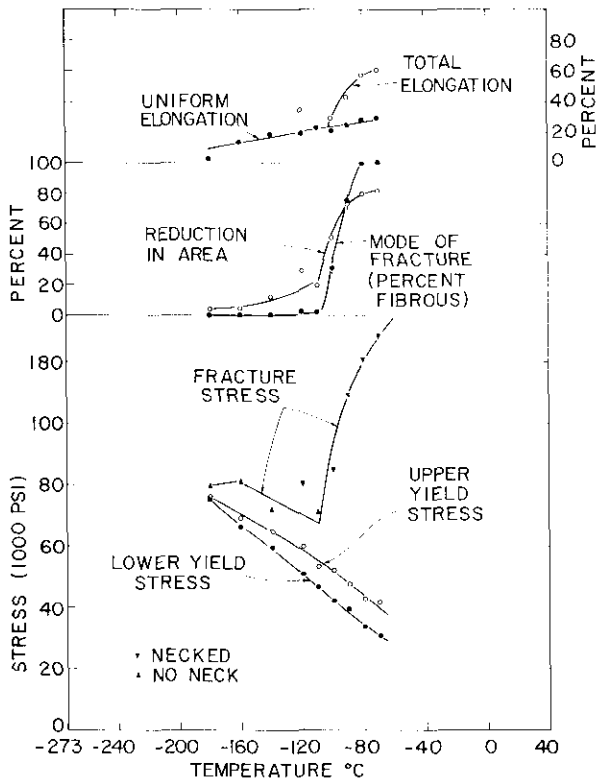


FIG. 25. TENSILE PROPERTIES OF F4 FERRITE-0.13 TO 0.17 MM GRAIN SIZE.

before fracture disappears. At the lower temperatures, mechanical twinning, punctuated by audible clicks, occurs and produces a marked effect on the yielding process. This effect is characterized by a gradual elimination of discontinuous yielding. The upper yield point is the first to disappear; the lower yield point vanishes at a lower temperature. Figures 20 and 21 show the details of the low temperature yielding behavior of VCG F4 and CG F5, and Figure 22 illustrates the increased amount of twinning with decreasing temperature in all three series of specimens. The twinning behavior of VCG F4 and CG F5 is essentially the same, whereas the twinning curve for moderately coarse-grained (MCG) F4 starts at a slightly lower temperature and remains lower than, but parallel to, the curve for the other two series. Grain size appears to be the most important variable, aside from temperature, controlling twinning. In all cases, this twinning takes place mainly within the first few percent of elongation. A complete representation of the tensile properties of the three materials in the temperature range of room temperature to -196°C is contained in Figures 23,

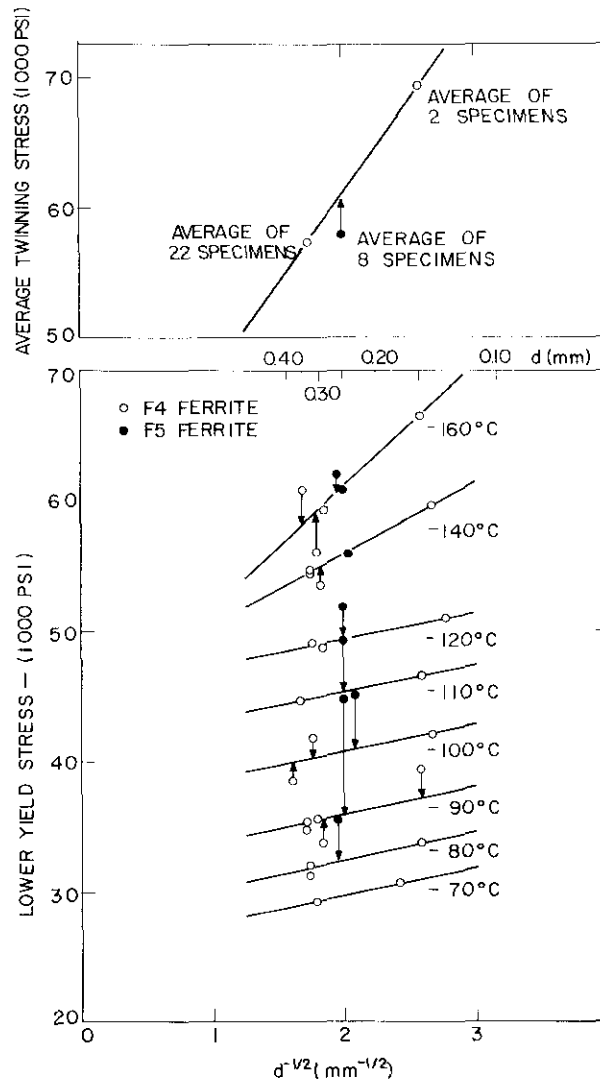


FIG. 26. DEPENDENCE OF LOWER YIELD STRESS AT VARIOUS TEMPERATURES AND OF AVERAGE TWINNING STRESS UPON GRAIN SIZE.

24 and 25.

Yielding Behavior

The effect of temperature on the yielding behavior can be summarized as follows:

In region I (Figures 23 and 24) yielding is discontinuous and takes place entirely by slip. No twins are found in specimens tested in this temperature region.

In region II, which starts at -90°C for VCG F4 and at -80°C for CG F5, twinning follows the onset of discontinuous yielding. Clicks are heard just after the upper yield point and

they die out during the lower yield extension. The number of grains containing twins increases as the temperature is lowered in this region.

Region III starts at about -130°C for VCG F4 and -140°C for CG F5. Here, the onset of twinning and discontinuous yielding occur almost simultaneously at the high end of this temperature range, but as the test temperature is lowered, twinning precedes the upper yield point. In the latter cases, a sudden offset or load-drop is seen at the end of the elastic portion of the load-elongation curve, and this is always accompanied by a loud click. At the lower end of this temperature region, the upper yield point is completely eliminated.

In region IV, which starts at about -160°C for VCG F4 and -170°C for CG F5, yielding is no longer discontinuous but is initiated by twinning and progresses by a series of short, audible load drops. In this region, the yield stress at 0.2 percent plastic elongation. The specimens undergo strain-hardening to this stress level by a mixture of slip and twinning.*

The stress at which the first audible load-drop or offset occurs in regions IV and III is taken to be the twinning stress. It can be seen from Figures 20 and 21 that the twinning stress is essentially independent of temperature. The line plotted as the twinning stress is the average value. The scatter about this average is comparable to the scatter observed in values of the upper yield stress at higher temperatures. This behavior is to be expected, since both the onset of twinning and discontinuous yielding should be quite sensitive to localized stress concentrations. Such concentrations could arise from deviations from perfectly uniaxial loading or from slight variations in the shape of the specimen should-

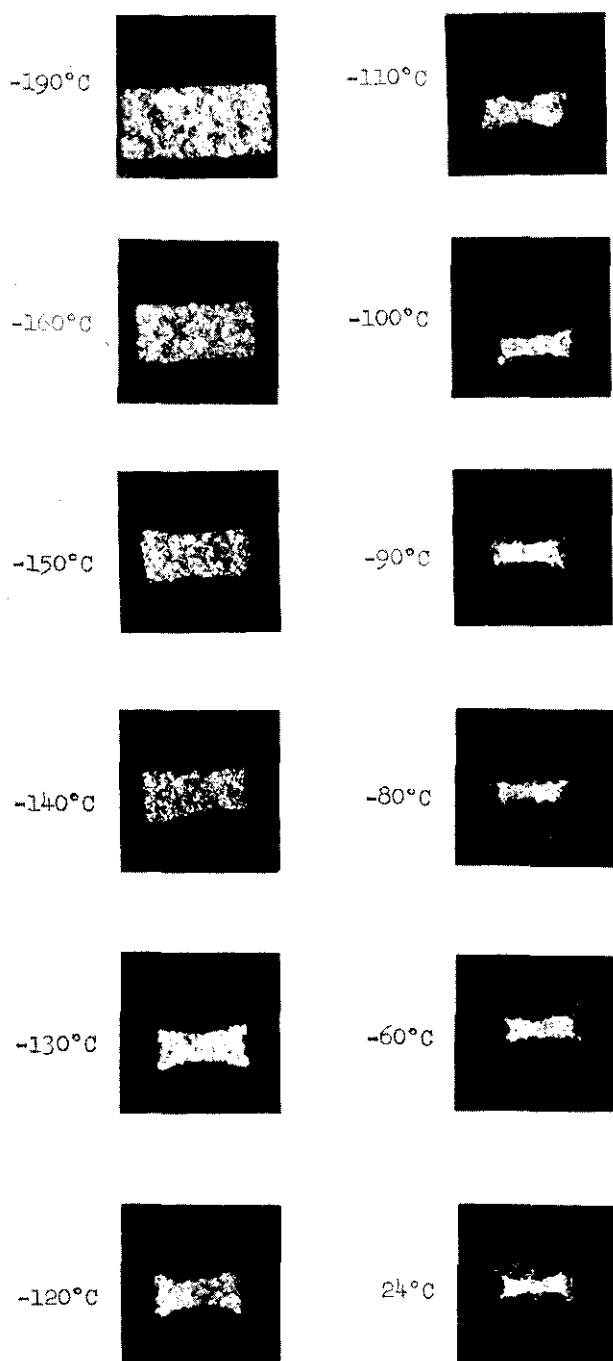


FIG. 27. THE CHANGE IN SHAPE OF THE FRACTURE AREA WITH INCREASING TEST TEMPERATURE. 3X

* The elimination of discontinuous yielding by the advent of twinning at low temperatures has been previously observed in mild steel by Erickson and Low⁷³.

ders or surface smoothness. In addition, there will be a statistical fluctuation of the orientation and size of the grain, or group of grains, most suitably situated to commence the yielding process.

In specimens which are unloaded after the first burst of twinning and examined under the microscope, almost the entire gauge section is found to contain twinned grains. In these specimens, twins which are stopped by grain boundaries often initiate twins in the neighboring grains. This can cause a chain reaction occurring over large distances. From these observations we can conclude that twinning is autocatalytic, that is, twinning, once triggered, provides the stress concentrations required for further propagation.

The lower yield stress and twinning stress of VCG F4, MCG F4 and CG F5 are plotted as a function of $d^{-1/2}$ in Figure 26. Since the range of grain sizes investigated is extremely limited for this type of plot, the resulting information is only indicative; however the following three points should be noted.

- (i) The lower yield stress of the F5 is, in nearly all cases, higher than would be expected for F4 specimens of the same grain size. Inasmuch as the F4 contains five times as much carbon as F5, this may appear curious at first glance. However, it has been shown³² that the presence of excess carbides will promote the precipitation of carbon during quenching of iron specimens, and that the rate of precipitation of carbon during quenching increases as the inter-carbide spacing decreases. Therefore, it is not unlikely that in the present materials, which are cooled from the austenitizing temperature at approximately the same rate, the F5 ferrite would retain more carbon in solid solution at room temperature, and thus should have a higher yield stress than F4.
- (ii) The twinning stress increases much more rapidly with decreasing grain size than does the lower yield stress. This phenomenon is commonly observed in b.c.c. metals. The average twinning stress of the F5 ferrite is lower than expected from grain size considerations alone. The reason for this is unclear.

- (iii) The VCG F4 specimens tested at -140 C and -160 C appear to have lower yield stresses that are anomalously low. It would seem that the twinning, which occurs during the lower yield extension, provides some of the stress concentration needed for the propagation of slip at the Lüders front, and that the applied stress required is thereby reduced.

Fracture Behavior

The transition from ductile to brittle behavior for the three groups of specimens is shown in Figures 23, 24 and 25. This transition is characterized by a shift from high stress level fracture in necked specimens to fracture without necking at lower stress levels. The curve of percent reduction in area at the fracture closely parallels the fracture stress curve in the ductile region. The mode of fracture changes from completely fibrous in the ductile region to completely cleavage in the brittle region by going through a stage of mixed fibrous and cleavage.

The transition temperature (Table III) of

TABLE III. TRANSITION TEMPERATURES

Material	Grain Size (mm)	Transition Temperature (°C)
F4	0.29 to 0.40	-90
F4	0.13 to 0.17	-110
F5	0.23 to 0.28	-160

VCG F4 is about -90 C and that of CG F5 is about -160 C. This large difference cannot be accounted for by the smaller grain size of F5, since the transition temperature of CG F4, which has an even smaller grain size, is only about -110 C. The two materials differed significantly in the amount of iron carbide which they contain. It will be seen in a later section that this factor provides an explanation for the observed differences in fracture properties.

The fracture stresses reported for the necked specimens are the load at fracture divided by the cross-sectional area of the fracture. This value is not the true flow stress at fracture (because the state of stress

in the neck is triaxial) but rather it represents only the average tensile stress across the fracture area. Therefore, it lacks the more fundamental significance that can be attached to the cleavage stress of unnecked specimens, which is a true flow stress.

There is no correction available for flat specimens, similar to the Bridgman correction for round specimens, which would enable one to calculate the true flow stress in the neck. Such a correction would be very sensitive to the width-to-thickness ratio and would be much more complex than the simple case of round specimens which neck symmetrically. Figure 27 shows the shapes of fracture cross sections found in the MCG F5 specimens. These are typical of the other series of specimens.

The fracture in the transition region in flat specimens is different from that in round specimens. In the latter, a fibrous void opens in the center of the neck and converts to a rim of cleavage as it grows in diameter^{5,11}. In the flat specimens, a fibrous tear usually starts at an edge or corner and converts to cleavage as it progresses across the specimen. This tear is sometimes initiated at the surface by a large cleavage microcrack which formed earlier and then opened up during the subsequent straining.

Microcrack Studies on Fractured Specimens

The number of microcracks which appeared on the broad surfaces of the VCG F4 specimens was relatively easy to determine, due mainly to the large grain size. On the other hand, in the CG F5 specimens, the finer grain size and the greater ductility at low temperature (which increased the distortion of the surface) served to make microcrack counting more difficult and less reliable. Hence, observations were also made on repolished surfaces as follows: About 2 mils were removed from both sides of the specimens by grinding on silicon carbide paper. The specimens were then electro-polished for 4 minutes (which removed less than 1 mil) and lightly etched. It was found that the number of microcracks visible after surface material had been removed was always larger than the number on the original surface. The reason for such differences will be discussed later. Every effort was made to ensure that a constant thickness was removed so that the numbers of cracks reported are self-

consistent.

Figures 28 and 29 show the numbers of cracks as a function of test temperature for the

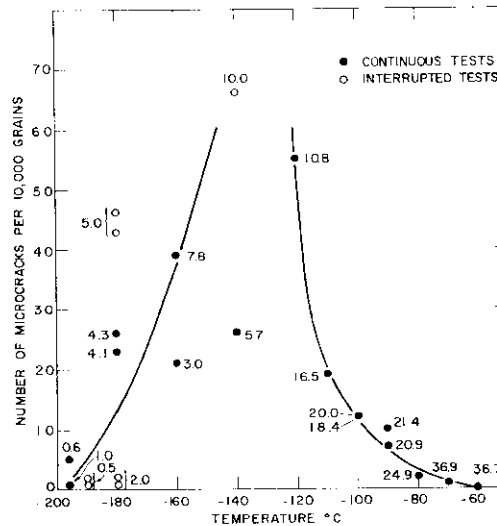


FIG. 28. INFLUENCE OF TEST TEMPERATURE ON THE NUMBER OF MICROCRACKS ON THE SURFACE OF FRACTURED VCG F4 TENSILE SPECIMENS. NUMBERS NEXT TO POINTS REFER TO PERCENT UNIFORM ELONGATION.

F4 and F5 specimens, respectively. Figure 30 indicates how these curves relate to the tensile properties of the two materials. Figures 31 and 32 relate the numbers of cracks to the uniform elongation of the fractured specimens. In the curves for the F4 specimens, the data obtained from the interrupted tests, which will be described later, are included for comparison.

It can be seen that the curves for number of cracks versus temperature and strain go through maxima. These maxima occur at the transition temperature for F5 specimens and at about 30 C below the transition temperature for F4. On the low temperature side of the maximum, the number of microcracks is more closely related to the strain at fracture than it is to the test temperature.

The angles which the surface traces of microcracks made with the tensile axis were measured from photographs. In both F4 and F5 specimens there is a strong tendency for

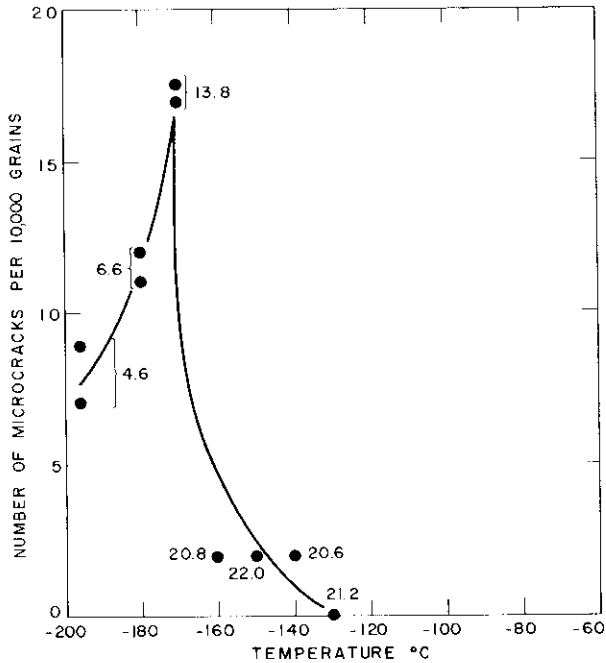


FIG. 29. INFLUENCE OF TEST TEMPERATURE ON THE NUMBER OF MICROCRACKS ON THE REPOLISHED SURFACE OF FRACTURED CG F5 TENSILE SPECIMENS. NUMBERS NEXT TO POINTS REFER TO PERCENT UNIFORM ELONGATION.

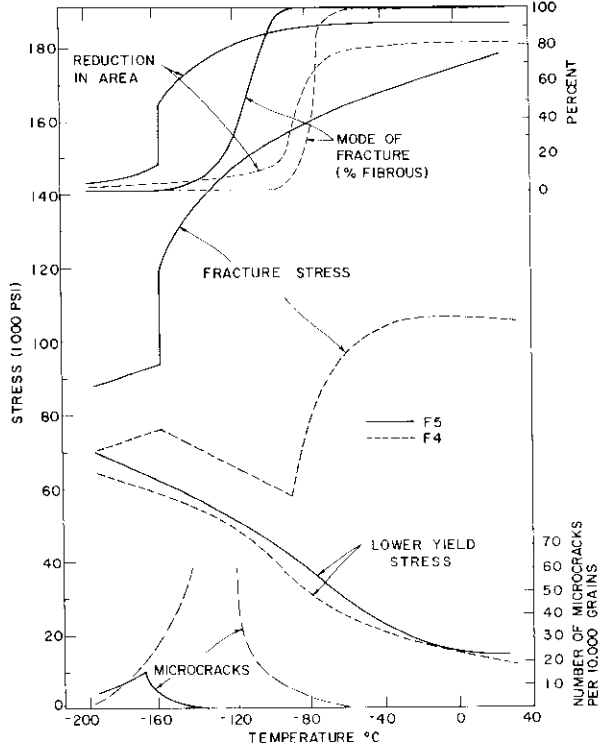


FIG. 30. COMPARISON OF TENSILE PROPERTIES AND MICROCRACKING TENDENCY OF VCG F4 AND CG F5 SPECIMENS.

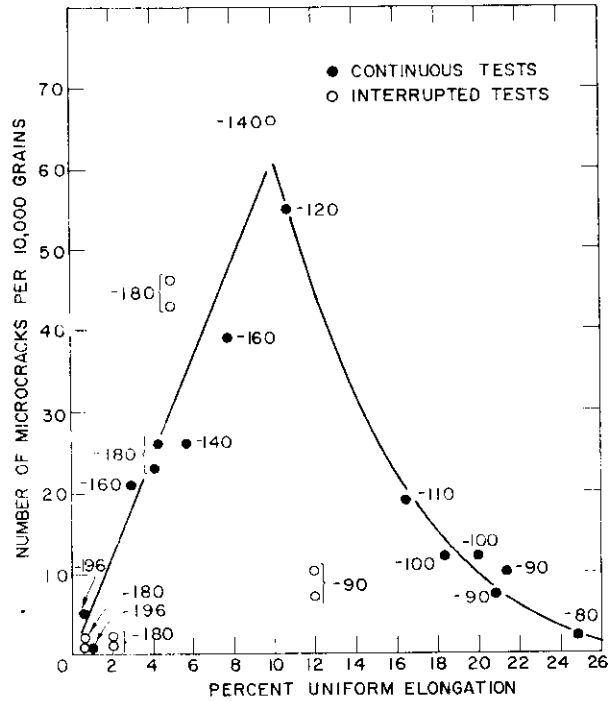


FIG. 31. INFLUENCE OF THE AMOUNT OF UNIFORM ELONGATION ON THE NUMBER OF MICROCRACKS ON THE SURFACE OF FRACTURED VCG F4 TENSILE SPECIMENS. NUMBERS NEXT TO POINTS REFER TO TEST TEMPERATURE.

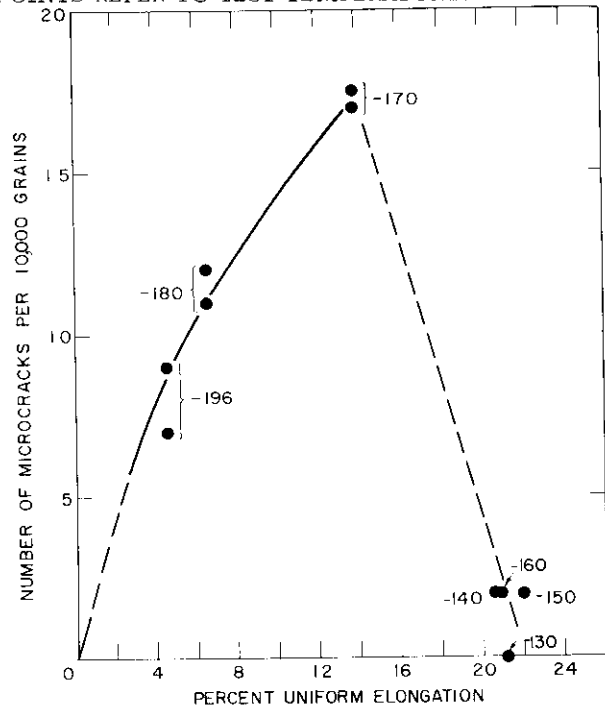


FIG. 32. INFLUENCE OF THE AMOUNT OF UNIFORM ELONGATION ON THE NUMBER OF MICROCRACKS ON THE REPOLISHED SURFACE OF FRACTURED CG F5 TENSILE SPECIMENS. NUMBERS NEXT TO POINTS REFER TO TEST TEMPERATURE.

the cracks to lie perpendicular to the tensile axis. An example of this is shown in Figure 33 in which 88 percent of the cracks lie within 20° of the plane normal to the tensile axis. This behavior was observed by Hahn⁶⁵ in microcrack studies in iron and mild steel, and it illustrates the importance of the normal stress in microcrack formation.

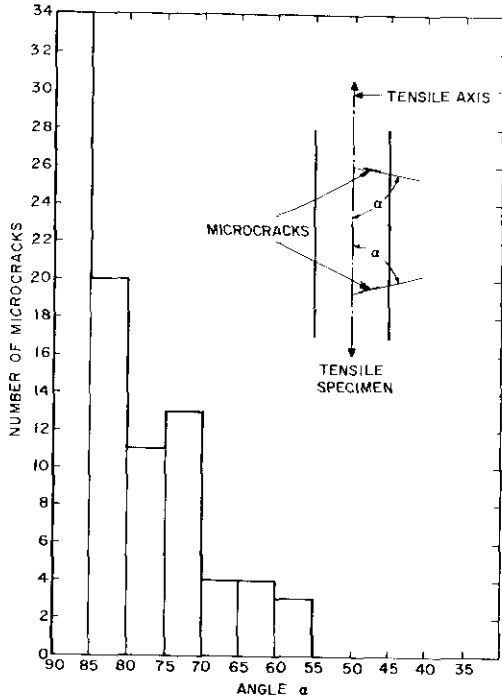


FIG. 33. FREQUENCY DISTRIBUTION OF ORIENTATIONS OF MICROCRACKS ON THE SURFACE OF AN F4 TENSILE SPECIMEN FRACTURED AT -180C WITH 5% PLASTIC ELONGATION.

It is found that the iron-carbide particles in the fractured F4 and the F5 specimens are severely fragmented. This cracking occurs in specimens tested at room temperatures but is more abundant at lower temperatures where the ferrite matrix has a higher flow stress. Examples of cracks in grain boundary carbides are shown in Figure 34*.

Some of the carbide cracks act as the source of cleavage microcracks in the ferrite. Figure 35 contains examples of some of the shorter microcracks formed in this manner which appear both on and beneath the surface of F4 and F5 specimens. The pearlite which is sparsely distributed throughout the F4 specimens also contains cracks, which start in the carbide envelopes around the pearlite patches. Figure 36(a) shows a ferrite microcrack which started in a pearlite patch, and Figure 36(b) shows a crack which is apparently contained entirely in the pearlite.

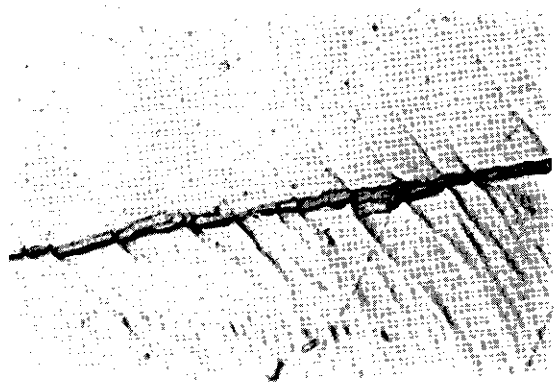
Unloading Effects in Interrupted Tensile Tests

Before proceeding with the interrupted tensile tests and replication studies, it was necessary to determine the effects of unloading and room temperature aging during the test. For this purpose, F4 specimens which had been prepared in the early stages of the program were used. These had been austenitized at 915 C for 1/2 hour and furnace cooled, and had a grain size of about 0.1 mm. They were tested at -170 C, with variations in the extent of unloading, temperature of aging, and the strain from which the unloading was carried out. The results are given in Figures 37 through 40.

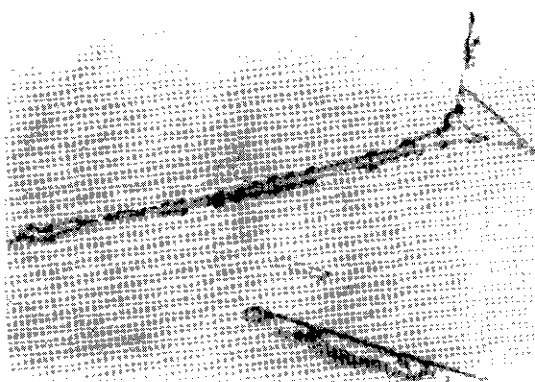
The stress-strain curve of a reloaded specimen follows the extension of the curve for the previous strain increment, except for a small yield effect. Figure 37 illustrates the yield effect which occurred after unloading completely after 7.4 percent elongation and aging 30 minutes at room temperature. A specimen completely unloaded after 6.5 percent elongation and aged 30 minutes at -170 C exhibits a similar, though smaller, effect (Figure 38). Figure 39 indicates that complete unloading after 12 percent elongation and aging only one minute at -170 C reproduces the effect obtained by previously unloading with less strain and aging 35 minutes at room temperature. This would not be expected if the effects were caused by the long-range diffusion of interstitials (strain aging). Figure 40 shows that the effect practically disappears when the specimen is only partly unloaded and then reloaded.

* In this work, the tensile axis is parallel to the long dimension of the photomicrographs, unless otherwise noted.

This type of yield effect has been observed in f.c.c. single crystals⁸⁴⁻⁸⁵ and in low carbon steel⁸⁶. It has been attributed to dislo-



(a) - VCG F4, -120°C, 10.8%,



(b) - CG F5, -170°C, 13.8%,



(c) - VCG F4, -120°C, 10.8%,



(d) - VCG F4, -180°C, 4.3%,

FIG. 34. EXAMPLES OF CRACKED GRAIN BOUNDARY CARBIDES IN FRACTURE F4 AND F5 SPECIMENS. TEST TEMPERATURE AND ELONGATION ARE INDICATED. 445X

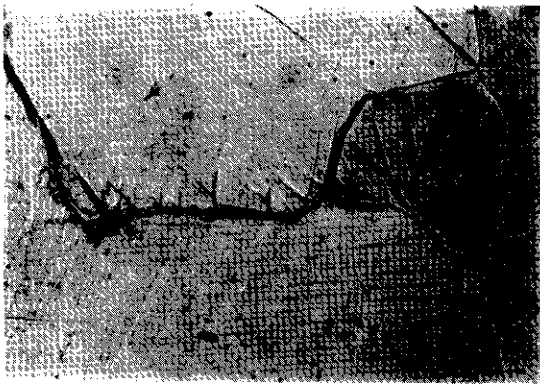
cation rearrangements during unloading¹¹⁷ in the f.c.c. crystals and to stress-induced ordering of interstitials in the stress fields of dislocations in the steel¹¹⁸. Whatever the cause, the effect cannot be avoided if a specimen is to be fully unloaded, but it apparently has little to do with the strain-aging phenomenon which involves the long-range diffusion of solute atoms to dislocations. While the coincidence of the stress-strain curves of the continuous and interrupted tensile tests is not exact, it is felt to be close enough for the present purpose.

Surface-Replication Studies

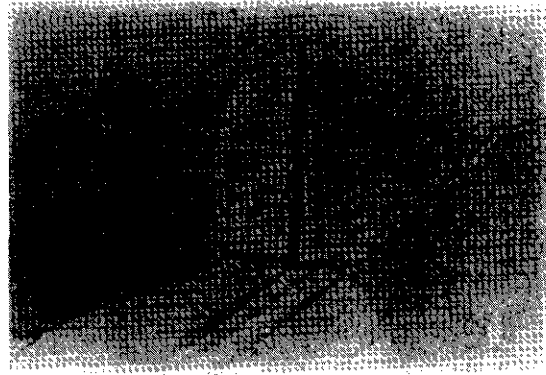
The stress-strain curves of the interrupted tensile tests which were carried out in conjunction with the surface-replication studies

are shown in Figures 41 through 45. Curves from continuous tests are included for comparison. These experiments were performed on VCG F4 specimens at -190, -180, -140 and -90 C and on a CG F5 specimen at -180 C. Figures 46 and 47 give the positions of the cracks observed on the F4 specimens tested at -180 and -140 C.

These results show that most microcracks form during the strain-hardening portion of the stress-strain curve and that new cracks continue to form right up to the moment of fracture. The F4 specimens tested at -90 and -140 C exhibit discontinuous yielding. No cracks are found upon unloading during the drop-in-load, and very few if any are present at the end of the Lüders strain.



(a) - VCG F4, -120°C, 10.8%,



(b) - VCG F4, -180°C, 5.0%,

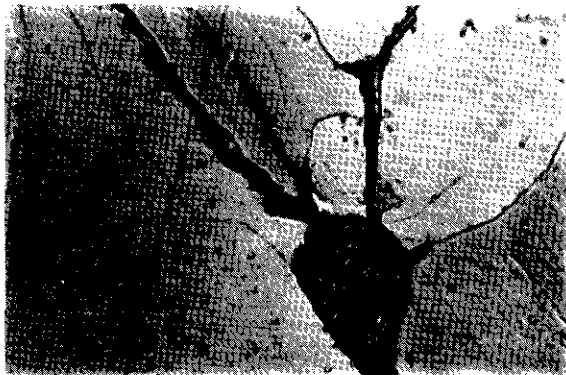


(c) - CG F5, -170°C, 13.8%,



(d) - CG F5, -170°C, 13.8%,

FIG. 35. EXAMPLES OF CLEAVAGE MICROCRACKS ORIGINATING AT CRACKED GRAIN BOUNDARY CARBIDES IN FRACTURED F4 AND F5 SPECIMENS. (b), (c) AND (d) FROM REPOLISHED SPECIMENS. TEST TEMPERATURE AND ELONGATION ARE INDICATED. (a) 180X (b) 445X (c) 890X (d) 890X.



(a) - VCG F4, -160°C, 3.0%, 500X.



(b) - VCG F4, -180°C, 4.3%, 500X.

FIG. 36. EXAMPLES OF CRACKS CONNECTED WITH PEARLITE PATCHES IN FRACTURED VCG F4 SPECIMENS. TEST TEMPERATURE AND ELONGATION ARE INDICATED.

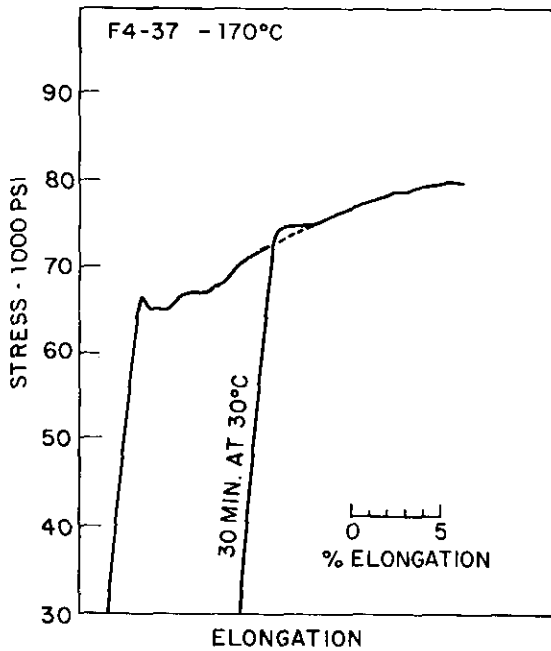


FIG. 37.

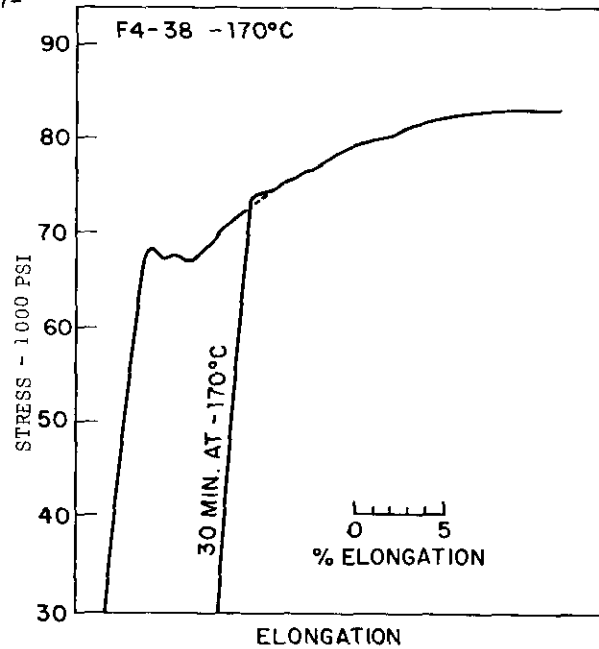


FIG. 38.

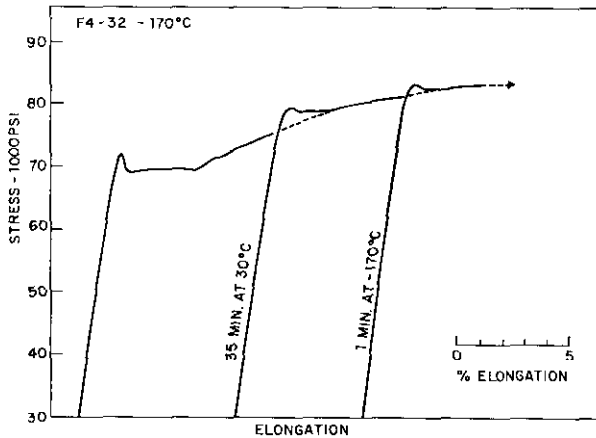


FIG. 39.

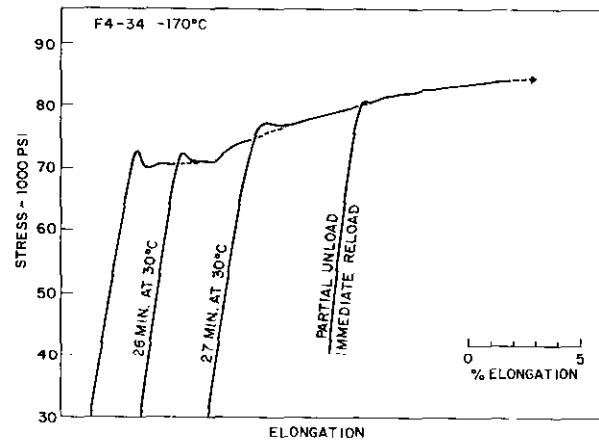


FIG. 40.

FIG. 37 through 40. STRESS-STRAIN CURVES OF INTERRUPTED TESTS ON F4 SPECIMENS AT -170°C SHOWING THE UNLOADING EFFECTS OBTAINED BY VARIOUS COMBINATIONS OF AGING TEMPERATURE AND TIME, EXTENT OF UNLOADING, AND STRAIN FROM WHICH SPECIMEN IS UNLOADED.

The increase in the total number of surface cracks with strain is shown in Figure 48 for the F4 specimens tested at -90, -140 and -180 C. The curve appears to level-off at about 10 percent elongation. This concurs with the observation of Hahn⁶⁶ that most microcracks in the iron and mild steel which he studied seemed to form during the first 10 percent strain. The upper curve in Figure 48 represents the microcrack formation behavior on the low temperature side of the maximum (Figure 28),

and the lower curve the behavior on the high temperature side.

It is apparent that microcrack formation is not connected with discontinuous yielding, per se, as would be required by the dislocation pile-up models of crack initiation. It would also seem that twinning is not a prime cause of crack initiation, at least in the temperature region above -180 C, since in these specimens most cracks are formed after twinning

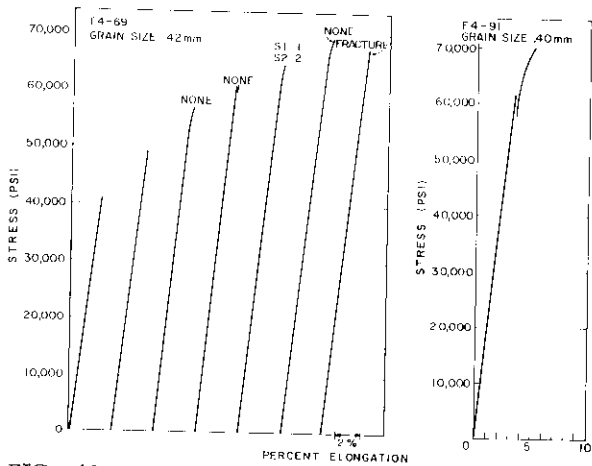


FIG. 41. F4 SPECIMENS AT -190C.

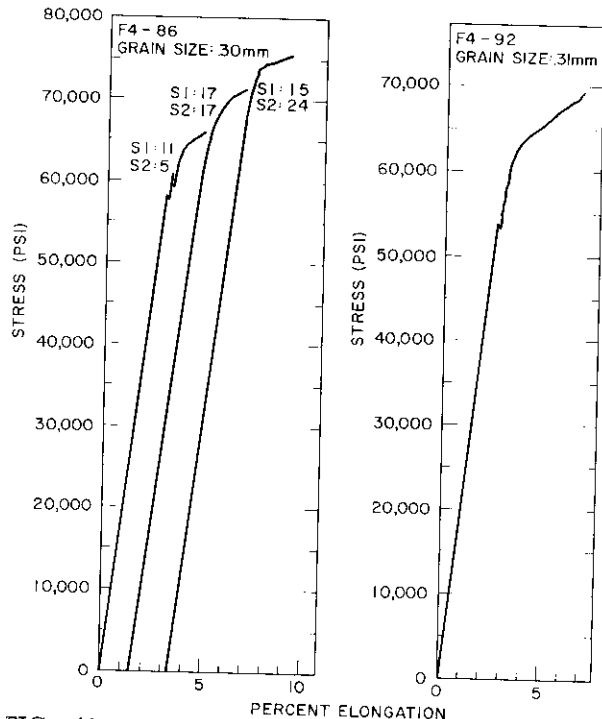


FIG. 42. F4 SPECIMENS AT -180 C.

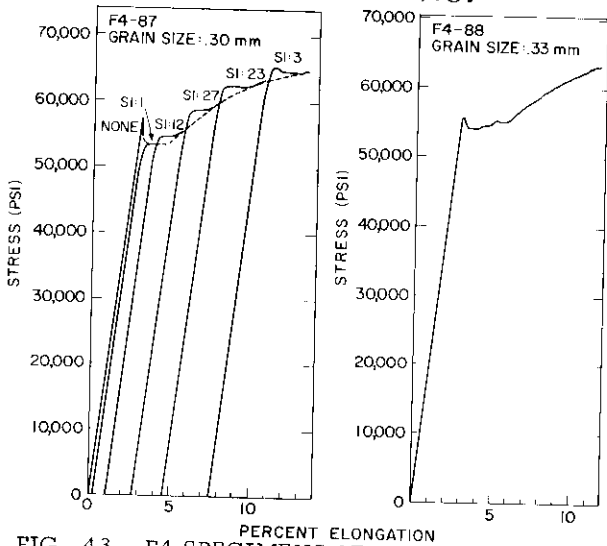


FIG. 43. F4 SPECIMENS AT -140 C.

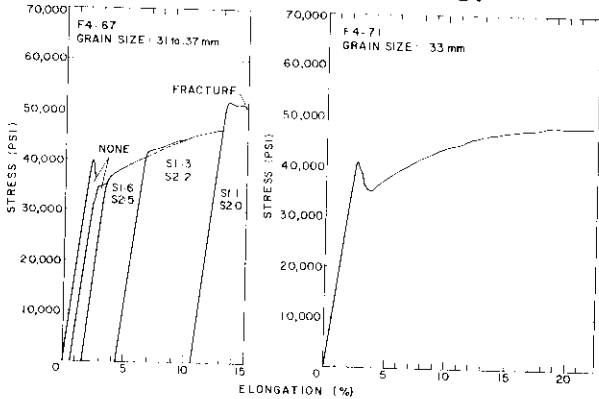


FIG. 44. F4 SPECIMENS AT -90 C.

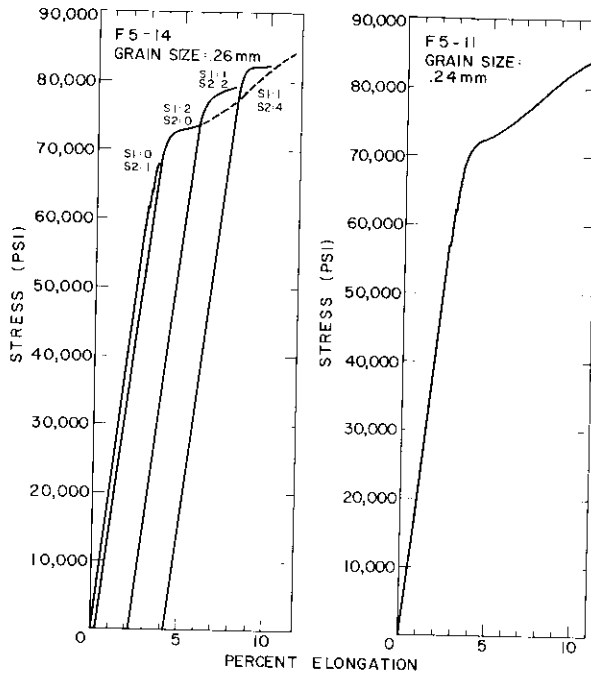


FIG. 45. F5 SPECIMENS AT -180 C.

FIGS. 41 through 45. STRESS-STRAIN CURVES OF INTERRUPTED AND CONTINUOUS TESTS ON F4 AND F5 TENSILE SPECIMENS AT VARIOUS TEMPERATURES. THE NUMBERS OF NEWLY FORMED MICROCRACKS OBSERVED ON EACH OF THE TWO SIDES (S1 AND S2) ARE SPECIFIED FOR EACH STRAIN INCREMENT. THE CURVES ARE TRACED FROM THE AUTOGRAPHIC RECORD AND ARE UNCORRECTED FOR THE ELASTIC EXTENSION IN THE MACHINE.

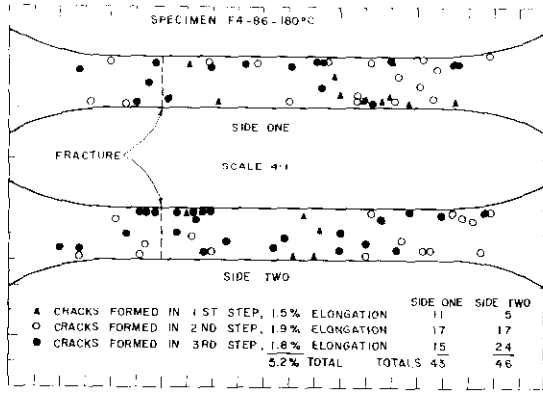


FIG. 46. OUTLINE OF F4 SPECIMEN TESTED AT -180 C SHOWING LOCATIONS OF SURFACE MICROCRACKS.

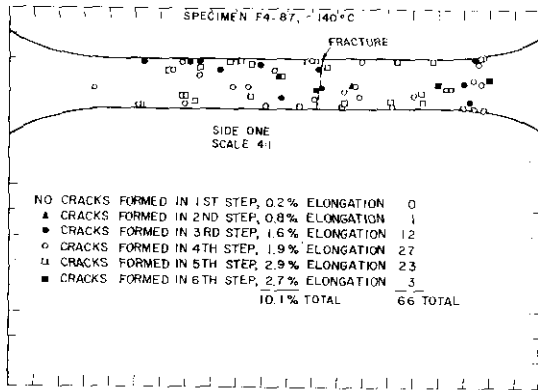


FIG. 47. OUTLINE OF F4 SPECIMEN TESTED AT -140 C SHOWING LOCATIONS OF SURFACE MICROCRACKS.

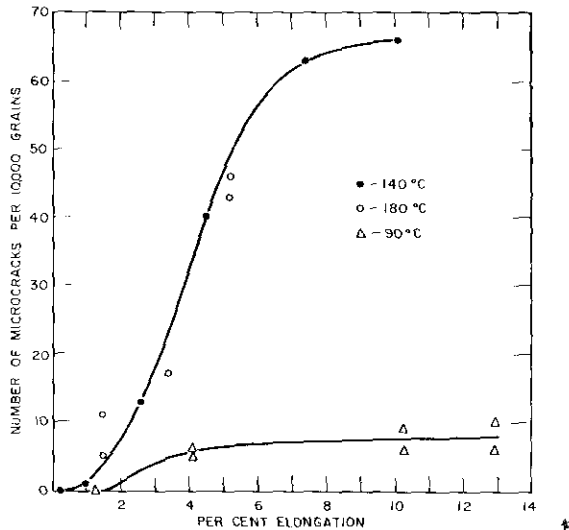


FIG. 48. EFFECT OF PLASTIC STRAIN ON THE NUMBER OF MICROCRACKS FORMED ON THE SURFACE OF VCG F4 TENSILE SPECIMENS IN INTERRUPTED TESTS.

has essentially ceased.

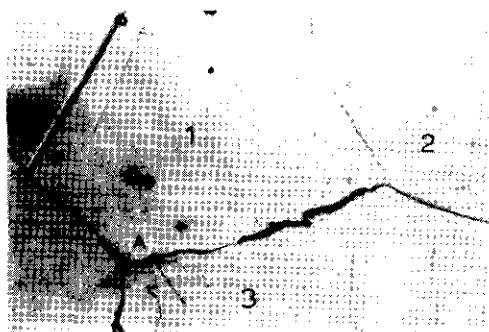
The fact that the Lüders strain in these coarse-grained specimens is only about 2 percent probably accounts for the small number of cracks formed at this stage. In finer-grained specimens with a large Lüders strain more crack formation in this stage would be expected. This type of behavior was observed in Hahn's mild steel specimens⁶⁶.

The positions of the microcracks in Figures 46 and 47 indicate that more cracks form near the edges of the specimens than in the central portion of the broad sides. Otherwise, the cracks formed in each loading increment are more or less randomly distributed.

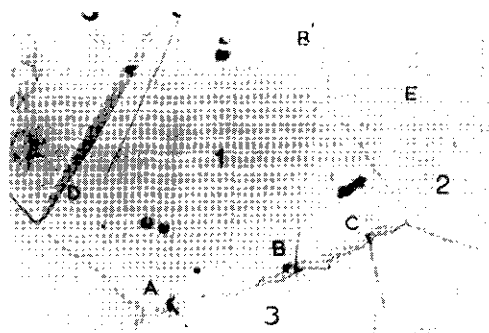
Figure 49 shows the stages of formation of a ferrite microcrack in the F4 specimen tested at -180 C. This crack was initiated by a crack in a carbide during the second loading increment and was stopped by a grain boundary. The initiation of ferrite microcracks by carbide cracking was found to be a common occurrence.

The only example of crack initiation by the intersection of mechanical twins out of all the specimens examined is shown in Figure 50. The sequence of events is given in the figure. The surface scratch, marked F in Figure 50 was originally present on the undeformed specimen and had nothing to do with the crack formation. The possibility exists that the crack was initiated in a cracked carbide below the surface and just happened to be stopped at the twin intersection, but this is highly unlikely. Figures 50(e) and 50(f) show that the end of the crack and the twin intersection still coincide after 2 mils have been removed from the surface by grinding.

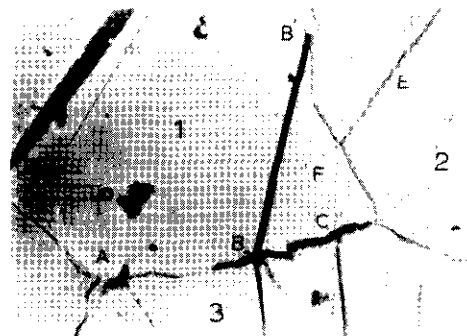
In general, microcracks, once formed, become wider but not much longer during further straining. Some cracks, however, are observed to lengthen slightly. An example of this is given in Figure 51 which shows a microcrack formed during the fifth loading step of the F4 specimen tested at -190 C (Figure 44). (In the first two steps, this specimen was unloaded in the elastic portion of the stress-elongation curve, and the replicas contained no evidence of plastic deformation.) It can be seen that the crack becomes slightly longer in both the sixth and seventh steps, and that it is apparently connected with the ultimate fracture in the seventh step. This is a



(a). Replica first loading step. Crack in carbide at (A) has initiated twins in grain 3.



(b). Replica second loading step. Cracks in carbide have initiated twins in grain 3 at (C) and (B) and a microcrack (BB') in grain 1. Twin (D) has thickened.



(c). Third loading step - fractured specimen. Microcrack (BB') has opened, causing localized deformation in grain 2. Twins have thickened. Thickening of twin (E) has produced new twin (F) in grain 1.

FIGS. 49 (a) through (c). STAGES OF MICROCRACK FORMATION IN SPECIMEN F4-86 (-180 C). 400X

case where a pre-existing microcrack could have been the starting point of the fracture. Another example of this is given in Figure 52 taken from specimen F4-87 (-140 C). Specimen F4-67 (-90 C) contained a similar example, but the fractures of specimens F4-86 (-180 C) and F5-14 (-180 C) did not pass through any known pre-existing cracks.

In any event, because new microcracks continue to form up to the time of fracture, one cannot determine whether the fracture is initiated by a pre-existing microcrack, or whether it is initiated by the formation of a new microcrack. This uncertainty prevails even when the ultimate fracture is found to pass through a previously observed microcrack. The essential feature of the fracture behavior in this temperature range is that the stress levels at which cracks can be initiated are lower than the stress necessary for long-range propagation. Once a stress is reached at which crack propagation is probable, then it seems to matter little where the fracture started. This issue will be discussed later in some detail.

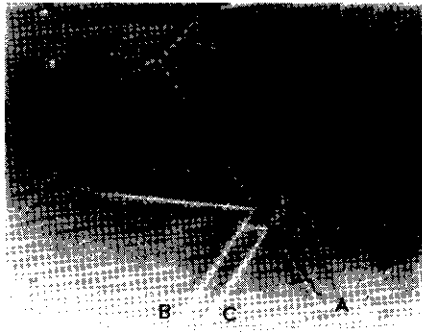
Cracks are sometimes observed to form beneath the surface during an early loading stage and to break through the surface at a latter stage. An example of this is shown in Figure 53. Here, again, is a case of a crack lengthening under increased stress.

The most common barriers at which microcrack propagation is arrested are twins and grain boundaries. However, it is not uncommon to find microcracks whose progress was apparently stopped by the initiation of twins and slip bands at the crack tip. An example of a microcrack that initiated at a grain-boundary carbide and stopped at a twin is given in Figure 54. Figure 55 shows a carbide-initiated microcrack which was apparently converted into a twin and slip band.

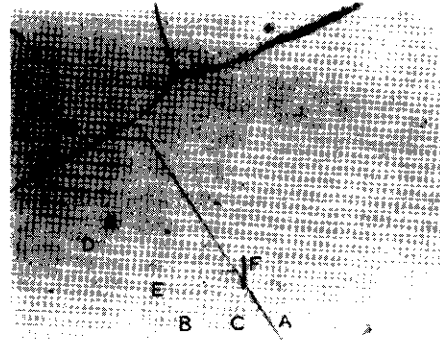
Subsurface Observations on Ground Specimens

Crack Sources

Approximately 20 percent of the cracks observed on the surfaces of F4 and F5 specimens were obviously initiated by cracking of grain-boundary carbides. The sources of the rest were not apparent from surface observations. In an attempt to determine some of these sources, selected specimens were ground

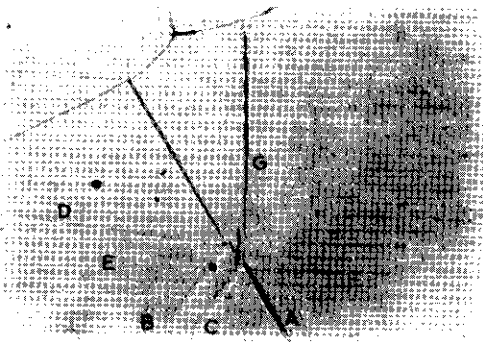


(a)

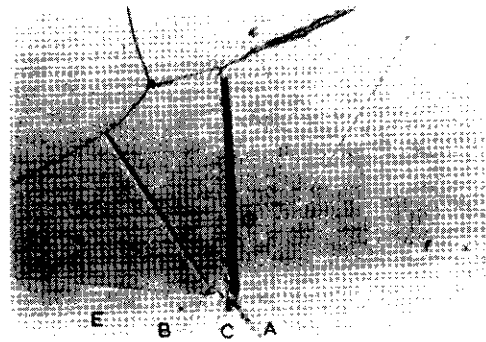


(b)

(a, b). Replica first loading step. Twin (A) formed first, followed by (B) and then (C). Accommodation slip band (D) formed when twin (B) hit twin (A). A similar band (E) formed when twin (C) hit twin (A) but was attenuated after crossing twin (B). (F) is a scratch originally present. (a) was taken under phase contrast illumination, and (b) with vertical illumination.



(c)



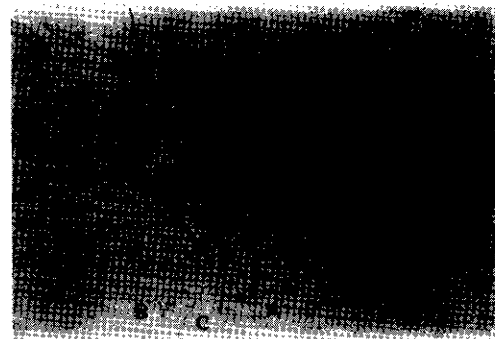
(d)

Replica second step. Microcrack (G) has formed at intersection of twins (C) and (A) and was stopped by grain boundary.

Third stage. Fractured specimen. Microcrack (G) has opened.



(e)



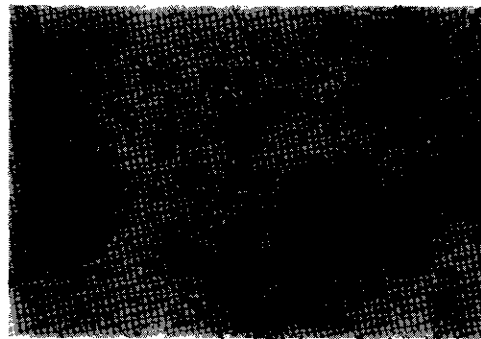
(f)

(e, f). Microcrack (G) after 2 mils are removed from surface of specimen.

FIG. 50. STAGES OF MICROCRACK FORMATION AT TWIN INTERSECTION IN SPECIMEN F4-86 (-180C). a, b, c, d, f, - 400X, e - 160X



(a). Replica fourth loading step. Twins and slip bands are present, as at (A), (B) (twins) and (C) (slip).



(b). Replica fifth step. Additional twins and microcrack (D) appear.

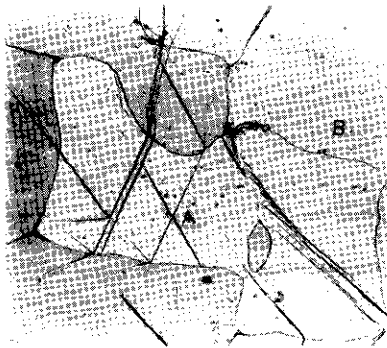


(c). Replica sixth step. Crack (D) is slightly longer.

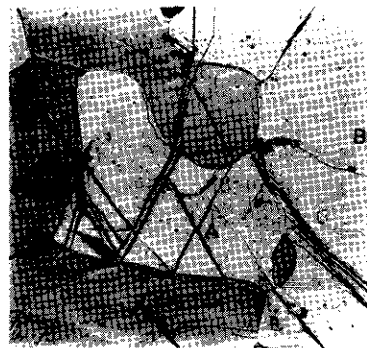


(d). Seventh step. Fractured specimen. Crack (D) is longer and is connected with fracture.

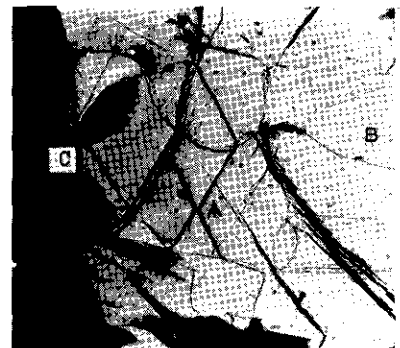
FIG. 51. STAGES OF FORMATION OF MICROCRACK IN SPECIMEN F4-69 (-190C) SHOWING LENGTHENING OF CRACK AND CONNECTION WITH FRACTURE. 160X



(a). Replica second loading step. Only twins, as at (A) and slip lines, as at (B) appear.

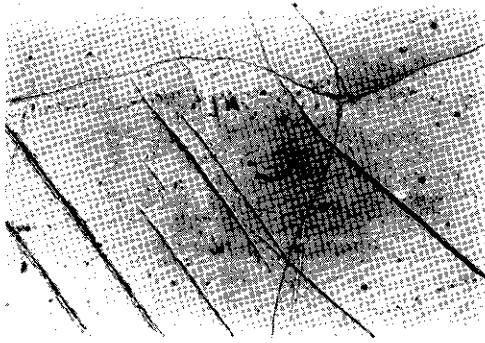


(b). Replica fourth loading step. Microcrack (C) formed in third step and appears unchanged here.



(c). Sixth loading step. Fractured specimen. Fracture passes through microcrack (C).

FIG. 52. MICROCRACK WHICH FORMED IN THE THIRD LOADING STEP OF SPECIMEN F4-87 (-140C) AND WHICH LATER BECAME PART OF THE FRACTURE IN THE SIXTH STEP. 80X



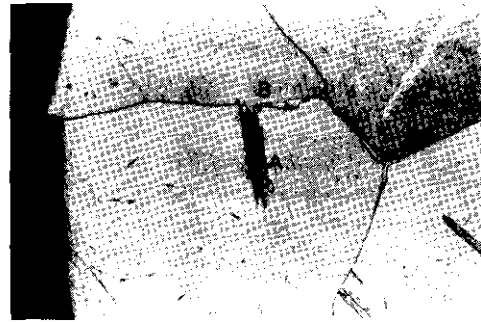
(a). Replica third loading step showing twins and depression (A) caused by crack below the surface.



(b). Replica fourth step. The depression has deepened.



(c). Sixth step. Fractured specimen. Crack has broken through the surface at (A).

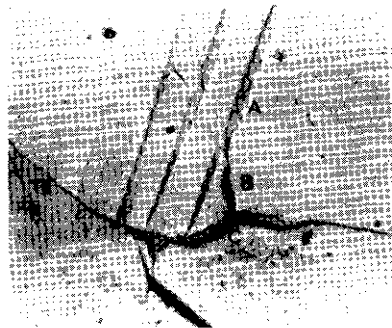


(d). After 2 mils removed from surface the cracked carbide which initiated the microcrack is found at (B).

FIG. 53 (a, b, c, d). THE BREAKTHROUGH ON THE SURFACE OF A MICROCRACK FORMED IN THE INTERIOR OF A GRAIN IN SPECIMEN F4-87 (-140 C). 160X



(a). Replica fourth loading step. Twin (A) has cracked the carbide in the grain boundary.



(b). Replica fifth loading step. Microcrack (B) has formed at a carbide crack (C) and has been stopped by Twin (A).



(c). Sixth step. Fractured specimen. Microcrack (B) has widened.

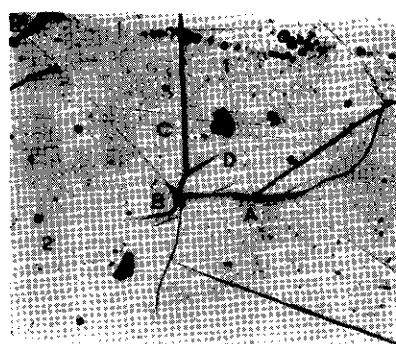
FIG. 54. EXAMPLE OF A MICROCRACK INITIATED AT A GRAIN-BOUNDARY CARBIDE AND STOPPED AT A TWIN IN SPECIMEN F4-87 (-140 C), 400X



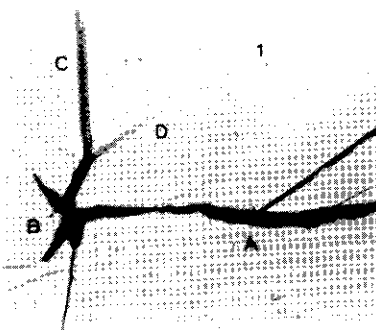
(a). Replica fourth loading step. Crack in carbide at (A) has given rise to a twin in grain 1.



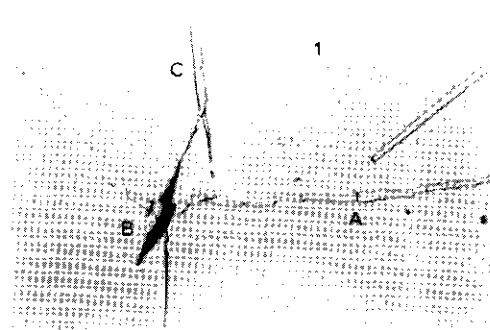
(b). Replica fifth loading step. Carbide cracked at (B) causing a microcrack in grain 1 which has, in turn, initiated twin (C) and slip band (D). A smaller crack has formed in grain 2. Twin in grain 1 has thickened.



(c). Sixth loading step. Fractured specimen. Cracks have opened; twin (C) and slip band (D) have thickened, as has the slip band at the end of the crack in grain 2.



(d). Details of (c).



(e). Same as (d) after 1 mil removed from surface. Twin (C) goes past the microcrack below the surface and twin in grain 1 no longer reaches the carbide at (A).

FIG. 55. EXAMPLE OF A MICROCRACK WHOSE PROPAGATION WAS APPARENTLY STOPPED BY THE INITIATION OF A TWIN AND A SLIP BAND. SPECIMEN F4-87 (-140 C). a, b, c - 160X, d, e, 400X

and polished in steps of 1 mil. This was carried out on both sides of specimen F4-86 (-180 C) and one side of F4-87 (-140 C), which had been replicated, and on one side of F5-12 (-170 C) which had not.

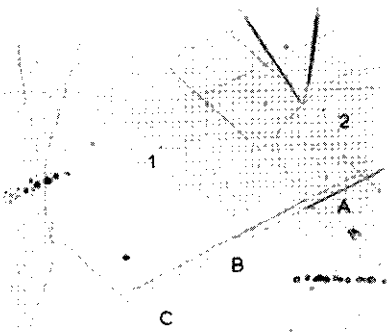
Figure 56(a), (b) and (c) show the sequence of formation of a microcrack in F4-86 (-180 C) which does not lie near a grain boundary on the surface and which has no apparent connection with a cracked carbide. After 2 mils are removed from the surface (Figure 56(e) and (f)), the cracked carbide initiating the crack can be seen.

In Figure 56 an example of the generation of slip bands by twins can be seen, as well as

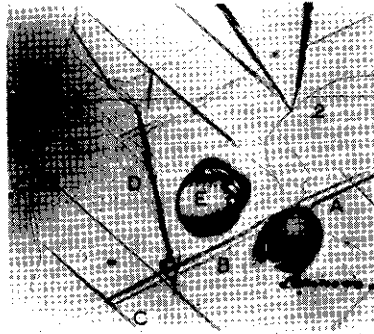
the passage of these slip bands through a twin. Although the slip bands, marked B, are indistinguishable from twins on the surface photographs, the fact that they disappear after repolishing signifies that they are slip bands.

Further examples of carbide sources of ferrite microcracks which were uncovered by grinding are given in Figures 57, 58 and 59. The carbide source in Figure 58 lies within a grain, rather than at the boundary, although it may be connected with a grain boundary at some lower level.

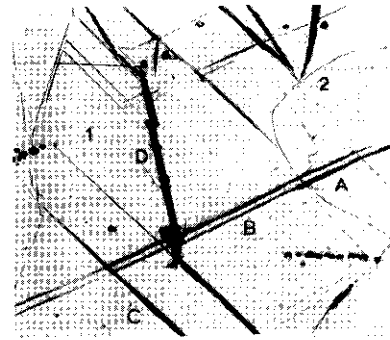
A summary of the crack sources on the four specimen sides which were ground to various depths are given in Table IV. Side 2 of speci-



(a). Replica first loading step. Twins (A) have caused slip bands (B) in grain 1 which have been attenuated after crossing twin (C).



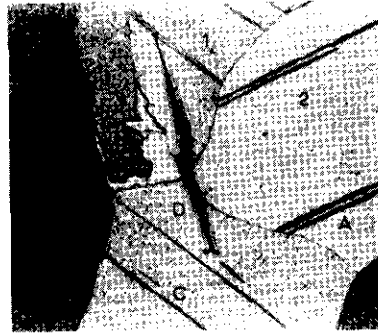
(b). Replica second loading step. Microcrack (D) has formed in grain 1. (E) and (F) are holes in the replica.



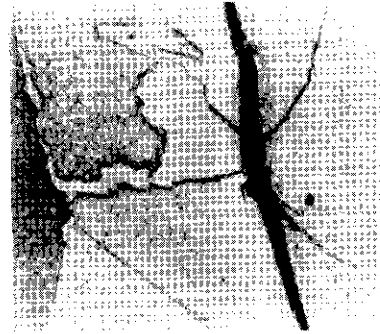
(c). Third loading step. Fractured specimen. Microcrack (D) has opened.



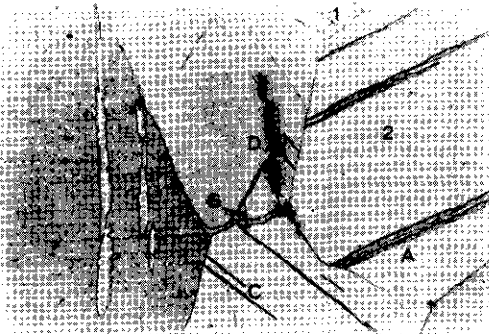
(d). 1 mil removed by grinding. Note disappearance of slip bands (B).



(e). Same as (f).

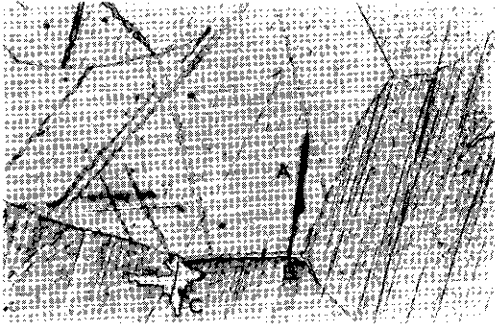


(f). 2 mils removed. Note large cracked carbide

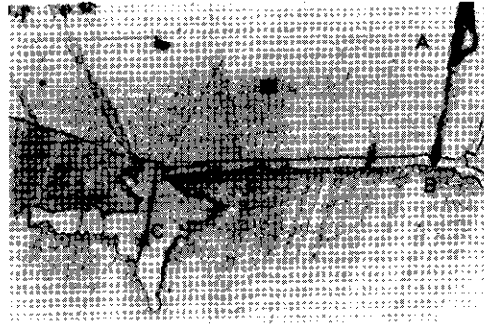


(g). 3 mils removed. A new crack can be seen at (G).

FIG. 56. (a, b, c). SEQUENCE SHOWING FORMATION OF MICROCRACK ON SURFACE OF SPECIMEN F4-86 (-180 C). CRACK HAS NO APPARENT CONNECT WITH CARBIDE. (d, e, f, g). SEQUENCE SHOWING CARBIDE SOURCE BENEATH THE SURFACE. NOTE THAT TWINS HAVE STOPPED CRACK PROPAGATION. a, b, c, d, e, g - 160X, f - 400X

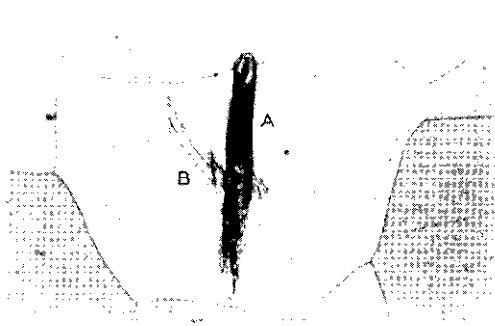


(a). 160X

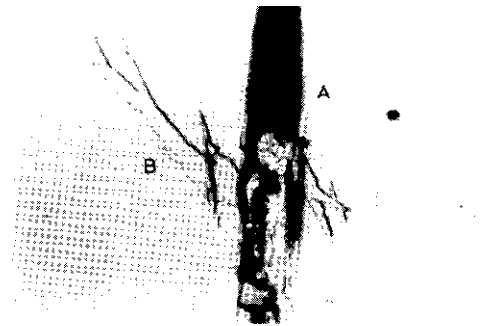


(b). 400X

FIG. 57. CRACK (A) ORIGINATING AT GRAIN BOUNDARY CARBIDE (B) WHICH WAS FOUND AFTER 3 MILS REMOVED FROM SURFACE. F4-87 (-140 C). CRACK STOPPED BY TWIN. NOTE LARGE CARBIDE CRACK (C) WHICH DID NOT NUCLEATE A FERRITE MICROCRACK.

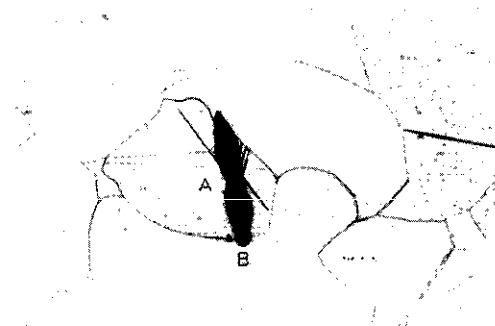


(a). 160X

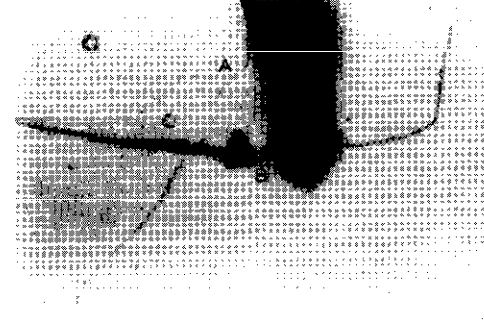


(b). - 400X

FIG. 58. MICROCRACK (A) ORIGINATING AT CARBIDE (B) WITHIN A GRAIN. 2 MILS REMOVED FROM SURFACE. F4-87 (-140 C). CRACK PARTLY FILLED WITH DEBRIS FROM POLISHING.



(a). 160 X



(b). 800 X

FIG. 59. MICROCRACK (A) ORIGINATING AT CRACKED GRAIN BOUNDARY CARBIDE (B) IN SPECIMEN F5-12 (-180 C). 1 MIL REMOVED FROM SURFACE.

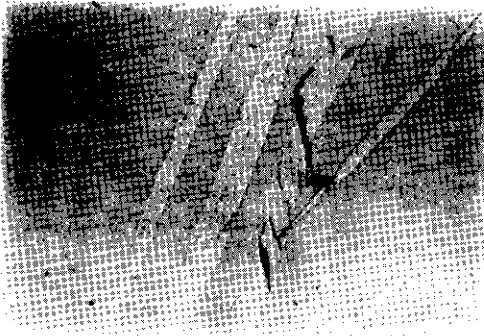
men F4-86 could not be examined in depth because of a mishap in grinding. More than 90 percent of the cracks on the other three sides originated in cracked carbides. Most of the rest appeared similar to the carbide-induced cracks, except that no carbide sources were actually found. It is probable that these also were initiated by carbides which were contained in material removed by grinding. Only one instance of crack initiation by twin intersection was found (Figure 50).

Two of the microcracks in the F5 specimen

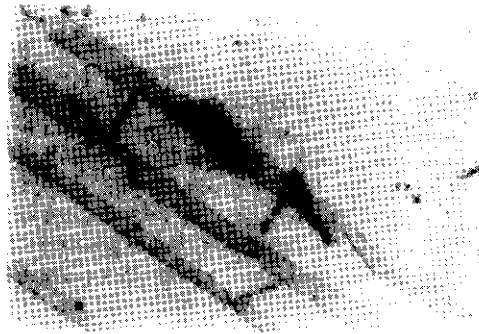
and one in F4-86, whose origin was uncertain, may have started at a twin-matrix interface. Examples of cracks contained within twins and in the twin-matrix interface are shown in Figure 60. No connection between these types of cracks and cleavage cracks in the matrix was ever observed in these materials, although such a connection has been reported for chromium²³. Figure 60(d) shows a crack formed at the intersection of two twins and a grain boundary in an F5 specimen. This was a fairly common occurrence in the F5 material, but it was never observed to be connected with a cleavage microcrack in the matrix.

TABLE IV. SOURCES OF MICROCRACKS IN F4 AND F5 FERRITE.

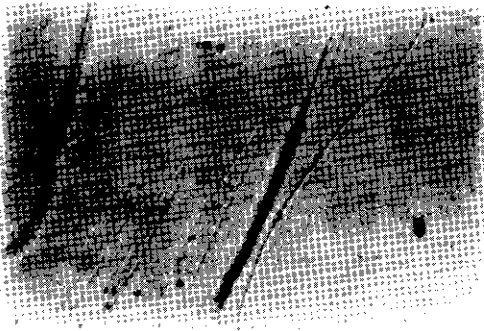
<u>Specimen/Side</u>	<u>F4-86/1</u>	<u>F4-86/2</u>	<u>F4-87/1</u>	<u>F5-12/2</u>
Test temperature	-180°C	-180°C	-140°C	-170°C
Total number of cracks observed	43	46	66	34
Number which originated at cracked carbide	42	23	63	25
Number which originated at twin intersection	--	1	--	--
Origin not certain -- probably cracked carbide	1	3	3	7
Origin not certain -- possibly twin-matrix interface	--	1	--	2
Origin completely undetermined due to loss of specimen in grinding accident	--	18	--	--



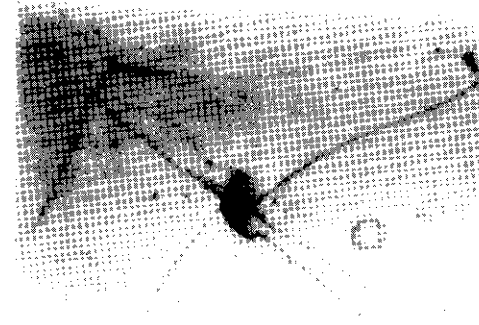
(a). Cracks in twins in F4-86 (-180C). 1 mil removed from surface.



(b). Cracks in twins in F5-12 (-180 C). 4 mil removed from surface.



(c). Crack along twin-matrix interface in F5-12 (-180 C). 1 mil removed from surface, then specimen electropolished.



(d). Crack formed where twins met at grain boundary in F5-11 (-170 C). 1 mil removed from surface, then specimen electropolished.

FIG. 60. CRACKS IN AND ALONG TWINS IN F4 AND F5 SPECIMENS. a, c - 400X, b, d - 800X

Modes of Crack Arrest

Observations on the manner in which crack propagation was arrested are summarized in Table V. Twins and grain boundaries are the most common barriers. More than half the cracks were stopped by twins at some point of their periphery.

Examples of a crack in F4 stopped by a twin and one stopped by the initiation of slip and twinning are given in Figures 54 and 55. An example of a crack, initiated at a carbide, which was stopped by a twin in an F5 specimen is shown in Figure 61. Figure 62 shows a crack in the same specimen which jogged when it passed through a twin and later through a grain boundary.

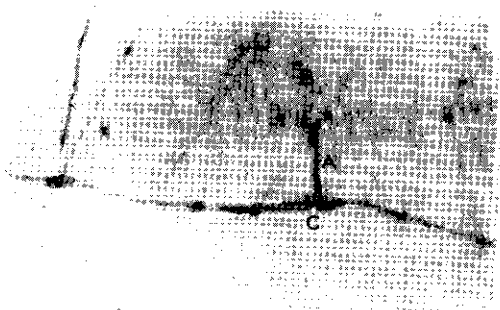
Examples of cracks as tributaries of the main fracture arc shown in Figure 63. In (a) a

TABLE V. MODES OF ARREST OF MICROCRACKS FORMED IN F4 AND F5 FERRITE.

Specimen/Side	F4-86/1	F4-86/2	F4-87/1	F5-12/2
Test temperature	-180°C	-180°C	-146°C	-170°C
Total number of cracks observed	43	46	66	34
Stopped by twin	23	24	23	13
Stopped by grain boundary	6	7	13	8
Stopped by both twins and grain boundary	--	7	11	10
Stopped by initiation of slip bands	6	3	4	--
Stopped by initiation of twins	3	4	4	--
Stopped by initiation of slip and twins	5	1	6	--
Not certain -- probably initiation of slip bands	--	--	--	3



(a). Microcrack (A) stopped by twin (B) in CG F5 specimen. 1 mil removed from surface. 400X



(b). Cracked carbide (C) source of microcrack (A). 2 more mils have been removed. 800X

FIG. 61. CRACK FROM CARBIDE STOPPED BY A TWIN IN F5-12 (-170 C).

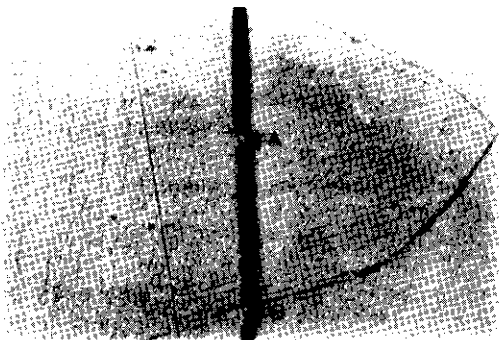
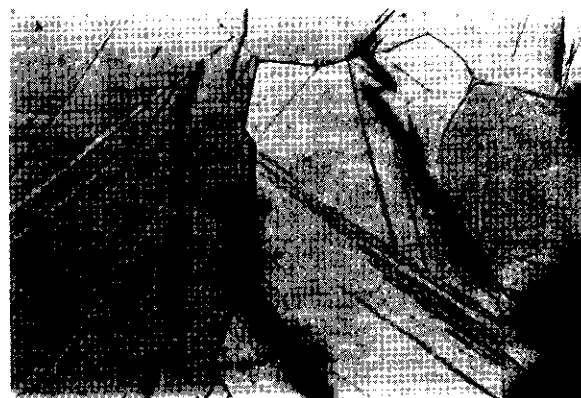


FIG. 62. JOGS IN CLEAVAGE CRACK PASSING THROUGH A TWIN (A) AND GRAIN BOUNDARY (B). SPECIMEN F5-12 (-170 C). 5 MILS REMOVED FROM SURFACE. 400X



(a). Crack (A) strikes twin (B), runs a short way along the twin boundary, then switches to a cleavage plane (nearly parallel to the tensile axis) and is finally stopped by twin (C). 8 mils removed from surface.



(b). Crack (M) hits grain boundary and opens it at (N) before coming to rest. 5 mils removed from surface.

FIG. 63. MODES OF ARREST OF TRIBUTARY CRACKS FROM MAIN FRACTURE IN F4-86 (-180 C). 160X

crack was diverted 90° into a direction nearly parallel to the tensile axis when it hit a twin. In (b) a crack was stopped by a grain boundary which was partly opened. Both types of behavior have also been observed in microcracks away from a fracture.

Lengths of Cracks

The lengths of the microcracks observed in the ground specimens are summarized in Figures 64 through 67. (The F4 specimens had been step-loaded and replicated; the F5 specimen was loaded continuously without replication.) It can be seen that most cracks are

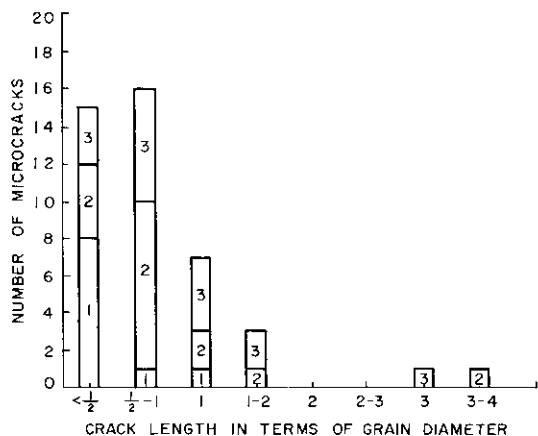


FIG. 64. LENGTHS OF MICROCRACKS ON SIDE 1 OF F4-86 INDICATING LOADING STEP IN WHICH MICROCRACKS FORMED. TESTED AT -180 C IN 3 STEPS.

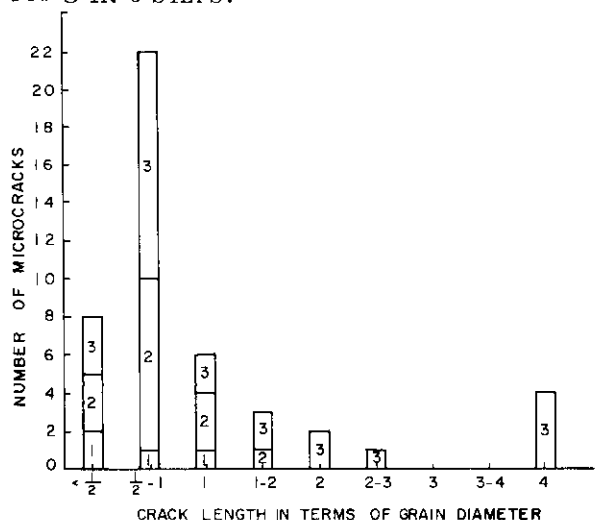


FIG. 65. LENGTHS OF MICROCRACKS ON SIDE 2 OF F4-86 INDICATING LOADING STEP IN WHICH MICROCRACKS FORMED. TESTED AT -180 C IN 3 STEPS.

equal to or less than the diameter of the grain in which they form. (The grain diameter referred to in these figures means the diameter of the grains in which the cracks are located; not to the average grain size of the specimen.) Specimen F4-87 (-140 C) has more cracks of 1-2 grain lengths than the specimens tested at lower temperatures. This may be a result of the smaller amount of twinning at this temperature (see Figure 22) which means that there are fewer crack barriers.

The data for the F4 specimens show that

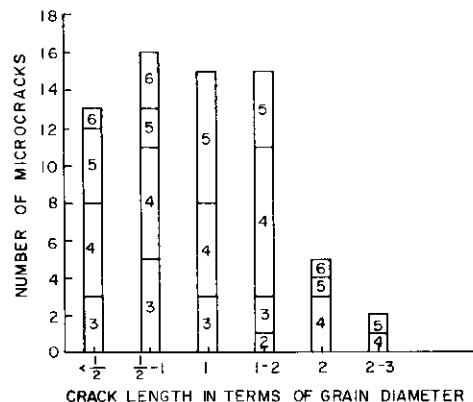


FIG. 66. LENGTHS OF MICROCRACKS ON SIDE 1 OF F4-87 INDICATING LOADING STEP IN WHICH MICROCRACKS FORMED. TESTED AT -140 C IN 6 STEPS.

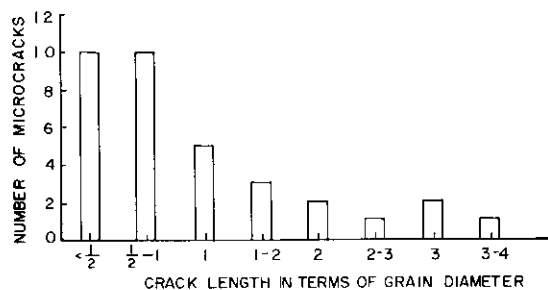


FIG. 67. LENGTHS OF MICROCRACKS ON SIDE 2 OF F5-12. TESTED AT -170 C IN 1 STEP.

the microcracks formed in the early steps tend to be short and that the longer cracks tend to be formed in the later steps. However, since about half the cracks formed in the later steps are less than one grain diameter in length, we cannot say that the later-formed cracks tend to be longer.

Occasionally, microcracks formed before the final loading stage are found to have propagated through several grains. Figure 68 shows two long cracks on a level 4 mils below the original surface of specimen F4-86 (-180 C) as formed in the second of three steps. Both cracks lie in 4 grains. Both come from cracked carbides, and they are joined by a ductile tear farther down in the specimen. The orientation of most of the grains through which the cracks pass appears to be nearly the same, as seen by the twin traces and etching characteristics of the grains. This would help explain the unusually long propagation. Although quite

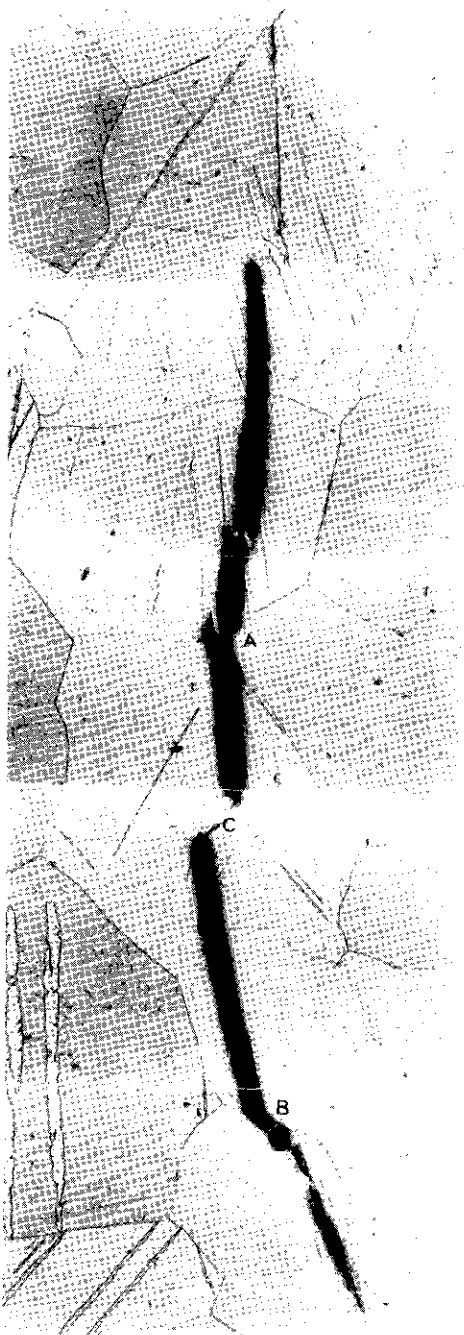


FIG. 68. TWO LONG CRACKS WHICH PASS THROUGH A GROUP OF GRAINS HAVING NEARLY THE SAME ORIENTATIONS. UPPER CRACK CAME FROM A CARBIDE AT (A); LOWER CRACK FROM A CARBIDE AT (B). THE CRACKS ARE JOINED AT (C) DEEPER IN THE SPECIMEN. F4-86 (-180 C). CRACKS FORMED IN SECOND STEP. 4 MILS REMOVED FROM SURFACE. 160X

long, this chain of cracks did not propagate further and was located more than an inch away from the fracture.

In contrast to the behavior shown in Figure 68, cases are also found where several cracks lie in one grain. An example is shown in Figure 69. All of the cracks in this figure originated from cracked carbides found during sectioning.

The Number of Microcracks in the Interior of Ground Specimens

The number of microcracks observed on an internal surface of a ground specimen is always greater than the number observed on the external (original) surface: Examples of this are shown in Table VI.

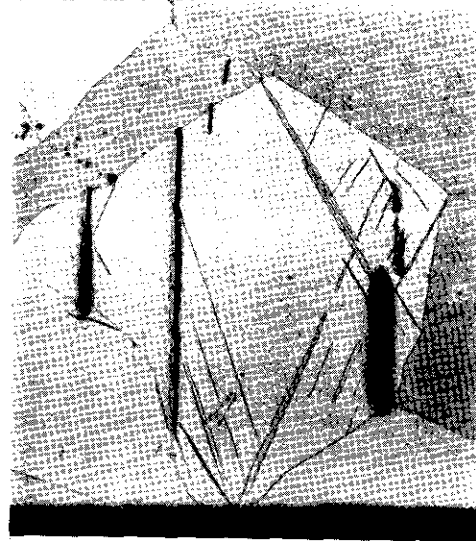


FIG. 69. FOUR MICROCRACKS LYING IN ONE GRAIN. ALL CAME FROM CRACKS IN CARBIDE. RIGHT-MOST CRACKS ARE JOINED LOWER IN SPECIMEN. F4-86 (-180 C) 9 MILS REMOVED FROM SURFACE. 160 X

Part of this increase is easily explained. On the external surface we see cracks which come from carbides lying on or below the surface. On an internal surface we see cracks which come from carbides lying on, below or above this surface. Thus, we may expect about a two-fold increase from this factor alone.

Some of the increase could also be due to a larger amount of carbide in the interior than near the surface. This situation, which was obvious in some specimens, could have re-

TABLE VI. INCREASE IN NUMBER OF CRACKS OBSERVED WHEN MATERIAL WAS REMOVED FROM THE SURFACES OF FRACTURED SPECIMENS BY GRINDING.

Specimen	Amount of material removed from original surface	Number of cracks observed
F4-86 (-180°C) short piece, side 1 (approximately 2500 grains)	none	7
	10 mils	27
F4-86 (-180°C) short piece, side 2 (approximately 2500 grains)	none	11
	10 mils	25
F5-12 (-170°C) long piece, side 2 (approximately 13000 grains)	none	3
	2 mils	24
	10 mils	35

sulted from either non-homogeneous carbon distribution in the as-received material, or more probably, to decarburization during heat treatment. Although the heat treatments were carried out in a dry argon atmosphere, it is likely that some amount of decarburization did occur. Because of the initially low carbon content of these materials, a small amount of decarburization would be hard to detect.

The Role of Carbides in the Ductile-Fracture Region

The role of cracked carbides in the fracture of the FCG F4 and CG F5 specimens above the transition temperature can be seen in Figures 70, 71 and 72. In the F4 specimens, the fragmented grain-boundary carbides provide the sites for the formation of large voids. The size of these voids increases with the extent of necking (Figure 71), and they provide a path of weakness through which fracture can occur by the rupture of the intervening material, whether by cleavage or by fibrous tearing. The connection of the voids with the cracked carbides is clearly shown in Figure 70. The carbides tend to become strung-out in the tensile direction in the neck, reminiscent of the appearance of inclusions in rolled or drawn materials. The voids formed at the cracked carbides play the same role as the voids formed around inclusions in the ductile fracture of copper³⁷. The deep cavities in the sponge-like fibrous fracture surface are undoubtedly due to some of the larger holes from the cracked carbides.

Figure 72 shows that the voids formed in F5 ferrite are much fewer in number and smaller in size than in F4, even in a specimen which

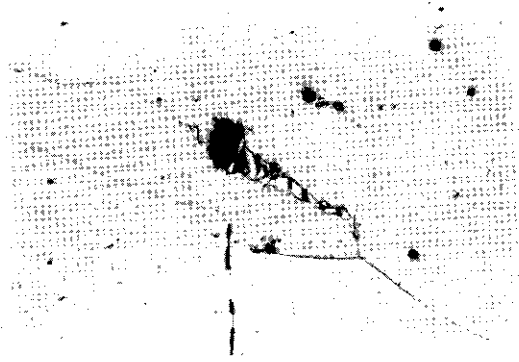
has undergone a larger reduction of area in the neck. The large amount of void formation in the necked F4 specimens causes them to fracture at a lower stress and to exhibit a smaller reduction in area.

DISCUSSION OF RESULTS

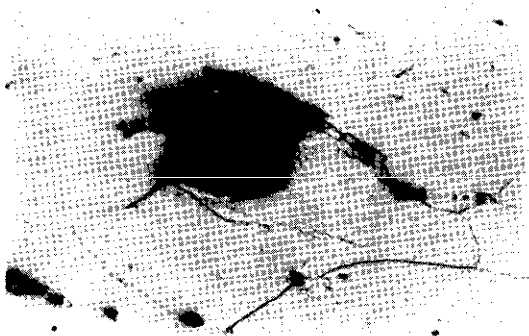
Crack Initiation

It now appears certain that in F4 and F5 ferrite, cleavage cracks are initiated by the cracking of iron carbide, either at ferrite grain boundaries or within the grains themselves. The brittle carbides crack under the influence of the tensile and bending stresses imposed upon them by the plastic deformation of the ferritic matrix. Webb and Forgeng⁸³ have estimated the elastic modulus of cementite to be 24.6×10^6 psi, which is less than the value for iron, 30×10^6 psi. They found that 1 to 2 μ crystals of Fe_3C , which were extracted from steel, could be bent to strains of 2 to 5 percent before fracturing in a brittle manner. In view of this, we would not expect the carbides to crack during the elastic deformation of the ferritic matrix, and this agrees with the present observations. (The thickness of typical grain-boundary carbides ranges from about 1 to 3 μ in F5 and 2 to 10 μ in F4.)

Carbides are found to crack at all temperatures from room temperature to -196 C, with the cracks tending to lie normal to the tensile axis. To examine this cracking more closely, the F4 specimen which was unloaded during the load-drop at yielding at -90 C was examined via a replica. It was found that carbide cracking occurs even at this strain of much less than 2 percent, as compared with the 2 to 5 percent fracture strain of the isolated carbides. The lowest estimate of the fracture strength of the isolated cementite, given by Webb and Forgeng, is more than an order of magnitude greater than the externally applied stress which causes cracking of the carbides contained in the ferrite. Thus, a stress concentration of at least a factor of 10 must be exerted on the carbide by the plastic deformation of the ferritic matrix to account for the cracking of the carbide. A calculation of the stress acting on any given carbide would be quite complex. One would expect it to depend on the size and shape of the carbide, the orientation of the carbide with respect to the tensile axis, the orientation of the ferrite grains adjoining the carbides, and the tem-



(a). Voids from cracked carbide in neck of F4-100 (-90 C) near fracture. 32.3% reduction in area.



(b). Large void from cracked carbide in neck of F4-102 (-70 C) near fracture. 70.0% reduction in area.

FIG. 70. VOIDS FROM CRACKED CARBIDES IN NECK OF VCG F4 SPECIMENS. GROUND APPROXIMATELY TO HALF-THICKNESS. 200X

perature (which would determine the character of the deformation of the ferrite). In addition, stress concentrations of at least a factor of 10 would be expected at the head of large slip bands or twins which impinge upon the carbides. The Zener model (Figure 1a) could well be applied here.

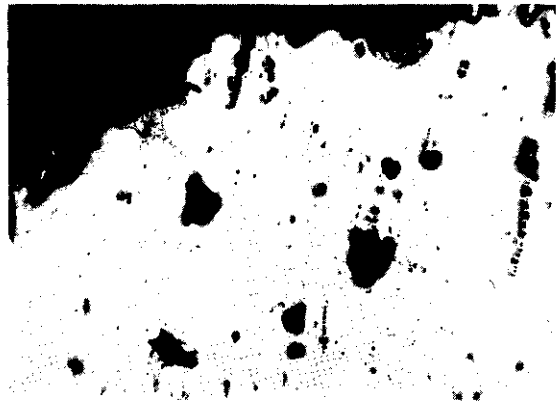
It may also be that Griffith-type flaws



(a). Voids in neck of F4-100 (-90C) 32.3% reduction in area. Note cracked carbides at (A) and cleavage cracks at (B). Fracture about 10% fibrous.



(b). Voids in neck of F4-101 (-80 C) 58.4% reduction in area. Fracture about 35% fibrous.



(c). Voids in neck of F4-102 (-70 C) 70.0% reduction in area. Note increase in size of holes from cracked carbides as strain in the neck increases. Fracture about 95% fibrous.

FIG. 71. VCG F4 SPECIMENS GROUND APPROXIMATELY TO HALF-THICKNESS, UNETCHED. TENSILE AXIS VERTICAL. 36X



FIG. 72. NECK OF F5-21 (-110 C) 83.0% REDUCTION IN AREA SHOWING ONLY A FEW SMALL VOIDS. LONGITUDINAL CLEAVAGE CRACK AT (A). FRACTURE ABOUT 60% FIBROUS. GROUND APPROXIMATELY TO HALF THICKNESS. 40X

exist on the surface of carbides formed in ferrite. Since the electrolytic extraction used by Webb and Forngeng probably dissolved some of the surface layer which would contain these flaws, we might then expect the isolated carbides to exhibit a higher strength.

It should be noted that the cementite-ferrite interface is apparently quite strong and was rarely seen to be opened up, even in carbides extending normal to the tensile axis. Figure 34(c) shows that cracking of the cementite is at least as easy as splitting of the interface.

The formation of a cleavage crack in ferrite may be visualized as follows: a crack is formed in a cementite plate. Since the carbide is a brittle material, the crack can be construed as a true Griffith crack while it is in the carbide. When the crack arrives at the carbide-ferrite interface, one of two possible situations will arise. If the ferrite is unable to respond by plastic flow to the stress concentration at the tip of the carbide crack, it will view the carbide crack as a Griffith crack. Considering the ferrite as a brittle material, for the moment, we can apply the Griffith equation for the plane strain case:

$$\sigma = \sqrt{\frac{2E\gamma}{\pi(1-\nu^2)c}}$$

Using the average cleavage strength of iron single crystals* as 3×10^{10} dynes/cm² and taking $E = 2 \times 10^{12}$ dynes/cm² and $\gamma = 10^3$ erg/cm², we find that $2c$, the critical Griffith crack size, is about 3μ . This is the thickness of the larger carbides in F5 ferrite and of the smaller carbides in F4. If the crack in the carbide is long enough, it will enter the ferrite and propagate until it hits a barrier strong enough to stop it, or until the relief of stress (and absorption of energy) by slip or twinning occurs ahead of the crack.

If the ferrite is able to deform plastically at the moment when the carbide crack reaches the interface, then the Griffith equation will not apply and no microcrack will form**. Thus, the formation of a cleavage microcrack is seen to be a statistical event. This is evidenced by the very large number of carbide cracks and the relatively small number of microcracks seen in the specimens tested. It should be noted that, in this picture of microcrack formation, a carbide crack causes cleavage in ferrite either at the instant it reaches the carbide-ferrite interface, or not at all.

TABLE VII. CRITICAL CRACK SIZE FOR F4 AND F5 FERRITES AT THE TEMPERATURES WHERE MICROCRACKS ARE FIRST OBSERVED.

Material	Temperatures at which microcracks are first observed *C	Lower yield stress (psi)	2c(μ)	Actual size of carbides (μ)
VCS F4	-70	29,300	5.6	2 to 10
DC F5	-140	25,950	1.6	1 to 3

* This is also about the stress at which microcracks form in the F4 and F5 polycrystals. To be more exact we may assume that the first microcracks form at about the lower yield stress, and use this to calculate the critical crack size at the temperature where microcracks first are observed in F4 and F5. This is done in Table VII. It can be seen that $2c$ is about the thickness of an average carbide.

** The word "microcrack" is used only to denote a cleavage crack in ferrite; it is not used to refer to a carbide crack.

There certainly must be a lower limit of carbide thickness, below which ferrite microcracks are not likely to be initiated by carbide cracks. However, a long carbide crack will not always form a microcrack more readily than a short one. This is shown in Figure 57, in which a short carbide crack has formed a ferrite microcrack, while a much longer one has not. Cleavage in ferrite depends on the right conditions existing at the right time, which was apparently not the case for the long carbide crack in Figure 27.

Clearly, it is not necessary to resort to mechanisms involving dislocation interaction to account for cleavage initiation in the materials studied. In addition, it can be seen that twin intersections, which can be important in single crystals, are of relatively little importance in these polycrystalline ferrites. This conclusion is supported by the following:

- (i) out of the several hundred ferrite microcracks observed, only one actually originated at a twin intersection;
- (ii) the twinning behavior of F4 and F5 ferrite is essentially the same, while the microcracking behavior is quite different;
- (iii) in the replicated specimens the majority of the microcracks are found to form after twinning has essentially ceased;
- (iv) at low temperatures the number of microcracks formed in fractured specimens decreases, while the amount of twinning continues to increase.

For the above reasons, the mechanism of cleavage initiation by the interaction of dislocations emitted by twins, as proposed by Sleeswyk^{5,7}, likewise has little or no relevance to these materials.

It might be noted that Sleeswyk used the peak in the microcrack frequency versus temperature in the "coarse-grained mild steel" (see Figure 8) tested by Hahn⁶⁶, in the justification of his theory. This material was actually Ferrovac E containing 0.039 percent carbon, and was furnace cooled from the austenitic region; therefore, it was quite similar to the F4 ferrite. The microcracks in this material must have come from cracked carbides, and so the peak in the curve has nothing to do with emissary dislocations.

Sleeswyk also concludes from his model that the twinning stress of a material will be 94.3 percent of the brittle fracture stress. This is not even approximately the case in the results obtained here.

The amount of carbide cracking increases with increasing strain. The likelihood of formation of microcracks from carbide cracks increases with increasing applied stress, and, thus, with decreasing temperature (as the yield stress rises). As temperature continues to decrease, the fracture strain decreases, that is, the stress required for long range microcrack propagation is reached at a smaller strain, and the specimen fractures. Therefore, two conflicting factors operate in microcrack formation as the temperature is lowered: increasing stress and decreasing fracture strain. This situation might well be expected to give rise to a maximum in the number of microcracks observed. Maxima are indeed observed in Figures 28 and 29 for F4 and F5 ferrite, and similar maxima have been found by Hahn⁶⁶ and Sullivan⁷⁶ in ferrite and mild steel. The dependency of the number of microcracks on the fracture strain on the low temperature side of the maximum can be most clearly seen in Figures 31 and 32.

Since the carbides in F5 are thinner than those in F4, the ferrite microcracks in F5 are first formed at a lower temperature (and higher stress level) than in the F4. Since the carbides in F5 are much fewer in number, there should be fewer microcracks in this material.

The Conditions for Brittle Fracture--Comparison of the Tensile Behavior of F4 and F5 Ferrite

Cleavage fracture of a polycrystalline aggregate occurs when a microcrack forms and is able to propagate initially along a path of low resistance. A low-resistance path could be a group of grains of abnormally large size, or a group of grains of nearly the same orientation (so that their cleavage planes are more or less aligned), or a group which contains relatively few twins which can act as barriers to cleavage. After propagating a certain distance along this path, the microcrack must be moving at a high enough velocity that it can penetrate barriers of high resistance. In order for ultimate cleavage fracture to occur, two conditions must be fulfilled. First, there must be enough sources to give a sizable probability that a microcrack can be initiated in the

vicinity of a low-resistance path. Secondly, the applied stress must be high enough for a microcrack to penetrate regions of high resistance at the end of a low-resistance path.

The length of the low-resistance path in which the fracture starts must be greater than one or two grain diameters, since microcracks of this length can form at the approximate level of the fracture stress without propagating. Furthermore, non-propagating microcracks of greater length have been observed. One of the longer low-resistance paths is shown in Figure 68. In specimen F4-86 tested at -180°C (see Figure 65), four microcracks, each passing through four grains, were formed in the third loading step (during which fracture occurred). These microcracks were quite thin and were apparently newly formed at the time of fracture. One or more of these microcracks may have been supercritical at this stress and it is possible that one of them would have caused the fracture, had it not already occurred elsewhere.

The microcrack which starts the fracture process in the F4 and F5 ferrite need not come directly from a carbide crack. It could be initiated by a microcrack that is already present; that is, an existing microcrack may act as a built-in notch. However, whether the final cleavage is initiated by an existing microcrack or directly by a carbide crack, the probability of final cleavage will increase with the amount of carbide present because cracks in the latter are also responsible for the formation of microcracks.

If the tensile stress on the specimen is too low for propagation, but the number of crack sources is high, we will find many non-propagating microcracks, as in the F4 specimens before fracture. If the tensile stress is high enough, but the number of crack sources is too small, we will find that the material is ductile, as in the F5 specimens above -160°C . At temperatures below -160°C in the CG F5 specimens, the applied stress is high enough (because the yield stress has been raised) so that even the fine carbides in this material can act as crack starters, and brittle behavior sets in.

Since plastically deformed but unfractured specimens are observed to contain microcracks, we are at first tempted to conclude that crack initiation does not control the

brittle fracture process. However, this conclusion appears to be too simple. The initiation event can be the controlling step, but only when it occurs under conditions suitable for propagation. We could say that the probability of brittle fracture equals the probability of initiation, times the probability of propagation, and that when either of latter probabilities is low, the probability of brittle fracture will be low. As will be pointed out below, the F4 and F5 materials seem to have approximately the same propagation tendencies.

The difference in tensile behavior between F4 and F5 ferrite is shown by the load-elongation curves and the reduction in area curves in Figures 73 and 74. From the similarity of the yield stress, grain size, twinning behavior, and shapes of the stress-strain curves of the two materials, we may assume that the probability of crack propagation at any given stress and temperature is about the same in the two cases. Accordingly, the difference in fracture behavior may be rationalized in terms of the number and size of carbides which are available for initiating cracks.

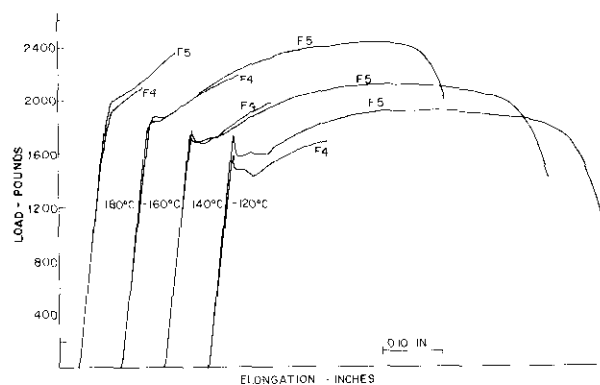


FIG. 73. COMPARISON OF LOAD-ELONGATION CURVES OF VCG F4 AND CG F5 FERRITE.

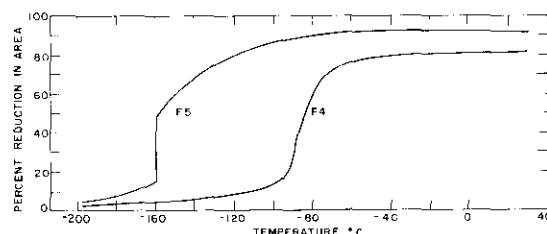


FIG. 74. COMPARISON OF REDUCTION IN AREA CURVES OF VCG F4 AND CG F5 FERRITE.

In Figure 73 the F4 and F5 load-elongation curves are superimposed for four temperatures. The original cross-sections of these specimens are the same within about 3 percent and are given in Table VIII. Initially the curves are alike at each temperature; however, the conditions for cleavage, described above, are reached in F4 before necking can occur. In the F5 at the higher temperature, no microcracks form in the ferrite because the stress is too low for the cracks in the thin carbides to be effective, and the specimen is completely ductile. At the two middle temperatures, cracks start to form in F5, but they are so few in number that the first condition (page 45) is not fulfilled. At the lower temperature the stress level is high enough that both conditions are fulfilled in F5. Thus, we can see that, at the three higher temperatures, the tendency for brittleness is determined mainly by the carbide content and carbide morphology.

The difference in ductility shown in Figure 74 can be explained for the whole range of temperatures. In the ductile region, the greater carbide content in F4 gives rise to the formation of more and larger voids in the neck of tensile specimens, leading to lower fracture strength and less reduction in area. In the transition region, the low number and small size of

carbides cause the F5 to remain ductile at lower temperatures, since the probability of microcrack initiation remains small. In the brittle region of both materials, the small carbide size means that the specimens must work harden to a higher stress level for fracture to take place, and the reduction in area will be larger.

The transition from ductile to brittle behavior in each material is seen to occur just below the temperature where microcrack formation first takes place. The difference in transition temperature between F4 and F5 (-160 C versus -90 C) corresponds closely to the difference in temperature at which microcracks start to form (-140 C versus -70 C). It may be noted that in this analysis, the temperature of the maxima in the microcrack-temperature curves (Figures 28 and 29) has no direct connection with the transition temperatures.

Since cleavage fracture, as described here, is of such a statistical nature, a fair amount of scatter is expected in the values of cleavage stress and total elongation. This scatter, as seen in Figure 23, is one of the hallmarks of brittle fracture.

The transition in fracture mode from completely fibrous to completely cleavage is more complex in flat specimens than it is in round specimens. In the transition region, where the fracture appearance is partly fibrous, the fracture starts with a ductile tear, which is usually initiated at an edge of the specimen. Sometimes the tear starts at a microcrack which has widened during the formation of the neck. As the tear progresses across the specimen, it converts to cleavage. Occasionally the ductile tear starts in the center of the specimen or at the center of one of the broad faces. In those cases the switch to cleavage occurs as the tear progresses toward the edges. The completion of the transition to complete cleavage does not always coincide with the disappearance of the necking phenomenon. Complete cleavage fracture has been observed in necked specimens of F4 ferrite, and it probably would also have been observed in F5 ferrite, had more specimens been tested.

TABLE VIII. ORIGINAL CROSS-SECTIONAL AREAS OF SPECIMENS REFERRED TO IN FIG. 73

Temperature (°C)	Specimen number	Area of original cross section (in. ²)
-180	F4-92	0.0302
	F5-11	0.0285
-160	F4-94	0.0301
	F5-13	0.0300
-140	F4-88	0.0308
	F5-19	0.0298
-120	F4-97	0.0291
	F5-22	0.0301

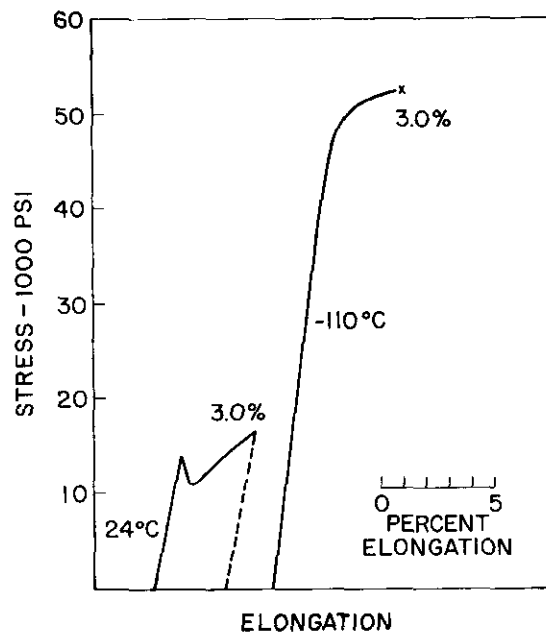
The Role of Twins in Crack Propagation

It was shown in the previous chapter that twins can provide effective barriers to crack propagation. Therefore, it would seem that an

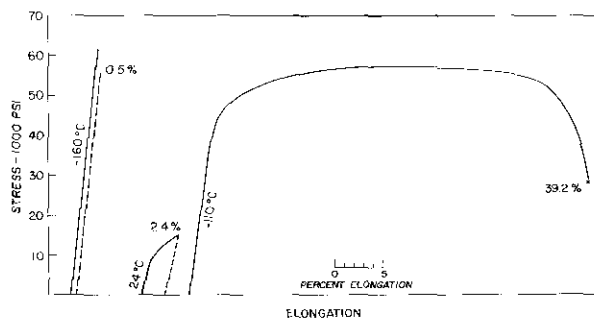
increase in the number of twins in a specimen would act to reduce the effective grain size, as far as fracture is concerned. A twin, after all, is a kind of grain boundary, and a thick twin may even be viewed as a double boundary. Unless a {100} cleavage plane in the twin is aligned with the plane on which the cleavage crack is moving in the matrix, the cleavage crack would be forced to become skewed upon both entering and leaving a thick twin. Honda has pointed out (private communication) that in a b.c.c. single crystal with the tensile axis in the vicinity of [100], the cleavage plane is coherent with a {100} plane in the twins which form, so that these twins will not be the most effective barriers, but this would not be the case, in general, in a polycrystal.

It has been shown by Gensamer and Weiner⁸⁹ that a decrease in the spacing of twins in zinc single crystals produces the same " $d^{-1/2}$ " increase in cleavage stress as the decrease in grain size in a polycrystal.

The work of Rosof⁹⁰ has provided a rather startling demonstration of the importance of twins in the ductile-brittle behavior of iron polycrystals. This is shown in Figure 75. In the present work it was found that in a VCG F4 specimen tested at -110 C , about 60 percent of the grains would contain twins and the specimen would fracture by cleavage after about 16 percent elongation. Rosof found that a room temperature prestrain of 2 to 3 percent would suppress all twinning at lower temperatures, except for those produced by the fracture itself. When a prestrained specimen was tested at -110 C immediately after the 3 percent prestrain, it failed by cleavage after only 3 percent elongation (Figure 75a). A similar specimen was strained at -160 C and unloaded after the first burst of twinning, and was observed to contain twins over the entire gauge section. It was immediately warmed to room temperature and prestrained to suppress further twinning and to give it the same starting point (except for the twins) as the other specimen. When then immediately tested at -110 C , the specimen containing the twins was quite ductile, with 39 percent elongation and a partly fibrous fracture (Figure 75(b)). Judging from the appearance of the fracture and the shape of the load-elongation curve, the transition temperature was lowered by about 30 C by the presence of twins. Thus, it can be seen that twins, instead of causing brittle fracture,



(a)



(b)

FIG . 75 (a, b). INFLUENCE OF ROOM TEMPERATURE PRESTRAIN, (a) WITHOUT, AND (b) WITH THE PRESENCE OF TWINS INDUCED AT -160 C , ON THE SUBSEQUENT DUCTILITY AT -110 C IN FURNACE-COOLED F4 FERRITE.

can actually prevent it in some cases.

The increase in cleavage stress in the VCG F4 ferrite between -90 and -160 C (Figure 23) is probably caused by the increase in the number of cleavage barriers due to the twins formed in this temperature range (Figure 22). This behavior is not seen in CG F5 because the latter is ductile in this temperature range for reasons previously explained. Below -160 C the cleavage stress decreases for both mate-

rials. Here the applied stress is so high that the increase in the number of twins is not able to offset the increased probability of long-range propagation. The higher cleavage stress in F5 is mainly due to the fineness of the carbides, i.e., a higher stress is needed to make the smaller carbide cracks become critical Griffith cracks.

The decrease in cleavage stress of both F4 and F5 in the temperature range below -160 C is a result of the increasing difficulty of slip at low temperatures. As the temperature is lowered, the probability that carbide cracks will initiate microcracks increases and the applied stress necessary for the microcracks to penetrate high-resistance regions decreases. This leads to the decrease in fracture strain and fracture stress. The maximum in the cleavage stress in the F4 specimens is caused by the conflicting tendencies of an increased amount of twinning and a decreasing ease of slip.

Applicability of these Results to other Materials

It is pertinent to ask how the experimental findings and explanation of brittle fracture, presented in this work, relate to the ductile-brittle behavior of mild steel. Aside from grain-size control, the two most effective means of reducing the transition temperature of steel are the addition of manganese and fast cooling from the hot-working or normalizing temperature. We are now in a position to explain the reasons for this in terms of carbide morphology.

It has been shown by Allen et al⁶⁵ that the addition of manganese inhibits the formation of carbide films in grain boundaries and around pearlite patches, and that manganese tends to change the shape of the carbide in pearlite from plates to nodules. The latter effect has also been shown by Hahn et al³⁷. Rees et al¹³ reported that manganese does not improve low temperature toughness if iron is essentially free of carbide. In addition it has long been known that fast cooling rates produce finer pearlite and inhibit the tendency to form carbide films. In general, we should expect that anything which refines the size of the carbide particles will lower the ductile-brittle transition of steel. This could account for the very low transition temperatures of quenched and tempered steels.

Since voids from carbide cracks reduce the

fracture strength above the transition temperature, we should expect manganese and fast cooling to improve this property, also. The beneficial effect of manganese in this regard has been demonstrated by Hahn et al³⁷, and Sullivan⁷⁶ has shown that fast cooling improves the ductile strength of mild steel.

It is not meant to imply that carbide cracking is the only mechanism of crack initiation in iron. Non-metallic inclusions, if present and of sufficient size, could serve just as well. Normalized steels made by vacuum melting of fairly pure starting materials have been found to have a lower transition temperature than commercial steels of similar nominal composition⁵²⁻⁵³.

On the other hand, even if all brittle phases were removed, iron may become brittle at some still lower temperature and high stress level, particularly if interstitial impurities are present in solid solution. In this case the crack might be initiated by a twin intersection, or even by a slip-band intersection. Here, the stress level for crack initiation could well be greater than that necessary for propagation; if so, microcracks would not be found. It should be noted that Smith and Rutherford³⁴ have found that polycrystalline specimens of zone refined iron are ductile at 4.2 K. It is not known whether single crystals of this purity would exhibit similar ductility.

SUMMARY AND CONCLUSIONS

The mechanical-twinning behavior of F4 (0.035 percent carbon) and F5 (0.007 percent carbon) ferrite can be summarized as follows:

- (i) The temperature at which mechanical twinning is first observed decreases as the ferritic grain size decreases.
- (ii) The number of grains of ferrite containing twins increases as the test temperature is lowered.
- (iii) Most twinning takes place during the first few percent of elongation, and at lower temperatures twinning causes a disappearance of the discontinuous yielding phenomenon.
- (iv) The stress for the onset of twinning is essentially independent of temperature, but it increases with decreasing grain

size much more rapidly than does the lower yield stress; the slope of the line representing the twinning stress in the stress versus $d^{-1/2}$ plot is about 7 times greater than the slope of the yield-stress line.

A small yield drop is observed when a specimen is reloaded after being unloaded in an interrupted tensile test. The magnitude of the effect depends on the extent of unloading, being largest when the load is removed completely. This effect has been observed by others in both f.c.c. and b.c.c. metals and is apparently not connected with strain aging. Aside from this yield effect, the stress-strain curve of a specimen tested at low temperatures is essentially unchanged by unloading and re-loading, even with in-between aging at room temperature for times up to about 30 minutes.

The tensile properties of polycrystalline iron in the ductile, brittle, and transition-temperature regions can be profoundly affected by changes in the amount and size of iron-carbide particles present. The carbides contained in the F4 and F5 ferrite, mainly as grain-boundary precipitates, crack during plastic deformation in tension at temperatures ranging from room temperature to -196°C . The role which this carbide cracking plays in the fracture of iron can be described as follows:

- (i) In the ductile and transition temperature regions, cracks in carbides lead to the formation of voids as the cracks open up with increasing strain. The void formation is especially pronounced in the necked region of the F4 ferrite and leads to lowering of the fracture stress and reduction-in-area values. The tendency for void formation is greatly reduced in the F5 ferrite because the carbides are fewer in number and smaller in size.
- (ii) In the brittle temperature region, carbide cracks initiate cleavage microcracks in the ferrite, which can eventually lead to cleavage fracture. Virtually all ferrite microcracks observed in F4 and F5 were originated by carbide cracks.
- (iii) The initiation of microcracks by carbide cracks can be understood in terms of the Griffith theory of crack propagation in brittle materials by considering that the ferrite has a statistical probability of be-

having (locally) as a brittle material, i.e., that the ferrite will fail to respond to a carbide crack by plastic relaxation. The highest temperature at which microcracks can be observed increases with the thickness of the carbides, since the stress level necessary for microcrack formation is reduced as the carbide crack length increases. Both carbide cracks and ferrite microcracks tend to lie normal to the tensile axis.

The observations regarding microcrack formation and propagation in the ferrite can be summarized as follows:

- (i) Microcracks appear mainly during the strain-hardening region of the stress-strain curve. The number of microcracks increases with increasing strain, and they continue to form up to the moment of fracture.
- (ii) Microcrack propagation can be stopped by grain boundaries, twins, or by the formation of slip bands and/or twins at the tip of the advancing crack. Twins lying across the path of cracks can act as effective barriers, and an increase in the twin content of a specimen behaves much like a decrease in grain size, as far as crack propagation is concerned. Accordingly, the presence of twins can significantly raise the cleavage stress and increase the ductility of ferrite.
- (iii) Microcracks generally become wider, but not longer, as straining of a tensile specimen continues, although crack lengthening is occasionally observed. Sometimes the final fracture passes through an existing microcrack; in such cases, it was not possible to determine whether the fracture had been triggered by the microcrack acting as a sharp notch, or whether the fracture started elsewhere and passed through the existing microcrack by coincidence.
- (iv) Microcracks arising early in the strain history of a specimen tend to be short, whereas the longer microcracks tend to be formed later. However, later-formed microcracks may be long or short with about equal probability.

- (v) The number of microcracks observed in a fractured specimen goes through a maximum when plotted against temperature due to the opposing tendencies of:
 - (a) increasing probability of microcrack formation with decreasing temperature (increasing stress for a given amount of strain) and
 - (b) decreasing fracture strain caused by the increase in probability of microcrack propagation with decreasing temperature.
- (vi) The ductile-brittle transition of these ferrites lies about 20 C below the temperature where microcracks are first observed.
- (vii) Twinning is not important in microcrack formation in the coarse-grained ferrite polycrystals studied here, and should be of even less significance in commercial steels which have a much finer grain size.

It is postulated that cleavage fracture in F4 and F5 ferrite occurs in the following manner: A microcrack is initiated by a carbide crack and is able to propagate along a path of low resistance for a distance large enough for the crack to attain the velocity required for the penetration of barriers of high resistance. A low-resistance path may be a group of grains of abnormally large size or with a similar orientation of cleavage planes. The conditions under which cleavage fracture can occur are (1) the density of crack sources, e.g., carbides, must be large enough so that an active source will have a high probability of lying in a low-resistance path, and (2) the applied stress must be high enough to allow the propagating crack to penetrate regions of high resistance without stopping.

It is suggested that the lowering of the ductile-brittle transition temperature of mild steel by manganese additions and by normalizing results from the refinement of the iron carbide which these treatments bring about. The increased fracture strength and ductility above the transition temperature seems to be caused by the same effect.

ACKNOWLEDGMENTS

The author would like to express his most sincere appreciation for the assistance rendered to him in the pursuit of this work. Professor Morris Cohen provided continued guidance throughout the experimental work and the writing of the thesis. Dr. Ryukishi Honda contributed countless hours of assistance and advice. Drs. C. P. Sullivan, A. R. Rosenfield and M. F. Comerford also aided in the initial stages of the work. The expert assistance of Mr. R. C. Whittemore in many phases of the experimentation was invaluable. Mr. Barry Rosof and Miss Miriam Yoffa also provided much technical assistance. Mr. R. V. Huston ably performed the many machining operations involved. Financial support for the work was provided by the Ship Structure Committee under contract number NObs-88279.

REFERENCES

1. Ludwik, P., Elemente der Technoligische Mechanik, Berlin (1909).
2. Griffith, A. A., "The Phenomena of Rupture and Flow in Solids," *Phil. Trans. Roy. Soc. A* 221 (1920) 163.
3. Andrade, E. N. da C., and Tsien, L. C., "On Surface Cracks in Glasses," *Proc. Roy. Soc. A* 159 (1937) 346.
4. Poncelet, E. F., "A Theory of Static Fatigue for Brittle Solids," Fracturing of Metals, ASM, Cleveland (1948) p. 201.
5. Shand, E. B., "Experimental Study of Fracture of Glass: II, Experimental Data," *J. Amer. Ceramic Soc.* 37 (1954) 559.
6. Anderson, O. L., "The Griffith Criterion for Glass Fracture," Fracture, John Wiley and Sons, New York (1959) 331.
7. Griffith, A. A., "Theory of Rupture," *Proc. First Inst. Conference on Applied Mechanics*, Delft (1924) p. 55.
8. Petch, N. J., "The Fracture of Metals," *Prog. Metal Phys.* 5 (1954) 1.
9. Zener, C., "The Micro-Mechanism of Fracture," Fracturing of Metals, ASM, Cleveland (1948) p. 3.
10. Eshelby, J. D., Frank, F. C., and Nabarro, F. R. N., "The Equilibrium of Linear Arrays of Dislocations," *Phil. Mag.* 42 (1951) 351.
11. Koehler, J. S., "The Production of Large Tensile Stresses by Dislocations," *Phys. Rev.* 85 (1952) 480.
12. Stroh, A. N., "The Formation of Cracks as a Result of Plastic Flow," *Proc. Roy. Soc. A* 223 (1954) 404.
13. Stroh, A. N., "The Formation of Cracks in Plastic Flow II," *Proc. Roy. Soc. A* 232 (1955) 548.
14. Stroh, A. N., "A Theory of the Fracture of Metals," *Advances in Phys.* 6 (1957) 418.
15. Hall, E. O., "The Deformation and Aging of Mild Steel," *Proc. Phys. Soc. (London) B* 64 (1951) 747.
16. Petch, N. J., "The Cleavage Strength of Polycrystals," *J. Iron Steel Inst.* 174 (1953) 25.
17. Low, J. R. Jr., "The Relation of Micro-Structure to Brittle Fracture," *Relation of Properties to Microstructure*, ASM, Cleveland (1954) 163.
18. Wronski, A. S., and Johnson, A. A., "The Deformation and Fracture Properties of Polycrystalline Molybdenum," *Phil. Mag.* 7 (1962) 213.
19. Greenwood, G. W., and Quarrel, A. G., "The Cleavage Fracture of Pure Polycrystalline Zinc in Tension," *J. Inst. Metals (London)* 82 (1954) 551.
20. Hauser, F. E., Landon, P. R., and Dorn, J. E., "Fracture of Magnesium Alloys at Low Temperatures," *Trans. AIME* 206 (1956) 589.
21. Cottrell, A. H., and Bilby, B. A., "Dislocation Theory of Yielding and Strain Aging of Iron," *Proc. Phys. Soc. (London) A* 62 (1949) 49.
22. Tjerkstra, H. H., "The Effect of Grain Size on the Stress-Strain Curve of Alpha-Iron," *Acta. Met.* 9 (1961) 259.
23. Marcinkowski, M. J., and Lipsitt, H. A., "The Plastic Deformation of Chromium at Low Temperatures," *Acta. Met.* 10 (1962) 95.
24. Carreker, R. P., and Hibbard, W. R., "Tensile Deformation of High-Purity Copper as a Function of Temperature, Strain Rate, and Grain Size," *Acta. Met.* 1 (1953) 654.
25. Thomas, D. A., and Averbach, B. L., "The Early Stages of Plastic Deformation in Copper," *Acta. Met.* 7 (1959) 69.
26. McLean, D., Grain Boundaries in Metals, Oxford University Press (1957) p. 176.
27. McLean, D., Mechanical Properties of Metals, John Wiley and Sons, New York (1962) p. 104.

28. Low, J. R. Jr., "The Fracture of Metals," to be published in Prog. in Material Science.
29. Biggs, W. D., and Pratt, P. L., "The Deformation and Fracture of Alpha-Iron at Low Temperatures," Acta. Met. 6 (1958) 694.
30. Cottrell, A. H., "Theory of Brittle Fracture in Steel and Similar Metals," Trans. AIME 212 (1958) 192.
31. Mott, N. F., "Fracture of Metals: Some Theoretical Considerations," Engineering 165 (1948) 16.
32. Yoffe, E. H., "The Moving Griffith Crack," Phil. Mag. 42 (1951) 739.
33. Berry, J. M., "Cleavage Step Formation in Brittle Fracture Propagation," Trans. ASM 51 (1959) 556.
34. Stroh, A. N., "Crack Nucleation in Body-Centered Cubic Metals," Fracture, John Wiley and Sons, New York (1959) p. 117.
35. Chou, Y. T., Garofalo, F., and Whitmore, R. W., "Interactions between Glide Dislocations in a Double Pile-up in Alpha-Iron," Acta. Met. 8 (1960) 480.
36. Cottrell, A. H., "Theoretical Aspects of Fracture," Fracture, John Wiley and Sons, New York (1959) p. 20.
37. Hahn, G. T., Cohen, M., and Averbach, B. L., "The Yield and Fracture Behavior of Mild Steel, with Special Reference to Manganese," J. Iron Steel Inst. 200 (1962) 634.
38. Adams, M. A., Roberts, A. C., and Smallman, R. E., "Yield and Fracture in Polycrystalline Niobium," Acta. Met. 8 (1960) 328.
39. Stokes, R. J., Johnston, T. L., and Li, C. H., "The Relationship between Plastic Flow and the Fracture Mechanism in Magnesium Oxide Single Crystals," Phil. Mag. 4 (1959) 920.
40. Parker, E. R., "Fracture of Ceramic Materials," Fracture, John Wiley and Sons, New York (1959) p. 181.
41. Petch, N. J., "The Ductile-Cleavage Transition in Alpha-Iron," Fracture, John Wiley and Sons, New York (1959) p. 54.
42. Petch, N. J., "The Ductile Fracture of Polycrystalline Alpha-Iron," Phil. Mag. 1 (1956) 186.
43. Koehler, J. S., "The Nature of Work-Hardening," Phys. Rev. 86 (1952) 52.
44. Low, J. R., and Guard, R. W., "The Dislocation Structure of Slip Bands in Iron," Acta. Met. 7 (1959) 171.
45. Low, J. R. Jr., and Turkalo, A. M., "Slip Band Structure and Dislocation Multiplication in Silicon-Iron Crystals," Acta. Met. 10 (1962) 215.
46. Hornbogen, E., "Observations of Yielding in an Iron-3.17 At% Phosphorus Solid Solution," Trans. ASM 56 (1963) 16.
47. Hull, D., "Nucleation of Cracks by the Intersection of Twins in α -Iron," Phil. Mag. 3 (1958) 1468.
48. Hull, D., "Twinning and Fracture of Single Crystals of 3% Silicon Iron," Acta. Met. 8 (1960) 11.
49. Hull, D., "Twinning and the Nucleation of Cracks in Body-Centered Cubic Metals," AIME International Conference on Fracture, Seattle (1962).
50. Honda, R., "Cleavage Fracture in Single Crystals of Silicon Iron," J. Phys. Soc., Japan 16 (1961) 1309.
51. Honda, R., "Cleavage Fracture in Single Crystals of Iron," to be published.
52. Edmondson, B., "The Effect of Composition and Structure on the Tensile Properties of High-Purity Iron Single Crystals, with Particular Reference to the Question of Brittle Fracture," Proc. Roy. Soc. A 264 (1961) 176.
53. Cahn, R. W., "Mechanical Twinning in Molybdenum," J. Inst. Metals (London) 83 (1954-55) 493.
54. Bell, R. L., and Cahn, R. W., "The Initiation of Cleavage Fracture at the

- Intersection of Deformation Twins in Zinc Single Crystals," J. Inst. Metals (London) 86 (1958) 433.
55. Hornbogen, E., "Observation of Slip, Twinning and Cleavage in Iron-Phosphorus Solid Solutions," Trans. AIME 218 (1960) 634.
56. Hornbogen, E., "Dynamic Effects During Twinning in α -Iron," Trans. AIME 221 (1961) 711.
57. Sleeswyk, A. W., "Twinning and the Origin of Cleavage Nuclei in α -Iron," Acta. Met. 10 (1962) 803.
58. Sleeswyk, A. W., "Emissary Dislocations: Theory and Experiments on the Propagation of Deformation Twins in α -Iron," Acta. Met. 10 (1962) 705.
59. Allen, N. P., Hopkins, B. E., and McLennan, J. E., "The Tensile Properties of Single Crystals of High-Purity Iron at Temperatures from 100 to -253 C," Proc. Roy. Soc. A 234 (1956) 221.
60. Hopkins, B. E., and Tipler, H. R., "The Effect of Phosphorus on the Tensile and Notch-Impact Properties of High-Purity Iron and Iron-Carbon Alloys," J. Iron Steel Inst. 188 (1958) 218.
61. Wessel, E. T., "A Tensile Study of the Brittle Behavior of a Rimmed Structural Steel," Proc. ASTM 56 (1956) 540.
62. Allen, N. P., "The Mechanism of the Brittle Fracture of Metals," Fracture, John Wiley and Sons, New York (1959) p. 123.
63. Hanemann, H., and Schrader, A., "Atlas Metallographicus," Vol. 1, Verlag von Gebrüder Borntraeger, Berlin (1933) 86-91.
64. Bruckner, W. H., "The Micro-Mechanism of Fracture in the Tension-Impact Test," Welding Journal-Research Supplement 29 (1950) 467S.
65. Allen, N. P., Rees, W. P., Hopkins, B. E., and Tipler, H. R., "Tensile and Impact Properties of High Purity Iron-Carbon and Iron-Carbon-Manganese Alloys of Low Carbon Content," J. Iron and Steel Inst. 174 (1953) 108.
66. Hahn, G. T., Sc.D. Thesis, Massachusetts Institute of Technology, Cambridge, Massachusetts (1959).
67. Josefsson, Ake, "Impact Transition Temperatures of Some Pearlite-Free Mild Steels as Affected by Heat Treatments in the Alpha Range," Trans. AIME 200 (1954) 652.
68. Danko, J. C., and Stout, R. D., "The Effect of Subboundaries and Carbide Distribution on the Notch Toughness of an Ingot Iron," Trans. ASM 49 (1957) 189.
69. Brick, R. M., "Mechanical Properties of High Purity Fe-C Alloys at Low Temperatures," Final Report SSC-94 to Ship Structure Committee (31 March 1959).
70. Low, J. R., and Feustel, R. G., "Inter-crystalline Fracture and Twinning of Iron at Low Temperatures," Acta. Met. 1 (1953) 185.
71. Orowan, E., "Fracture and Strength of Solids," Reports on Progress in Physics (London) 12 (1949) 185.
72. Felbeck, D. K., and Orowan, E., "Experiments on Brittle Fracture of Steel Plates," Welding Journal 34 (1955) 570S.
73. Tetelman, A. S., and Robertson, W. D., "Direct Observation and Analysis of Crack Propagation in Iron-3% Silicon Single Crystals," Acta. Met. 11 (1963) 415.
74. Tetelman, A. S., "The Plastic Deformation at the Tip of a Moving Crack," AIME International Conference on Fracture, Seattle (1962).
75. Owen, W. S., Averbach, B. L., and Cohen, M., "Brittle Fracture in Mild Steel in Tension at -196 C," Trans. ASM 50 (1958) 634.
76. Sullivan, C. P., to be published.
77. Jacquet, P. A., "Improved Electrolytes for the Anodic Polishing of Certain

- Metals," Sheet Metal Industry 26 (1949) 577.
78. Wessel, E. T., and Olleman, R. D., "Apparatus for Tension Testing at Sub-atmospheric Temperatures," ASTM Bulletin No. 187 (1953) 56.
79. Erickson, J. S., and Low, J. R. Jr., "The Yield-Stress Temperature Relation for Iron at Low Temperature," Acta. Met. 5 (1957) 405.
80. Lement, B. S., Averbach, B. L., and Cohen, M., "Microstructural Changes on Tempering Iron-Carbon Alloys," Trans. ASM 46 (1954) 851.
81. Smith, C. S., and Guttman, L., "Measurement of Internal Boundaries in Three Dimensional Structures by Random Sections," Trans. AIME 197 (1953) 81.
82. Young, A. P., and Marsh, L. L., "A Method for Observing the Progress of Deformation in Tensile Samples," Trans. AIME 212 (1958) 247.
83. Stark, P., Averbach, B. L., and Cohen, M., "Influence of Microstructure on the Carbon Damping Peak in Iron-Carbon Alloys," Acta. Met. 6 (1958) 149.
84. Haasen, P., and Kelly, A., "A Yield Phenomenon in FCC Single Crystals," Acta. Met. 5 (1957) 192.
85. Birnbaum, H. K., "Unloading Effects in Crystals - I. The Unloading Yield Point Effect," Acta. Met. 9 (1961) 320.
86. Wilson, D. V., and Russell, B., "Stress-Induced Ordering and Strain-Ageing in Low Carbon Steels," Acta. Met. 7 (1959) 628.
87. Puttick, K. E., "Ductile Fracture in Metals," Phil. Mag. 4 (1959) 964.
88. Webb, W. W., and Forgeng, W. D., "Mechanical Behavior of Microcrystals," Acta. Met. 6 (1958) 462.
89. Gensamer, M., "The Structure of Metals and the Strength of Metal Structures," Trans. AIME 215 (1959) 2.
90. Rosof, B. H., S. B. Thesis, Massachusetts Institute of Technology, Cambridge, Massachusetts (1963).
91. Rees, W. P., Hopkins, B. E., and Tipler, H. R., "Tensile and Impact Properties of Iron and Some Iron Alloys of High Purity," J. Iron and Steel Inst. 169 (1951) 157.
92. Gensamer, M., private communication.
93. Grounes, M., private communication.
94. Smith, R. L., and Rutherford, J. L., "Tensile Properties of Zone Refined Iron in the Temperature Range from 298 to 4.2 K," Trans. AIME 209 (1957) 857.

SHIP HULL RESEARCH COMMITTEE

Division of Engineering & Industrial Research
National Academy of Sciences-National Research Council

Chairman:

RADM A. G. Mumma, USN (Ret.)
Vice President
Worthington Corporation

Members:

Mr. Hollinshead de Luce
Assistant to Vice President
Bethlehem Steel Co., Shipbuilding Div.

Professor J. Harvey Evans
Professor of Naval Architecture
Massachusetts Institute of Technology

Mr. M. G. Forrest
Vice President - Naval Architecture
Gibbs & Cox, Inc.

Mr. James Goodrich
General Manager
Todd Shipyards, Los Angeles Div.

Professor N. J. Hoff
Head, Dept. of Aeronautics & Astronautics
Stanford University

Mr. M. W. Lightner
Vice President, Applied Research
U. S. Steel Corporation

Arthur R. Lytle
Director

R. W. Rumke
Executive Secretary